Sexual mating in *Neurospora crassa*

Hsiao-Che Kuo

Doctor of Philosophy Thesis

The University of Edinburgh

2008

This thesis is dedicated to my parents, my brothers and my wife

Abstract

Little is known about the initial stages of mating during sexual reproduction in filamentous fungi. The research described in this thesis has focused primarily on this process in *N. crassa* in which a specialized hypha, the trichogyne, grows out chemotropically from the ascogonium (female cell) towards a sex pheromone releasing male cell which is commonly a macroconidium of opposite mating type. Following macroconidium-trichogyne fusion, the male and female nuclei became arrested in nuclear division. The female nuclei became immobilized, rounded up and clumped together whilst all of the male nuclei from the macroconidium moved unidirectionally and sequentially towards the ascogonium with an 'inchworm-like', repeated elongation and condensation pattern of movement. Male nuclei were transported along microtubules and actin microfilaments. Dynein, kinesins and myosins played a role in regulating perithecial formation and the behaviour of male and female nuclei during mating. The dynein subunits DYN-2, DLC, DIC and DYN-27, the kinesins NKIN-2 and KAR-3, and the myosin MYO-2 encoded by the female influenced male nuclear behaviour whilst the dynein subunit RO-3, the kinesin KIP-2 and the myosins MYO-1 and MYO-2 encoded by male influenced female nuclear behaviour. Non-self recognition of nuclei of opposite mating type occurs immediately following mcroconidium-trichogyne fusion. A novel mechanism underlying non-self (male-female) nuclear recognition in filamentous fungi was proposed, and involves the co-operative functioning of motor proteins encoded by the male and female partners at different stages following macroconidium-trichogyne fusion. A new type of hypha produced by conidia, the conidial sex tube (CST), was discovered. It was found to be induced by sex pheromone from the opposite mating type and to be regulated by red, green and blue light. The red light photoreceptors, phytochrome-1 (PHY-1) and phytochrome 2 (PHY-2), the putative green light photoreceptor, Opsin Related Protein-1 (ORP-1), and the blue light photoreceptors White Collar-1 (WC-1) and Cryptochrome

(CRY-1), were found to have photostimulatory and photoinhibitory roles in CST induction, The clock control protein Frequency (FRQ) was also found to be involved in the photoinhibition of CST induction. The emergence of CSTs from conidia was shown to display a positive phototropism.

Acknowledgements

After 3 years, 3 months and 26 days (14/Sep/2004 - 4/Jan/2008), I completed my PhD study. This was an unforgetable journey for me and without the following people I would never have finished and survived my PhD in the United Kingdom.

I would like to thank:

My supervisor, **Prof. Nick Read**, who taught me a lot not only about my PhD study but also about life in the UK. Also for his constant enthusiasm about my work and guidance that will be with me forever.

My parents and family for their never ending support, especially, my wife, **I-Ching**, for taking care of me and for encouragement.

All members of the Fungal Cell Biology Group, past and present, especially Gabriela Roca, Patrick Hickey, Graham Wright, Mari Valkonen, Eric Kalkman, Pete Marris, Verena Seidl, Javier Palma-Guerrero, Ulrike Binder, Kirsten Altenbach, Kathryn Lord, Alex Lichius and Meiling Chu for their advice, friendship and inspiration.

External collaborations:

Michael Frietag for the GFP and RFP labelled strains.

Katherine Borkovich for the sex pheromone and pheromone receptor KO mutant strains.

FGSC for providing all the other KO strains I used in my PhD.

Thanks to the British Mycological Society and the British Society for Cell Biology for their stimulating meetings and generous travel bursaries.

Thanks to ORS (Overseas Research Studentship) who funded some of my PhD and all the help from Prof. Keith Charnley at Bath University to get the funding.

Contents

Abbreviations

ATP	adenosine triphosphate
ATPase	adenosine triphosphatase
BLAST	basic local alignment search tool
Bml	β-tubulin
CATs	conidial anastomosis tube
CST	conidial sex tubes
DIC	differential interference microscopy
dH_2O	demineralized water (MilliQ grade)
DMSO	dimethylsulfoxide
EtOH	ethanol
FGSC	Fungal Genetics Stock Center
FITC:	fluoresceinisothiocynate
FM4-64	N-(3-triethylammoniumpropyl)-4-(6-(4-(diethylamino)phenyl) hexatrienyl pyridinium dibromide
GFP	green fluorescent protein
GPCR	G-protein coupled receptor
H1-GFP	histone 1 labelled with GFP
his	histidine
H1-RFP	histone 1 labelled with RFP
h	hour(s)
hyg	hygromycin

KO	knock out
LED	light emitting diode
min	minute(s)
N.A.	numerical aperture
NCBI	National Center for Biotechnology Information
NJ	neighbour-joining
PBS	phosphate buffered saline
pccg-1	ccg-1 promoter
PWA	Pokeweed agglutinin
RFP	red fluorescent protein
RIP	repeat induced point-mutation
SC	synthetic crossing
SEM	scanning electron microscopy
WGA	wheat germ agglutinin
WT	wild type
w/v	weight by volume
UV	ultraviolet light

CHAPTER 1

Introduction

Neurospora crassa has a long history as an excellent model for genetic, cellular, and biochemical research (Davis, 2000; Akins & Lambowitz, 1985; Seiler & Plamann, 2003). In 1843, bakeries in France were infested by a mould that produced luxuriant, conspicuous crops of powdery orange spores. This mould, known at the time as *Monilia sitophila*, is commonly found on bread and other carbohydrate-rich foodstuffs, on residues of sugar-cane processing (Davis & Perkins, 2002) and on burnt trees (Jacobson *et al.*, 2004). A century passed before the discovery of sexual fruiting bodies allowed the mycologists Cornelius L. Shear and Bernard O. Dodge to place this fungus in a new genus, *Neurospora* (Galagan *et al.,* 2003). By 1939, *N. crassa* had become a genetic textbook example to illustrate genetic segregation and crossing over in meiotic tetrads (Davis & Perkins, 2002). Even at this time *N. crassa* was recognized as a useful model system. It could be grown on a simple minimal growth medium. It is haploid, and therefore recognition of recessive, loss-of function mutations was straightforward (Davis & Perkins, 2002). In the 1940s, Beadle and Tatum analysed the role of certain metabolic genes in *N. crassa* (Beadle & Tatum, 1941). Their 'one-gene-one-enzyme' hypothesis, which established the relationships between genes and proteins, led quickly to a revolution in genetics in the mid-20th century (Galagan, *et al.,* 2003). With its genetically complex and biochemically tractable life cycle, *N. crassa* has become a popular experimental model microbe that has played a major role in the progress of biochemistry, genetics, molecular and cell biology in the latter half of the 20th century (Davis & Perkins, 2002). Research on this organism has ranged from molecular genetics, biochemistry, physiology, cell biology, developmental biology, photobiology, biological clock, gene silencing, genome defence systems, mitochondrial protein import, DNA repair, ecology, population genetics, and evolution (Davis & Perkins, 2002; Borkovich *et al.,* 2004).

In 2003, *N. crassa* became the first filamentous fungus to have its genome published, and is now a primary model for genome-wide experimental approaches. The approximately 40-megabase genome encodes about 10,000 protein-coding genes (Galagan, *et al.,* 2003; Borkovich *et al.,* 2004), approximately twice as many as in the yeasts *S. cerevisiae,* (5600) and *S. pombe,* (4900), and only about 25% fewer than in *Drosophila melanogaster* (14,000), and approximately half as many as *Caenorhabditis elegans* (19,000) (Seiler & Plamann, 2003; Stein, *et al.,* 2003). Analysis of the *N. crassa* gene set has yielded unexpected insights into its biology, including the identification of genes potentially associated with red light photobiology, genes implicated in secondary metabolism, and differences in Ca^{2+} signalling as compared with plants and animals (Galagan, *et al.,* 2003). The legacy of 70 years of intense research with this organism continues to be driven by a large and interactive research community that has also served to draw together a wider group of scientists working together. This coupled with the availability of advanced molecular and genetic tools, offers enormous potential for continued discovery using *N. crassa* as a model experimental system.

1.1 Life cycle of *Neurospora crassa*

Neurospora crassa is a multicellular organism and produces at least 28 morphologically distinct cell types, many of which are derived from hyphae (Bistis *et al.,* 2003). *Neurospora* vegetative hyphae are tip-growing cellular elements that undergo regular branching (Trinci, 1984) and are multinucleate (Freitag *et al.,* 2004). In its life cycle, *N. crassa* reproduces asexually by conidia and sexually by ascospores produced in perithecia (Fig. 1.1); the latter develop from protoperithecia (female structures) after they have been fertilized (Elliott, 1994). The asexual cycle is mitotic, while the sexual cycle involves mating and meiosis (Springer, 1993). For sexual reproduction, *N. crassa* requires that parents be of different mating type, determined by alternative forms (called idiomorphs) of the genetically complex mating type *mat A* and *mat a* loci (Glass & Nelson, 1994) (also see section 1.4).

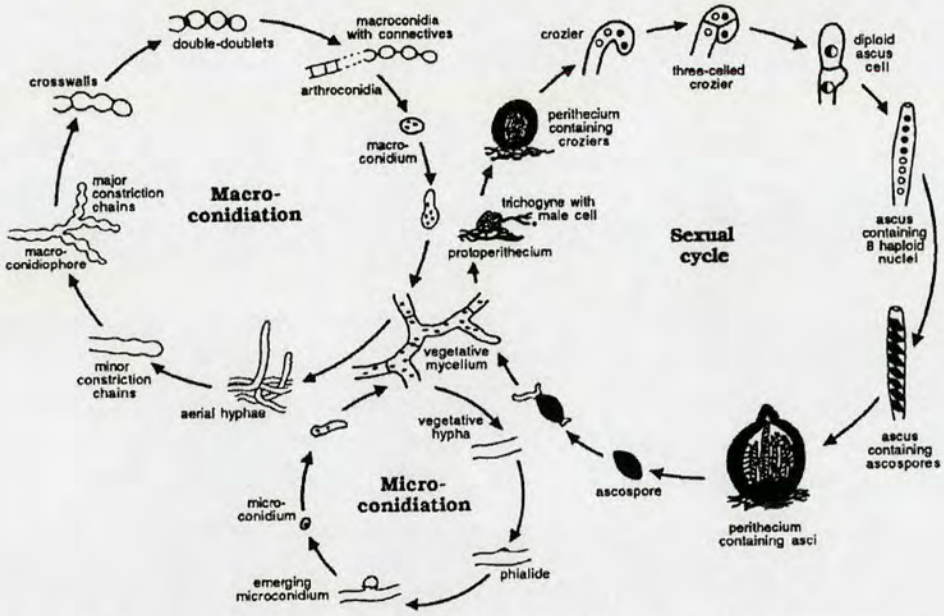

Figure 1.1 Life cycle of *N. crassa* (reproduced from Seale, 1973). *N. crassa* reproduces asexually by conidia, microconidia and macroconidia, and sexually by ascospores produced in perithecia; the latter develop from protoperithecia after they have been fertilized.

1.2 Asexual reproduction in *Neurospora crassa*

Neurospora crassa produces three types of asexual spores (macroconidia, microconidia, and arthroconidia) (Fig. 1.2) (Davis, 2000). They are produced in response to nutrient deprivation, desiccation, or various environmental stresses (Springer & Yanofsky, 1989).

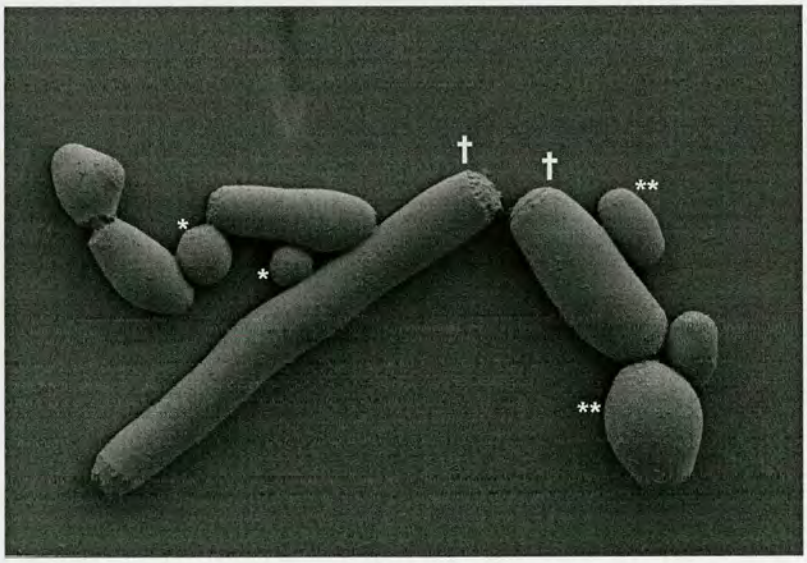

Figure 1.2 *Neurospora crassa* (WT 74A, FGSC 2489) produces three types of asexual spores: macroconidia, microconidia, and arthroconidia (Roca, M.G., Jeffree C.E., & Read, N.D., unpubl). *, microconidia. **, macroconidia. †, arthroconidia.

Macroconidiation is influenced by a circadian rhythm, which in turn is modulated by exposure to blue light (Springer & Yanofsky, 1989; Loros & Dunlap, 2001). Following a

period of growth, conidiophores switch to an apical budding mode of growth that results in a chain of macroconidia being formed (Fig. 1.1). As the macroconidia reach maturity, they separate and dispersal occurs primarily by means of air currents (Springer & Yanofsky, 1989). The macroconidia typically contain from two to five nuclei, the nuclear number being influenced by the nutrient status of the growth medium. Macroconidia also germinate rapidly allowing efficient reproduction of the fungus (Turian & Bianchi, 1972; Michán *et al.,* 2003). The second type of asexual spore is a microconidium and is normally uninucleate. It emerges by budding laterally from microconidiophores or directly from vegetative hyphae (Springer & Yanofsky, 1989; Maheshwari, 1999). The third type of asexual spore, the arthroconidium, arises by fragmentation of conidiophore hyphae (Springer & Yanofsky, 1989).

1.3 Sexual reproduction in *Neurospora crassa*

Sexual development typically starts after asexual sporulation once conidial production is well under way (Davis, 2000). Sexual reproduction is involved in the union of two compatible nuclei which can be brought together by different methods (Mukerji *et al.,* 1983). Protoperithecia begin to form as a small knot of hyphae that surround a specialized coiled hypha called the ascogonium (the 'female cell'). The hyphae around the ascogonium become interwoven and adhere together to form the protective wall of the protoperithecium (Read, 1983, 1994). One or more filamentous trichogynes grow out from the ascogonium through the protoperithecial wall and may grow for a considerable distance and branch (Backus, 1939; Bistis 1981). Trichogynes usually respond to a pheromone emitted by the male fertilizing agent (e.g. of the opposite mating type by growing towards it until contact and fusion occurs) (Fig 1.3) (Bistis, 1981).

The fertilizing agent is most commonly a macroconidium, microconidium, or arthroconidium (Nelson & Metzenberg, 1992; Davis, 2000). After the fertilizing agent has fused with a trichogyne then one or a few nuclei from the conidium migrate(s) through the trichogyne to the ascogonium (Davis, 2000). The protoperithecium is normally fertilized by a single conidial nucleus, although mixed male parentage and mixed female parentage of resulting perithecia have occasionally been observed (Johnson, 1976). Ascogenous hyphae and asci subsequently develop (Davis, 2000) as the protoperithecium enlarges and differentiates into the perithecium, from which ascospores are ultimately discharged.

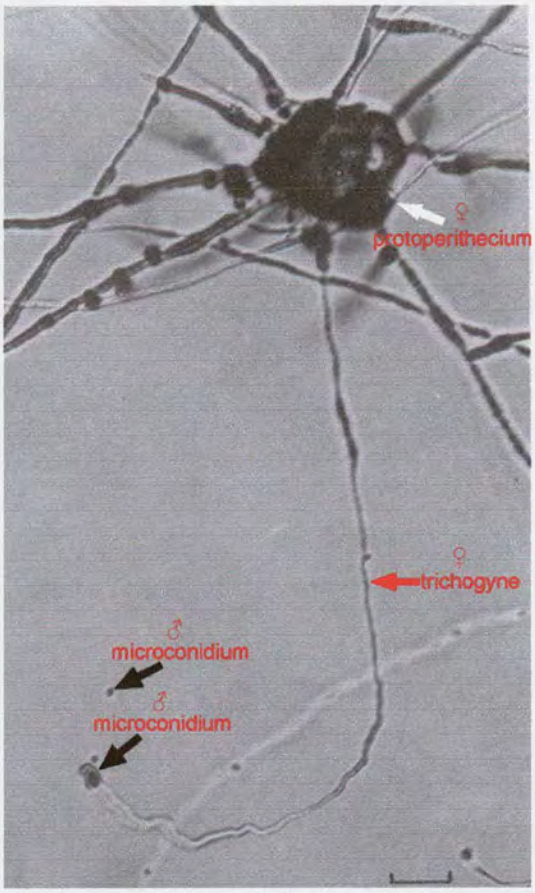

Figure 1.3 A protoperithecium of *N. crassa*. Note the trichogyne is homing towards a microconidium of opposite mating type. Microconidia (male cells) of strain mat *a* (black arrow indicated) were placed on the agar surface near a mat *A* protoperithecium (female) (white arrow indicated). 7.5 h later the trichogyne (red arrow indicated) has reached one of the microconidia in and begun to coil around it. Bar = 20 μm (reproduced from Bistis, 1981).

The dikaryon is set up within the ascogenous hyphae and is propagated by conjugate nuclear divisions such that each hyphal compartment of the ascogenous hyphae contains one male nucleus and are female nucleus (i.e. one of which is *mat A* and the other *mat a*). The initiation of the dikaryon is believed to be important for the transition from the protoperithecial to perithecial stage to occur. Fusion of the *mat A* and *mat a* nuclei occurs in the penultimate cell of the ascogenous hyphae and gives rise to a very short-lived diploid phase. The diploid cell is the ascus mother cell. Within the young ascus meiosis followed by mitosis occurs, and eight linearly ordered haploid ascospores are formed. The ascospore cell wall became melanized and ridged.

Figure 1.4 Ascus rosette of *Neurospora crassa*. Each ascus contains eight ascospores (reproduced from Raju & Newmeyer, 1977).

All of these asci (Fig 1.4) are usually derived from a single pair of haploid parental nuclei (Davis, 2000). If the parents have two different alleles of one gene, asci will contain four of one parental type and four of the other. The perithecium possesses a neck ('beak') through which mature asci extend and discharge their ascospore from the ostiolar pore (Read & Beckett, 1996).

1.4 Regulation of sexual reproduction by mating-type genes

Neurospora crassa has two mating types, *A* and *a*, which regulate mating (Glass & Nelson, 1994). The mating types are determinated by dissimilar DNA sequences at the mating-type locus (*mat*) and have been termed idiomorphs (Metzenberg & Glass, 1990). There are three genes, *mat A-1*, *mat A-2* and *mat A-3* at the *mat A* locus but only one gene *mat a-1*, at the *mat a* locus (Fig. 1.5). The mating-type genes are 'master regulators' of mating, postfertilization development, and nuclear identity during sexual reproduction in *N. crassa* (Glass & Nelson 1994). The *mat A-1* gene is required for *mat A* mating identity, postfertilization functions, and vegetative incompatibility with *mat a* strains. The Δ*mat A* strain is morphologically similar to wild type during vegetative growth, but it is sterile and heterokaryon compatible with both *mat A* and *mat a* strains. In *mat a* individuals, a single gene, *mat a-1*, is required for mating identity, postfertilization functions, and for vegetative incompatibility with *mat A* strains (Saupe & Glass, 1997; Wu & Glass, 2001; Glass & Kaneko, 2003). Mutations in *mat A-2* or *mat A-3* do not dramatically affect sexual development nor do they result in the production of uniparental asci. *mat A-1* and *mat a-1* are the critical factors for both mating and sexual development (Ferreira *et al.*, 1996; Saupe *et al.*, 1996). It has been proposed that MATA-1 functions as a transcriptional regulator that controls expression of

genes involved in mating and post-fertilization functions (Ferreira *et al.*, 1996).

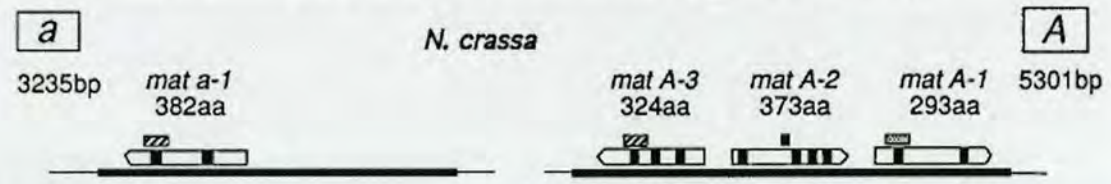

Figure 1.5 Structural and functional regions of the mating-type genes of *N. crassa.* The sizes (in base pairs) correspond to the unique sequences (idiomorphs) indicated by thick lines. The bordering identical sequences are indicated by thin lines. Arrows interrupted by solid boxes represent the coding sequences of the identified genes and the introns, respectively. The approximate position of the sequence encoding the putative DNA binding motifs is indicated by a box above each gene. This sequence is generally interrupted by an intron. Symbols: hatched boxes, HMG proteins; stippled boxes, protein with a a1 domain; solid boxes, a conserved 19-aa peptide domain in MAT A-2 (reproduced from Coppin *et al.*, 1997).

1.4.1 Vegetative incompatibility

During sexual reproduction, which involves the formation of a heterokaryon containing both *mat A* and *mat a* nuclei, heterokaryon incompatibility is suppressed. This is in contrast to heterokaryons containing *mat A* and *mat a* nuclei which form by vegetative hyphal fusion, which are heterokaryon incompatible and undergo rapid cell death (Glass & Kaneko, 2002). Heterokaryon incompatibility is mediated by the *tol* locus; mutations in *tol* are recessive and suppress mating-type-associated heterokaryon incompatibility (Glass & Staben, 1990). The *tol* mutation only suppresses mating-type heterokaryon incompatibility; it does not suppress the incompatibility regulated by other *het* genes (Glass & Kuldau, 1992; Shiu & Glass, 2000). It is clear that different *het* genes encode very different gene products that function in different ways in causing heterokaryon incompatibility (Glass *et al.*, 2000; Glass & Kaneko, 2003).

1.4.2 Sex pheromones and sex pheromone receptors

In heterothallic fungi, pheromones play an important role in mating by facilitating recognition between strains of opposite mating type and by launching the complex pheromone response signalling mitogen activated protein (MAP) kinase pathway (O'Shea *et al.*, 1998; Bobrowicz *et al.*, 2002). Pheromones are diffusible mating-type specific substances produced in one individual that elicit in individuals of opposite mating type the responses required for fusion (Nelson, 1996). The expression of the pheromone precursor genes is mating-type specific and under the control of the mating-type locus (Bobrowicz *et al.*, 2002; Kim *et al.*, 2002). Genes linked to mating type encode putative pheromone precursors that are expressed specifically in *mat A* (CCG-4) or in *mat a* (MFa-1). MFa-1 (which encodes mating factor *a*-1), has been identified and has multiple roles in the sexual development of *N. crassa* (Pöggeler & Kück, 2000; Bobrowicz *et al.*, 2002). Clock-controlled gene-4 (*ccg-4*) was first identified as a

gene that is expressed with a 22 h rhythm under the control of the circadian biological clock (Bell-Pedersen *et al.*, 1996). Only *matA-1* is required for transcriptional regulation of CCG-4 (Bobrowicz *et al.*, 2002).

Cells of opposite mating type release different peptide pheromones that are recognized by seven transmembrane domain G protein-coupled pheromone receptors (GPCRs) encoding *pre-1* and *pre-2* genes and produced by cells of the opposite mating type (Pöggeler & Kück, 2001). *pre-1* is most highly expressed in *matA* strains under mating conditions, but low levels can also be detected in *mat a* strains. The pheromone receptor protein is homologous to other fungal pheromone receptors which belong to the rhodopsin-like superfamily of GPCRs (Wendland *et al.*, 1995; Vaillancourt *et al.*, 1997). The pheromone-receptor interaction initiates a signal transduction pathway involving G-protein signalling (Yang *et al.*, 2002) that activated a MAP kinase cascade that leads to cell cycle arrest in G1 and transcription of genes involved in cell and nuclear fusion (Bobrowicz *et al.*, 2002).

Both MFa-1 and CCG-4 transcripts are not abundant in mycelia grown in rich Vogel's medium. However, both MFa-1 and CCG-4 mRNA accumulated to higher levels in mycelia cultured on synthetic crossing medium that contains a low nitrogen level. The demonstration of rhythmic pheromone precursor gene transcript accumulation in *N. crassa* provides the first molecular connection between the sexual developmental pathway and the circadian clock (Bobrowicz *et al.*, 2002).

1.5 Nuclear distribution and movement in fungi

After a male conidium and a female trichogyne fuse, one or a few nuclei from the conidium migrate(s) through the trichogyne to the ascogonium (Davis, 2000). The nuclear movement is presumably mediated by cytoskeletal elements (microtubules and/or actin microfilaments) and their motor proteins. In filamentous fungi, microtubules, actin and probably motor proteins have been intensively analysed (Fischer, 1999; Steinberg, 2006).

Fungal hyphal tip growth is a highly polarized and dynamic process involving both actin microfilaments and microtubules. It is thought that microtubules are primarily responsible for the long distance transport of secretory vesicles to the Spitzenkörper, while actin microfilament primarily controls vesicle organization within the Spitzenkörper and their transport to the apical plasma membrane (Harris *et al.*, 2005). Nuclear positioning is generally dependent on microtubules, which are dynamic polymers of αβ-tubulin (Inoué & Salmon, 1995) and an associated microtubule-organizing centre (MTOC) from which they are originally derived. Microtubules have been proposed to contribute to nuclear movement in at least three ways (Reinsch & Gonczy, 1998): (a) microtubule pushing by microtubule polymerization (Dogterom & Yurke, 1998), (b) microtubule pulling through microtubule

motor proteins or microtubule depolymerization, and (c) microtubules acting as tracks on which the nucleus can travel using microtubule motor proteins (Steinberg, 2007).

1.6 Motor proteins in *Neurospora crassa* and other fungi

Two major classes of motor proteins have been described, microtubule-dependent and actin-dependent motors (Fig. 1.6). The first class comprises two subclasses: (a) dynein motor proteins which migrate along microtubules to the minus end and (b) kinesins which migrate either to the plus or to the minus end. The second major class of motor proteins is the actin-dependent myosins, some of which are involved in intracellular membrane trafficking (Steinberg, 2006).

All known and predicted motor proteins in *N. crassa* are listed in Table 1.1 (Borkovich *et al.*, 2004). There are 5 major groups, kinesin, myosin, dynein subunit, dynactin subunit and lis-1 complex in *N. crassa.*

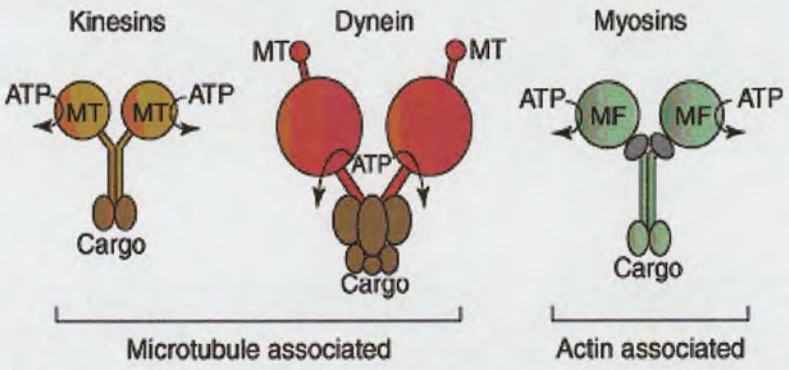

Figure 1.6. The organization of molecular motors. The known motors can be classified into three major types: the MT-associated kinesins and dyneins and the actin-associated myosins. In most cases, motors consist of a homodimer of heavy chains (light colors) and a variable number of associate light chains that often have regulatory roles (dark colors). The heavy chain forms the globular motor domain that binds microtubules (MT) or F-actin (microfilaments, MF). ATP cleavage leads to conformational changes in the two motor domains, which results in the coordinated 'walking' of the motor along the fibrous cytoskeleton. Note that myosin I and kinesin-3 motors are thought to be single-headed motors (reproduced from Steinberg, 2006).

Table 1.1 Comparison of fungal motor proteins

	Orthologs			
***N. crassa* gene (NCU no.)**	***S. cerevisiae* gene**	***S. pombe* gene**	**Family/class**	**Proposed role(s)**
		Dynein subunits		
Δ*dyn-2* (02610)	Dyn2p	Dlc (SPAC926.07)	Dynein light chain, LC8	
Δ*dlc* (03882)	NF	Dlc (SPAC1805.08)	Dynein light chain, Tctex-1	
Δ*ro-1* (06976)	Dyn1p	Dhc1	Dynein heavy chain	Nuclear movement, spindle elongation, retrograde vesicle transport
09095	NF	NF	Dynein light chain, LC7	
Δ*dic* (09142)	Pac11p	SPBC646.17	Dynein intermediate chain	
Δ*dlic* (09982)	NF	NF	Dynein light intermediate chain	
		Dynactin subunits		
Δ*ro-2* (00257)	NF	NF	Dynactin p62	Dynein-cargo interaction, nuclear movement, spindle elongation, retrograde vesicle transport
Δ*ro-3* (03483)	NIP100p	NF	Dynactin $p150^{Glued}$	
Δ*ro-7* (03563)	NF	NF	Dynactin Arp11	
Δ*dyn-27* (04043)	NF	NF	Dynactin p27	
Δ*ro-4* (04247)	Arp1p	Actin-like protein (SPBC1347.12)	Dynactin Arp1	
Δ*ro-12* (07196)	NF	NF	Dynactin p25	
08375	NF	NF	Dynactin p50/dynamitin	
		Lis-1 subunits		
04534	Pac1p	NF	LIS1	Dynein regulation,

04312	Pac1p	NF	LIS1	nuclear movement, spindle elongation, retrograde vesicle transport
Δ*ro-11* (08566)	NF	NF	NUDE/RO-11	
		Kinesins		
Δ*kip-1* (00927)	Kip1p, Cin8p	Cut7	BimC/Eg5	Spindle assembly and spindle pole body separation during mitosis
Δ*kip-2* (02626)	Kip2p	Klp4/Tea2	Kip2	Heterogenous group: Kip2p has mitotic functions (partly overlapping with Kip3p), while Tea2 seems to alter the dynamics of interphase microtubules
Δ*nkin-3* (03715)	NF	SPAC144.14		
Δ*kar-3* (04581)	Kar3p	Pkl1/Klp1	C-terminal	Spindle microtubule dynamics, counteracts BimC-like motors
		Klp2		
05180	NF	SPBC15D4.01 C	Fast evolving/pavarotti	Organization of the mitotic spindle
05028	NF	NF	KID	Chromosome alignment in metaphase
Δ*kip-3* (06144)	Kip3p	Klp5	Kip3	Spindle positioning, spindle elongation during anaphase, microtubule disassembly
		Klp6		
Δ*nkin-2* (06733)	NF[a]	NF	Unc104	Vesicular transport
Δ*kif-21* (06832)	NF	NF	Kif21/ chromokinesin	Vesicular transport, DNA binding
Δ*nkin* (09730)	Smy1p	Klp3	Conventional kinesin	Transport of secretory(?) vesicles, nuclear positioning, microtubule dynamics
		Myosins		
Δ*myo-1* (02111)	Myo3p, Myo5p	Myo1	Class I	Endo-/exocytosis

04350	NF	NF	Chitin synthase-myosin fusion protein	Specific for filamentous fungi
Δ*myo-2* (00551)	Myo1p	Myo2	Class II	Actin organisation, cytokinesis
		Myo3		
Δ*myo-5* (01440)	Myo2p, Myo4p	Myo5	Class V	Organelle transport
		Myo4		

[a] NF, not found by conventional BLAST searches.

This table is reproduced from Borkovich *et al.*, (2004)

1.6.1 Dynein and Dynactin subunits

Cytoplasmic dynein is a multi-subunit, MT-dependent mechanochemical enzyme that has been proposed to function in a variety of intracellular movements, including minus-end-directed transport of organelles (Paschal & Vallee, 1987; Vallee *et al.*, 1988). Dynein-mediated vesicle transport (Fig. 1.9) is stimulated *in vitro* by addition of the Glued/dynactin complex raising the possibility that these two complexes interacts *in vivo* (Plamann *et al.*, 1994). The dynein mutant, *ro-1* and *ro-3*, still had a prominent Spitzenkörper, demonstrating that apical transport was intact, but retrograde transport was inhibited completely (Seiler *et al.*, 1999; Riquelme *et al.*, 1998).

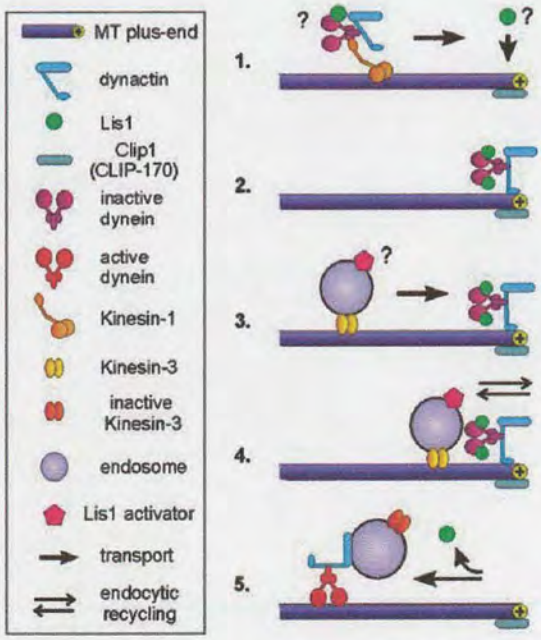

Figure 1.9 Dynein in minus-end directed traffic of early endosomes. (1) In the current model, Kinesin-1 takes dynein/dynactin to the microtubule plus-ends in the hyphal tip. Preliminary evidence indicates that a portion of Lis1 might hitchhike on the transported dynein/dynactin complex (not shown), but other mechanisms are also likely. (2) An inactive complex of dynein, dynactin and Lis1 accumulates at the plus-ends close to the growth region of the hypha. (3) Kinesin-3 transports early endosome along microtubules to the inactive dynein/dynactin/Lis1 complex, thereby delivering an unknown activator of Lis1. (4) When early endosome reach the plus-ends at the hyphal apex they quickly exchange material with the growing tip. This might involve the uptake of material for transport towards the cell body

as well as local membrane recycling processes. (5) Subsequently, the unknown activator triggers Lis1-dependent activation of the dynein/dynactin complex, which results in retrograde motility of the early endosome (reproduced from Lenz *et al.,* 2006).

In fungi, dynein is required for nuclear migration and requires dynactin for its functioning (Gill *et al.,* 1991). Dynactin is a protein complex that comprises two distinct structural components: a short, actin-like filament and a projecting sidearm (Yamamoto & Hiraoka, 2003). In *N. crassa,* the *ropy* (*ro*) mutants that are defective in genes encoding subunits of either cytoplasmic dynein or dynactin complex, have curled hyphae with abnormal nuclear distribution (Plamann *et al.,* 1994). Three *ro* genes, *ro-1*, *ro-3*, and *ro-4*, encode subunits of either cytoplasmic dynein or the dynein activator complex, dynactin (Minke *et al.,* 1999a).

In *ro-1* hyphae, the normally polarized distribution of organelles was disturbed and the motility and/or positioning of vesicles, mitochondria, and nuclei were altered, relative to the wild type hyphae. The apex of the *ro-1* hypha contained a Spitzenkörper with reduced numbers of apical vesicles but maintained a defined central core. Clearly, dynein deficiency in the mutant caused profound perturbation in microtubule organization and function and, consequently, organelle dynamics and positioning (Riquelme *et al.*, 2002).

RO-2 is proposed to play a role in mediating interactions between components of the dynein/dynactin motor complex or in linking this complex to the nucleus or cytoskeleton (Vierula & Maris, 1997).

ro-3 is predicted to encode the large subunit, $p150^{Glued}$, of cytoplasmic dynactin (Bruno *et al.*, 1996) and is defective in hyphal growth and nuclear distribution (Plamann *et al.,* 1994).

ro-4 encodes an actin-related protein that is a probable homologue of the actin-related protein Arpl which is the major component of the Glued/dynactin complex (Plamann *et al.,* 1994). The phenotypes of *ro-1* and *ro-4* mutants suggest that cytoplasmic dynein, as well as

the Glued/dynactin complex, are required to maintain the normal uniform nuclear distribution in hyphae (Plamann *et al.*, 1994).

Δ*ro-11* exhibit severe defects in nuclear distribution but this is not caused by an inability to generate or maintain cytoplasmic microtubules. The precise role of RO-11 in the movement and distribution of nuclei in *N. crassa* hyphae is unknown (Minke *et al.*, 1999b).

1.6.2 Kinesins

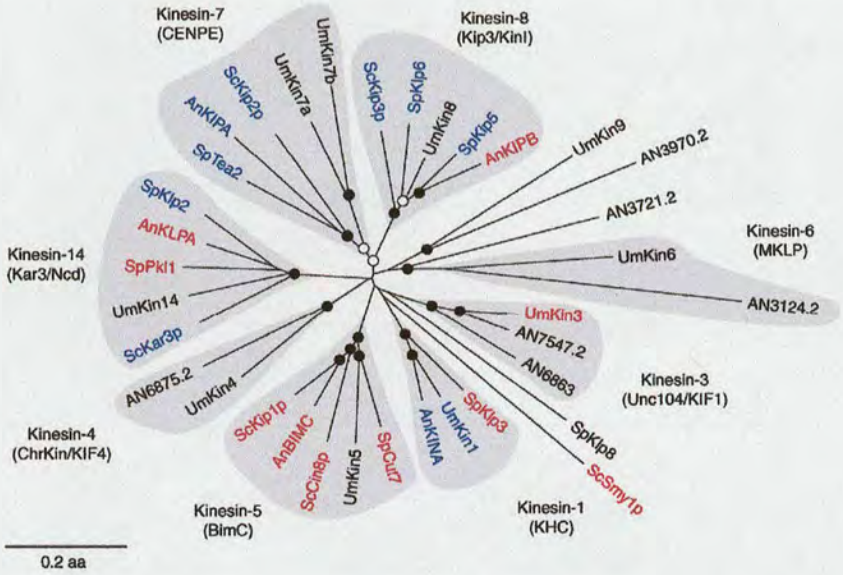

Figure 1.7 The biological role of fungal kinesins. Whereas the yeast fungi *Saccharomyces cerevisiae* (Sc) and *Schizosaccharomyces pombe* (Sp) contain six and eight kinesins, respectively, filamentous fungi such as *Aspergillus nidulans* (An or AN) and the dimorphic fungus *Ustilago maydis* (Um) encode 10–11 kinesin motors belonging to eight subfamilies. There is experimental evidence for the cellular role of many motors (names shown in red). Members of the subfamily kinesin-8, kinesin-14 and kinesin-5 are involved in mitosis, whereas members of kinesin-3 and kinesin-1 are predominantly organelle motors. However, members of almost all classes participate in the organization of microtubules (names shown in blue). Bootstrap values are indicated as 60–80% (open circles) and > 80% (closed circles). Alternative names for kinesin subfamilies are given in brackets (reproduced from Steinberg, 2006).

There are several groups of kinesins that can be classified according to their biological roles (Fig. 1.7). *Neurospora crassa* kinesin (*nkin*), was identified by Steinberg &

Schliwa (1995). In the Δ*nkin* mutant, regular nuclear spacing is lost, and nuclei often cluster in small groups separated by large gaps. Also, compared to bovine brain kinesin (0.6 - 0.8 μm/sec), NKIN is an unusually fast (2.1 - 3.8 μm/sec) microtubule motor protein (Grummt *et al.,* 1998). Its neck domain behaves differently from that of animal conventional kinesins and may be turned to drive fast, possessive motility (Kallipolitou *et al.,* 2001).

NKIN-2 and NKIN-3 are novel kinesin-related motor proteins of the Unc104/KIF1 subfamily and NKIN-2 is required for binding of mitochondria to microtubules (Fuchs & Westermann, 2005). There are other kinesins in *N. crassa* which are homologues of other known genes in *S. cerevisiae* (and *Ustilago maydis*) (e.g., Kar3p [kinesin-14), Kip3p [kinesin-8) and Kip2p [kinesin-7)) and that have been implicated in regulating microtubule stability. Kinesin-14 motors are minus-end-directed motors that have important roles in the mitotic spindle of all fungi (Prigozhina *et al.,* 2001), and might also organize the microtubule array in interphase in *S. pombe* (Carazo-Salas *et al.,* 2005).

Kip2p and Kip3p are kinesin-related proteins that function in regulating the dynamic organization of microtubule motors. Kip2p stabilizes microtubules and is required as part of the dynein-mediated pathway in nuclear migration and Kip3p function, in part, by depolymerizing microtubules in *S. cerevisiae* (Miller *et al.,* 1998). By contrast, in the filamentous fungus *A. nidulans,* the kinesin-7 KipA (similar to Kip2p family) focuses microtubules at the growing hyphal tip, thereby supporting growth directionality during tip growth. However, in *U. maydis* hyphal growth does not involve kinesin-7, but rather requires kinesin-1 and kinesin-3, which function in concert with myosin V (reviewed by Steinberg, 2006). Simple models showing the action of kinesins and dynein are shown in Figs 1.8.

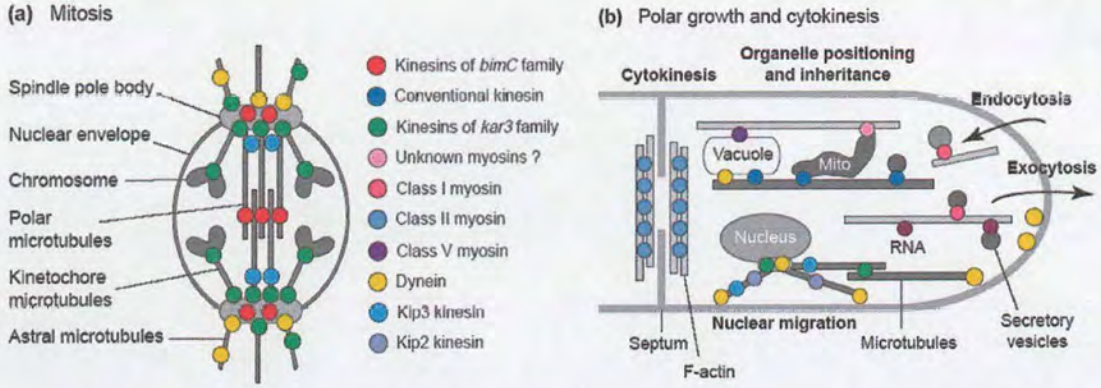

Figure 1.8 Localization and/or assumed site of action of fungal motors. (a) Mitosis. kar3-kinesins influence the dynamics of spindle microtubules and counteract bimC-like motors, which appear to crosslink polar microtubules. In addition, Kar3p might function within the chromosomal kinetochore. Anaphase is supported by cytoplasmic dynein that exerts pulling forces on astral microtubules and, in conjunction with Kip2p and Kip3p, probably modifies microtubule dynamics. Note that the localization of Kip3p within the spindle is not known. (b) Polar growth and cytokinesis. Motors are involved in a wide spectrum of organelle transport. In *S. cerevisiae*, F-actin is involved in mitochondrial motility, but the putative myosin has not yet been identified. Note that the figure summarizes data from several fungi (reproduced from Steinberg, 2000).

1.6.3 Myosins

Little is known about myosin function in filamentous fungi. In *U. maydis*, Myo5 has a crucial role in the morphogenesis, dimorphic switching, and pathogenicity of *U. maydis* (Weber *et al.*, 2003). Myosin I is essential for hyphal growth and is required for endocytic internalization of the endocytic marker dye FM4-64 (Steinberg, 2007).

1.7 Influence of environmental factors on sexual development

The decision whether to undergo asexual or sexual development is made on the basis of environmental signals perceived by vegetative hyphae (Bobrowicz *et al.*, 2002). Environmental factors such as temperature, aeration and nutrition influence the initiation and development of protoperithecia (Viswanath-reddy & Turian, 1975). Under conditions of nitrogen and carbon starvation (Davis & deSerres, 1970) and at temperatures between 15

and 30°C (McNelly-Ingle & Frost, 1965), vegetative hyphae undergo protoperithecial differentiation in preparation for sexual reproduction (Kim & Nelson, 2005).

Light plays a major role in *Neurospora* development (Davis 2000).Many physiological processes such as the induction of carotenoid synthesis (Harding & Turner, 1981), promotion of conidiation (Davis 2000) and protoperithecial development (Lauter & Russo, 1991), direction of perithecial neck development (Harding & Melles, 1983) and entrainment of the circadian rhythm (Sargent & Briggs, 1967; Franchi *et al.,* 2005) are regulated by blue light. Biological functions for light of other wavelengths are unknown in *Neurospora.*

1.8 *Neurospora crassa* photoreceptors and light-regulation genes

N. crassa is ideal for investigating photobiology and has more predicted photoreceptors (3 blue light, 2 green light and 2 red light photoreceptors) (Fig. 1.10) than any of the other fungi that have had their photobiology studied (Purschwitz *et al.,* 2006).

1.8.1 WC-1, WC-2, VIVID and FRQ proteins

A number of blue light activated regulated photoresponses are already known in *N. crassa* including carotenoid biosynthesis, macroconidiation, perithecial neck development and the regulation of circadian rhythms (Purschwitz *et al.,* 2006). The blue light photoreceptors White Collar-1 (WC-1) and VIVID (VVD) contain LOV domains that bind the flavin chromophore. WC-1, the most studied fungal photoreceptor, is a transcription factor which forms a heterodimer with White Collar 2 (WC-2) and activates a battery of light-induced genes (Fig 1.11). The White Collar complex is a key component of the circadian oscillator in which it regulates VVD expression. The third flavin-binding blue light photoreceptor is cryptochrome (CRY-1) which shows strong sequence homology to plant and animal cryptochromes, although its role in fungal blue light signalling is unknown (Purschwitz *et al.* 2006).

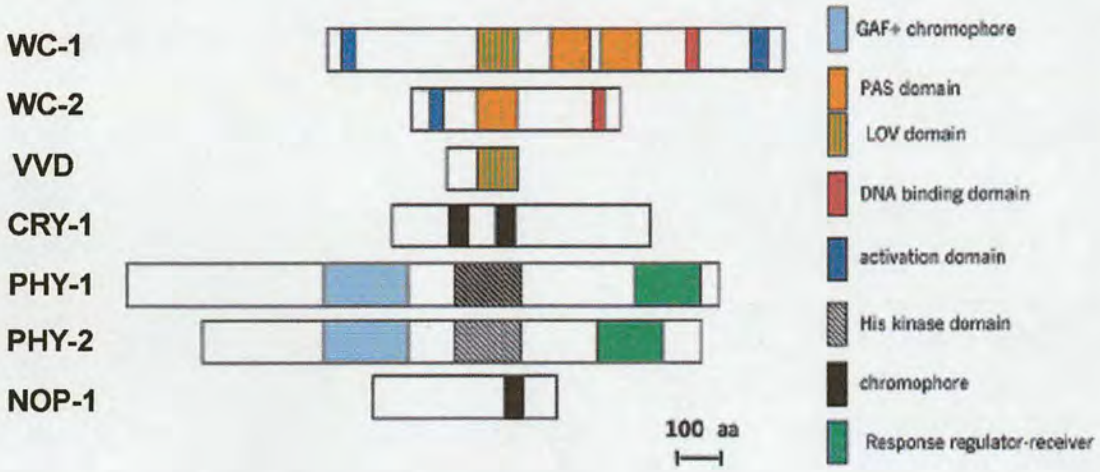

Figure 1.10. Real and predicted photoreceptors encoded in the *N. crassa* genome. The approximate sizes and locations of pertinent protein functional domains having known or plausible roles in photobiology are shown. WC-1 and WC-2 work together as the White Collar Complex (WCC) and comprise a photoreceptor that appears to be the main circadian photoreceptor and a major blue light photoreceptor in *N. crassa*. VVD is also a blue light photoreceptor that is responsible for modulating the WCC and contributing to photoadaptation. NOP-1 binds retinal and undergoes a photocycling. CRY-1, PHY-1, and PHY-2 all show strong sequence homologies to known photoreceptors from other organisms. aa, amino acids (from Blumenstein *et al.*, 2005). Another protein, not shown here, that may also be a green light photoreceptor is ORP-1 (reproduced from Borkovich *et al.*, 2004).

The frequency (frq) locus of *N. crassa* plays a key role in the regulation of circadian rhythms (Lewis & Feldman, 1996). In the dark (Fig 1.11), WC-1 and WC-2, activate *frequency* (*frq*) transcription by binding to its promoter (Froehlich *et al.*, 2002; 2003; Denault *et al.*, 2001). Thus the White Collar Complex (WCC) acts as a positive element. FRQ, on the other hand, acts as a negative element of this circadian negative feedback loop (Fig. 1.11) (Dunlap, 1999). In the *Neurospora* circadian clock, WCC is already bound to the *frq* promoter when the day begins (i.e. at dawn), and actively drives *frq* transcription. FRQ is translated with a short lag period, dimerizes and assembles with FRQ related helicase (FRH) into the FRQ-FRH Complex (FFC), and moves to the nucleus. FRQ, in the FFC, participates in several interactions here, and these determine the kinetics of the circadian cycle. There is less FRQ than WC-1 in the nucleus and the FFC promotes the phosphorylation of one or both

elements of the WCC thereby rendering them transcriptionally less active. Indeed, phosphorylation of both WC-1 and WC-2 in the dark requires FRQ, and phosphorylation of the WCC reduces its ability to bind to DNA. FRQ disappears through proteasomal degradation, and this too is triggered by its phosphorylation. As soon as it appears, it begins to be phosphorylated by a host of kinases. The end result of all this is a daily cycle in FRQ phosphorylation resulting in the precipitous turnover of FRQ around the middle of the night. When FRQ disappears, the phosphorylation-mediated inactivation of the WCC is reversed and the expression of *frq* (and the circadian cycle) begins anew (reviewed by Dunlap, 2006).

The *Neurospora* protein VIVID (VVD) is a second fungal blue light photoreceptor which non-covalently binds a flavin chromophore and shows partial sequence similarity with plant blue light photoreceptors. VIVID is localized in the cytoplasm and is only present after light induction (Schwerdtfeger & Linden 2003). The vivid (Δ*vvd*) mutant shows an increased accumulation of carotenoids under constant illumination, which is due to a sustained expression of carotenoid genes in the light (Perkins *et al.,* 1997; Schwerdtfeger & Linden, 2001). Furthermore, VIVID was found to be controlled by the circadian clock and to modulate the light input to the circadian pacemaker (Heintzen *et al.,* 2001).

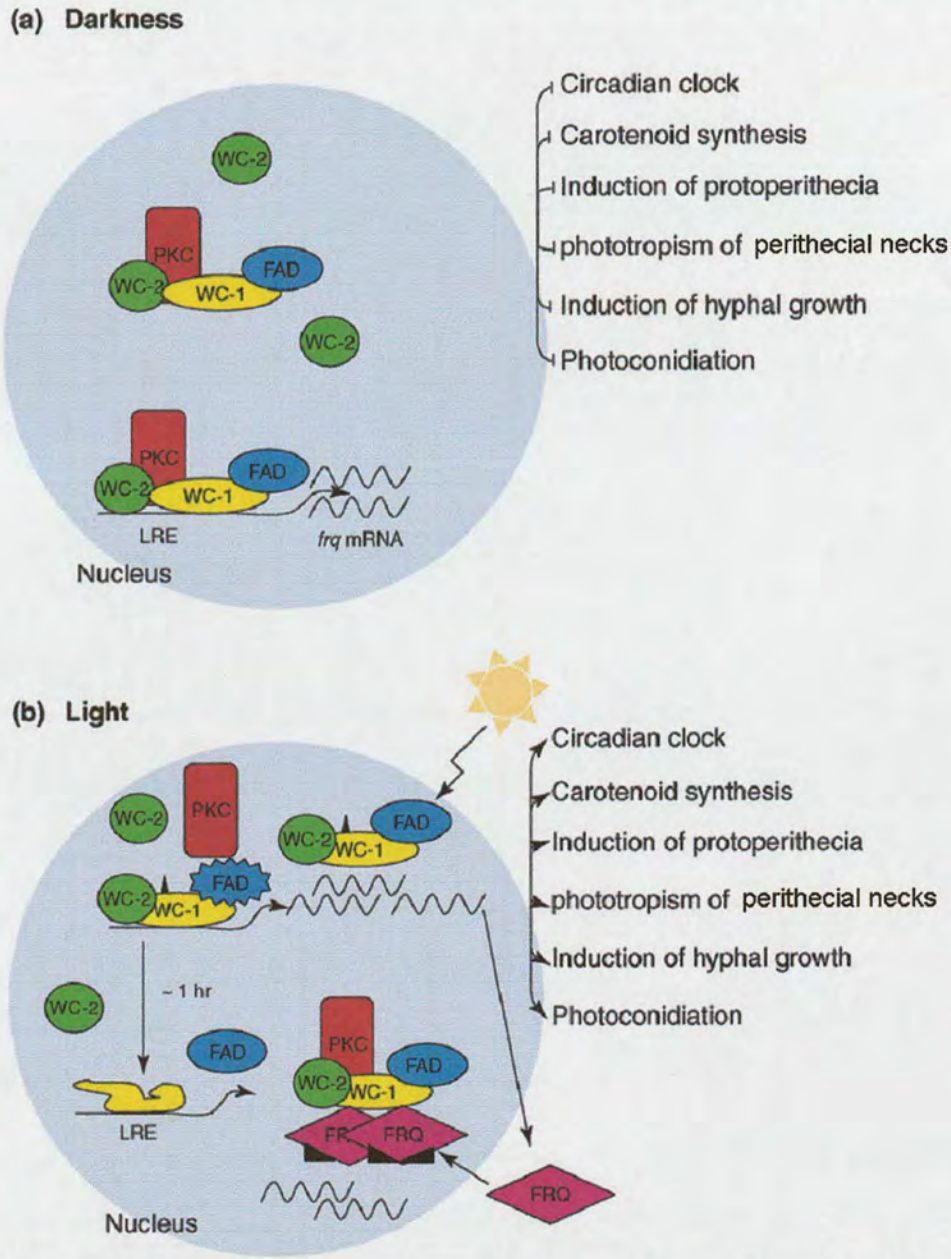

Figure 1.11 Model of blue-light sensing in *N. crassa*. In darkness, the White Collar Complex (WCC) associates with protein kinase C (PKC) and binds to cis-acting elements (LREs) at the promoter of the *frq* gene. The *frq* transcript level is very low under these conditions. Upon light exposure the frq mRNA level increases immediately and *wc–1* expression is also induced. By contrast, the WC–2 level is high under all conditions. PKC dissociates from WCC in light, leaving a phosphorylated WCC behind at the LRE site. Transcription of *frq* reaches its peak and FRQ is synthesized. One hour after light exposure, WCC experiences hypophosphorylation and is subsequently degraded. FRQ binds newly synthesized WCC and prevents its own transcriptional activation. As a result *frq* expression is again reduced to a basal level and the photo-cycle can start again (reproduced from Blumenstein *et al.*, 2005; Purschwitz *et al.*, 2006).

1.8.2 Opsins

No green light photoresponses are known in fungi. However, *N. crassa* possesses two 7 transmembrane helix opsins (NOP-1 and ORP-1) that are putative green light photoreceptors (Borkovich *et al.* 2004).

Opsins are integral membrane proteins that bind to the chromophore retinal to form light-absorbing pigments known as rhodopsins (Bieszke *et al.,* 1999). They serve as photosensors in the eyes of animals and as photosensors and light-dependent ion (H^+ or Cl^-) pumps in archaea. The first fungal opsin characterized was NOP-1 of *N. crassa* (Borkovich *et al.,* 2004) and is not transcribed in liquid cultures or in the absence of light (Bieszke *et al.,* 1999). The NOP-1 protein shows green light-absorbance properties and no evidence of H^+ pumping. An opsin from the plant pathogen *Leptosphaeria maculans* (Idnurm & Howlett, 2001) has a similar photochemistry to *N. crassa* NOP-1, but additionally is capable of light dependent H^+ pumping (Bahn *et al.,* 2007). So far *Δnop-1* mutants in *N. crassa* have no related defects in light signalling or other biological function (Bieszke *et al.,* 1999).

1.8.3 Cryptochrome

Cryptochromes are blue photoreceptors that are found in all plants and some animals (Cashmore *et al.,* 1999; Somers *et al.,* 1998). In plants, cryptochrome can interact with phytochromes (Martinez-Garcia *et al.*, 2000). The direct interaction between the plant phytochrome PHYB and plant cryptochrome CRY2 suggests that cryptochrome signal transduction may involve phytochrome-mediated regulation of transcription. Another plant cryptochrome, CRY1, has been reported to interact with another phytochrome PHYA in a yeast two-hybrid assay (Ahmad *et al.,* 1998). CRY1 also may interact with PHYB, at least indirectly (Yang *et al.,* 2001).

In animals, cryptochrome can interact with opsin. For example, opsins, as well as cryptochrome, are believed to function in the entrainment of the fly's behavioural rhythms

(Stanewsky *et al.,* 1998). Mutant mice lacking CRY2 undergo photoentrainment of their behavioural rhythms, which indicates a role in this process for at least one other photoreceptor (Thresher *et al.,* 1998). Whether opsins support rhythm entrainment in mammals, as they appear to in flies, is not so clear. Potential interacting partners in this process are phytochromes for plant cryptochromes, and opsins for animal cryptochromes (Cashmore *et al.,* 1999).

So far, virtually nothing is known about cryptochromes in *N. crassa* or other fungi.

1.8.4 Phytochromes

Phytochromes are an important class of photoreceptors in all plants, most algae, as well as certain fungi and many prokaryotes, including most cyanobacteria. Typically phytochromes absorb light in the 600–750 nm wavelength range: the red-absorbing form Pr (k_{max} ca. 660 ± 10 nm) is photoconverted to the far red (k_{max} ca. 720 ± 15 nm) absorbing Pfr form. Far red light photoconverts the Pfr form back to the Pr form. In plants the active state is the Pfr form and the inactive state is the Pr form. In bacteria it is the opposite (Yeh *et al.,* 1997; also reviewed by Strauss *et al.,* 2005). Figure 1.12 shows the different domains of the plant, bacterial and fungal phytochromes.

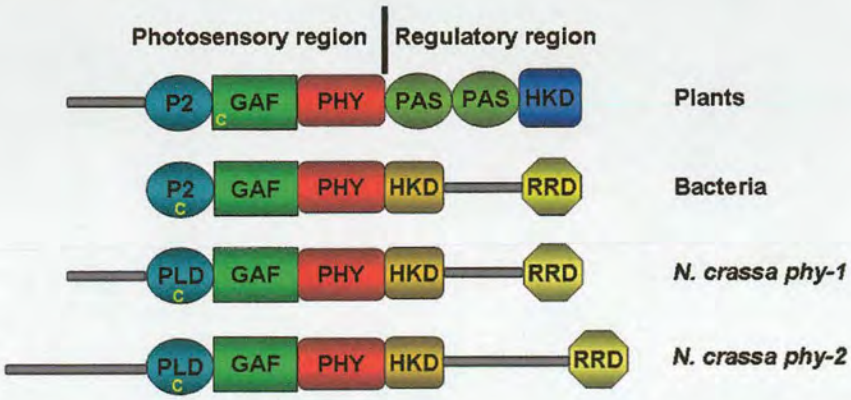

Figure 1.12 The specific domains of phytochromes in plant, bacterial and *N. crassa*. P2: C–terminal regulatory module; PHY, phytochrome. HKD, histidine kinase domain. RRD, response regulator domain which is the chromophore-binding site in *N. crassa*. GAF, cGMP-specific phosphodiesterases. PAS, photosensory input domain that comprises the

Per-Arnt-Sim (PAS) motif. The term PAS is an acronym of the names of genes in whose protein products these domains were identified for the first time: PER (*period*) of Drosophila, ARNT (*aryl hydrocarbon receptor nuclear translocator*) of mammals, and SIM (*single-minded regulator*) of *Drosophila* (modified from Blumenstein *et al.,* 2005).

1.8.4.1 Plant phytochromes

It is believed that phytochrome has evolved from the biliproteins present in cyanobacteria (Sharma, 2001). In *Arabidopsis*, the phytochrome apoproteins are encoded by a small gene family, *PHYA*, *PHYB*, *PHYC*, *PHYD*, and *PHYE* (Clack *et al.,* 1994).

The *PHYA* gene encodes the so-called type I photo-labile phytochrome A. It is abundant in etiolated seedlings in the dark, but its level drops 50 to 100 times in green plants in the light (Quail *et al.,* 1995). The other four have been suggested to encode the so-called type II photo-stable phytochromes B-E (Furuya, 1993) Plant phytochrome photoreceptors, contain two domains, the N-terminal photosensory and the C-terminal domains (Fig. 7, Oka *et al.,* 2004), that play a central role in the regulation of plant development. Phytochromes are red/far-red photochromic proteins with a covalently bound linear tetrapyrrole (bilin) prosthetic group. As indicated earlier, plant phytochromes exist in two forms: an inactive Pr form and an active Pfr form. The chromophore of the Pr form absorbs red light and photoconversion results in conformational changes that culminate in the formation of the signalling Pfr state (Fig. 1.13) (Bhoo *et al.,* 2001; Hahn *et al.,* 2006).

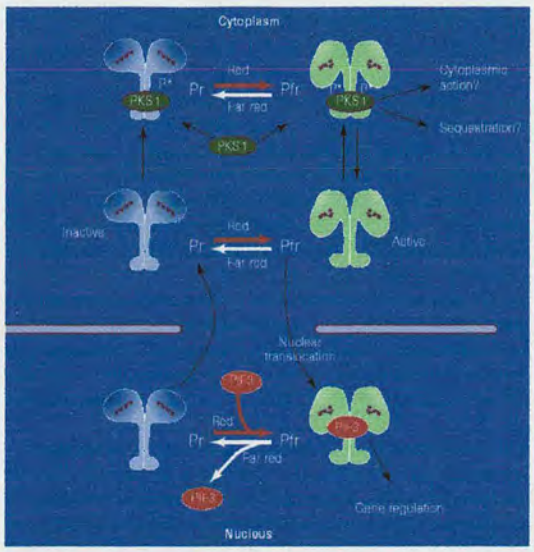

Figure 1.13 Main steps in plant phytochrome action. Absorption of a red photon by the inactive Pr form of a phytochrome causes a conformational change in the dimeric photoreceptor molecule. In the Pfr form, the phytochrome translocates to the nucleus where it binds to a putative reaction partner, PIF3, which is constitutively found in the nucleus and has the characteristics of a basic helix–loop–helix transcription factor. The Pfr–PIF3 complex initiates gene regulation, either directly or through unknown intermediates. Reversion of Pfr to Pr by far-red light results in rapid dissociation of PIF3, interrupting signal transduction. In the Pr form, the phytochrome slowly relocates to the cytoplasm. Here, in either the Pr or Pfr form, it can bind to a kinase substrate (PKS1), which may be involved in retention of the phytochrome in the cytoplasm or in its release for translocation. Phosphorylation of PKS1 is enhanced with Pfr, and may be the prelude to cytoplasmic action. So, several steps are susceptible to regulation by absorption of light by the photoreceptor: phosphorylation, nuclear translocation, association with PIF3 and transfer of signal transduction to PIF3 (reproduced from Smith, 1999).

PHYB is relatively light stable and is the primary high-intensity red light photoreceptor for circadian control (Somers *et al.*, 1998), It is the most abundant phytochrome in light-grown plants (Somers *et al.*, 1991)

The *PHY* domain of *PHYB* is dispensable for PHYB signal transduction but is required for stabilizing the Pfr form of PHYB (Oka *et al.*, 2004). Photosensory signalling by phytochrome B involves light-induced, conformer-specific recognition of the putative transcriptional regulator PIF3, providing a potential mechanism for direct photoregulation of

gene expression (Ni *et al.*, 1999). PHYA and PHYB are functionally the most important phytochromes in *Arabidopsis* (Gyula *et al.*, 2003) and their functions are summarized in Fig. 1.14 (Fankhauser & Chory, 1997).

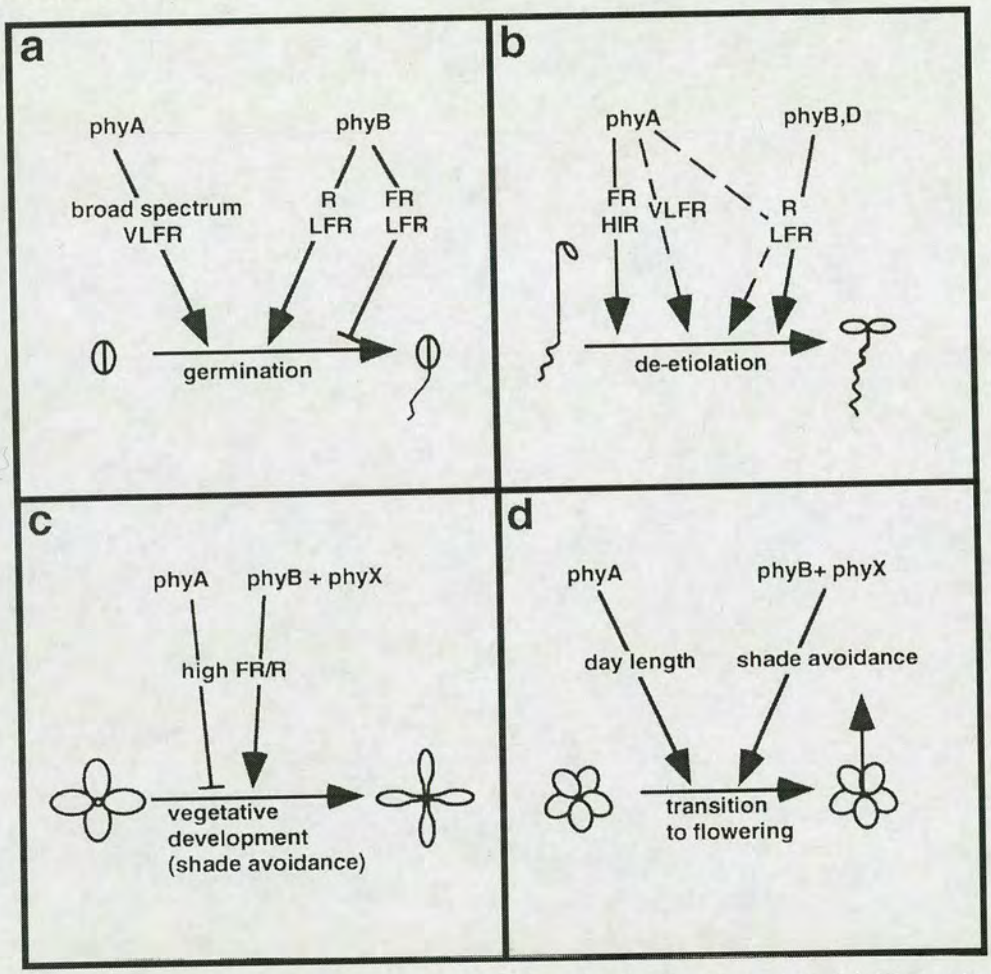

Figure 1.14 Phytochrome functions throughout the plant's development. (*a*) The role of phytochrome A and B in seed germination; (*b*) the role of phytochrome A, B, and D in de-etiolation; (*c*) phytochromes influencing vegetative development; (*d*) the transition to flowering is influenced by phytochromes. Red, R; far-red, FR; very low fluence response, VLFR; low fluence response, LFR; high irradiance response, HIR (reproduced from Fankhauser & Chory, 1997).

PHYC has motifs similar to bacterial sensor proteins of the 'two-component' regulatory system (Schneider-Poetsch, 1992). The relatively recent isolation of *phyC* mutans means less is known about this phytochrome compared with other members of the phytochrome family (Franklin et al., 2003 Monte et al. 2003; Li & Chinnappa, 2004; Balasubramanian et al., 2006).

A preliminary understanding of *phyC* in leaf development and leaf expansion was proposed based on the effects of the ectopic expression of the *PHYC* gene (Franklin *et al.*, 2003). The PHYC photoreceptor gene mediates natural variation in flowering and growth responses (Balasubramanian *et al.*, 2006). Plants lacking PHYC undergo early flowering in short days and exhibit reduced sensitivity to red light during seedling growth (Franklin et al., 2003).

PHYD acts in the shade-avoidance syndrome by controlling flowering time and leaf area (Devlin *et al.*, 1999)

PHYE was required for germination of *Arabidopsis* seeds in continuous far red light. However, inhibition of hypocotyl elongation by far red light, induction of cotyledon unfolding, and induction of agravitropic growth were not affected by loss of phytochrome E (Hennig *et al.*, 2002).

1.8.4.2 Bacterial phytochromes

The first phytochrome from a bacterial source to be discovered was Cph1 (cyanobacterial phytochrome 1) from *Synechocysis sp*. PCC6803 which was followed by the discovery of bacterial phytochromes from nonphotosynthetic bacteria (Davis *et al.*, 1999; Hughes *et al.*, 1997). Unlike plant and cyanobacterial phytochromes, most bacterial phytochromes carry a phytochromobilin or phycocyanobilin chromophore (Bhoo *et al.*, 2001) and lack the conserved cysteine residue in the conserved bilin lyase domain (BLD). This domain has been defined as the minimal GAF domain, capable of autocatalytic assembly with bilin chromophores (Wu & Lagarias, 2000). Bacterial phytochrome from the opportunistic pathogen *Pseudomonas aeruginosa* is synthesized in the dark in the red-light-absorbing Pr form and immediately converted into a far-red-light-induced photoreversibility of phytochromes (Tasler *et al.*, 2005). In *Afrobacterium tumefaciens*, a pair of bacterial phytochromes, AtBphP1 and AtBphP2, were identified and could function as opposing light sensors. The most interesting distinction is that AtBphP2 uses the Pfr and

not the Pr form as the inactive state, which is opposite to the situation with plant phytochromes (Montgomery & Lagarias, 2002; Karniol & Verstra, 2003).

1.8.4.3 Fungal phytochromes

The first phytochrome-mediated response to red light in fungi was recently demonstrated in *Aspergillus nidulans* (Blumenstein *et al.,* 2005). Red light stimulates asexual conidiation and represses sexual development in *A. nidulans* which possesses only one phytochrome (FphA). *Neurospora crassa* on the other hand possesses two phytochromes (PHY-1 and PHY-2) but no red light/phytochrome-mediated responses have been previously reported for it. Fungal phytochromes are more closely related to bacterial than to plant phytochromes. The output module of fungal and bacterial phytochromes comprises a histidine kinase domain and a response regulator domain, whereas plant phytochromes possess only a histidine kinase-related domain which is separated from the photosensory module by two PAS domains (Fig. 1.12). In *N. crassa*, binding of PHY-2 to its bilin chromophore has been demonstrated. The levels of *phy* transcripts do not appear to be light-regulated, but the abundance of *phy-1* mRNA is clock controlled (Froehlich *et al.,* 2005). So far there is no evidence of Pr/Pfr photoreversibility in fungi.

1.9. Introduction to the research described in this thesis

Sexual reproduction in *Neurospora crassa* is a very complex process that has been investigated for nearly a century but is still little understood.

The aims of my research were as follows:

1. To characterize the basic cytology of mating involving the chemotropic growth of the female trichogyne hypha towards to the male conidium, fusion of these cells, and the movement of the male nuclei through the trichogyne towards the female ascogonium.

Using live-cell imaging, I was able to analyse the dynamics of male and female nuclei during mating for the first time in a filamentous fungus.

2. To determine the roles of different motor proteins in the transport of the male nuclei through the trichogyne. In this part of study, GFP–labelled nuclei were imaged living cells and their dynamics analyzed in different mutants with different defective kinesin, dynein and myosin motor proteins. Using this experimental approach I was able, for the first time, to identify which motor proteins are involved in male nuclear transport through the trichogyne. I have also provided the first evidence for motor proteins encoded by both male and female partners contributing to this process.
3. To characterize a new type of hypha (the conidial sex tube) produced by conidia that I discovered. I have shown that the conidial sex tube is involved in sexual reproduction, and have provided morphological, physiological and genetic evidence that conidial sex tubes are different from conidial germ tubes or conidial anastomosis tubes.
4. To analyse the role of blue, green and red light, and different photoreceptors, in conidial sex tube formation. Important findings were (a) the first demonstration of a phytochrome-mediated response in *N. crassa*, and the second in filamentous fungi, (b) the first example of a cryptochrome mediated response in fungi, and (c) the first example of a green light response outside the animal kingdom.

References

Ahmad, M., Jarillo, J.A., Smirnova, O., Cashmore, A.R. 1998. The CRY1 blue light photoreceptor of *Arabidopsis* interacts with phytochrome A *in vitro*. *Mol. Cell* 1, 939-948.

Akins, R.A., Lambowitz, A.M. 1985. A general method for cloning *Neurospora crassa* nuclear genes by complementation of mutants. *Mol Cell. Biol.* 5, 2272-2278.

Backus, M.P. 1939. The mechanics of conidial fertilization in *Neurospora sitophila*. *Bull. Torrey Bot. Club* 66, 63-76.

Bahn, Y.S., Xue, C., Idnurm, A., Rutherford, J.C., Heitman, J., Cardenas, M.E. 2007. Sensing the environment: lessons from fungi. *Nature Rev. Microbiol.* 5, 57-69.

Balasubramanian, S., Sureshkumar, S., Agrawal, M., Michael, T.P., Wessinger, C., Maloof, J.N., Clark, R., Warthmann, N., Chory, J., Weigel, D. 2006. The PHYTOCHROME C photoreceptor gene mediates natural variation in flowering and growth responses of *Arabidopsis thaliana*. *Nature Genet.* 38, 711 – 715.

Beadle, G.W., Tatum, E.L. 1941. Genetic control of biochemical reactions in *Neurospora*. *Proc. Natl. Acad. Sci. U.S.A.* 27, 499-506.

Bell-Pedersen, D., Shinohara, M., Loros, J.J., Dunlap, J.C. 1996. Clock-controlled genes isolated from *Neurospora crassa* are late night- to morning-specific. *Proc. Natl. Acad. Sci. U.S.A.* 93, 13096-13101.

Bhoo, S.H., Davis, S.J., Walker, J., Karniol, B., Vierstra, R.D. 2001. Bacteriophytochromes are photochromic histidine kinases using a biliverdin chromophore. *Nature* 414, 776-779.

Bieszke, J.A., Braun, E.L., Bean, L.E., Kang, S., Natvig, D.O., Borkovich, K.A. 1999. The nop-1 gene of *Neurospora crassa* encodes a seven transmembrane helix retinal-binding protein homologous to archaeal rhodopsins. *Proc. Natl. Acad. Sci. U.S.A.* 96, 8034-8039.

Bistis, G.N. 1981. Chemotropic interactions between trichogyenes and conidia of opposite mating type in *Neurospora crassa*. *Mycologia* 73, 959-975.

Bistis, G.N., Perkins, D.D., Read, N.D. 2003. Cell types of *Neurospora crassa*. *Fungal Genet. Newsl.* 50, 17–19.

Blumenstein, A., Vienken, K., Tasler, R., Purschwitz, J., Veith, D., Frankenberg-Dinkel, N., Fischer, R. 2005. The *Aspergillus nidulans* phytochrome FphA represses sexual development in red light. *Curr. Biol.* 15, 1833-1838.

Bobrowicz, P., Pawlak, R., Correa, A., Bell-Pedersen, D., Ebbole, D.J. 2002. The *Neurospora crassa* pheromone precursor genes are regulated by the mating-type locus and the circadian clock. *Mol. Microbiol.* 45, 795-804.

Borkovich, K.A., Alex, L.A., Yarden, O., Freitag, M., Turner, G.E., Read, N.D., Seiler, S., Bell-Pedersen, D., Paietta, J., Plesofsky, N., Plamann, M., Goodrich-Tanrikulu, M.,

Schulte, U., Mannhaupt, G., Nargang, F.E., Radford, A., Selitrennikoff, C., Galagan, J.E., Dunlap, J.C., Loros, J.J., Catcheside, D., Inoue, H., Aramayo, R., Polymenis, M., Selker, E.U., Sachs, M.S., Marzluf, G.A., Paulsen, I., Davis, R., Ebbole, D.J., Zelter, A., Kalkman, E.R., O'Rourke, R., Bowring, F., Yeadon, J., Ishii, C., Suzuki, K., Sakai, W., Pratt, R. 2004. Lessons from the genome sequence of *Neurospora crassa*: Tracing the path from genomic blueprint to multicellular organism. *Microbiol. Mol. Biol. Rev*, 68, 1–108.

Bruno, K.S., Tinsley, J.H., Minke, P.F., Plamann, M. 1996. Genetic interactions among cytoplasmic dynein, dynactin, and nuclear distribution mutants of *Neurospora crassa*. *Proc. Natl. Acad. Sci. U.S.A.* 93, 4775–4780.

Carazo-Salas, R.E., Antony, C., Nurse, P. 2005. The kinesin Klp2 mediates polarization of interphase microtubules in fission yeast. *Science* 309, 297–300.

Cashmore, A.R., Jarillo, J.A., Wu, Y.J., Liu, D. 1999. Cryptochromes: blue light receptors for plants and animals. *Science* 284, 760-765.

Clack, T., Mathews, S., Sharrock, R.A. 1994. The phytochrome apoprotein family in Arabidoposis is encoded by five genes- the sequences and expression of PHYD and PHYE. *Plant Mol. Biol.* 25, 413-427.

Coppin, E., Debuchy, R., Arnaise, S., Picard, M. 1997. Mating types and sexual development in filamentous Ascomycetes. *Microbiol. Mol. Biol. Rev.* 61, 411–428.

Davis, R.H. 2000. *Neurospora*: contributions of a model organism. Oxford University Press, New York.

Davis, R.H., deSerres, F.J. 1970. Genetic and microbial research techniques for *Neurospora crassa*. *Methods Enzymol.* 17A, 79-143.

Davis, R.H., Perkins, D.D. 2002. *Neurospora*: a model of model microbes. *Nature Rev.* 3, 7-13.

Davis, S.J., Vener, A.V., Vierstra, R.D. 1999. Bacteriophytochromes: phytochrome-like photoreceptors from nonphotosynthetic eubacteria. *Science* 286, 2517–2520.

Denault, D.L., Loros, J.J., Dunlap, J.C. 2001. WC-2 mediates WC-1-FRQ interaction within the PAS protein-linked circadian feedback loop of *Neurospora*. *EMBO J.* 20, 109–117.

Devlin, P.F., Robson, P.R.H., Patel, S.R., Goosey, L., Sharrock, R.A., Whitelam, G.C. 1999. phytochrome D acts in the shade-avoidance syndrome in *Arabidopsis* by controlling elongation growth and flowering time. *Plant Physiol.* 119, 909–915.

Dogterom, M., Yurke, B. 1998. Microtubule dynamics and the positioning of microtubule organizing centers, *Phys. Rev. Lett.* 81, 485–488.

Dunlap, J.C. 1999. Molecular bases for circadian clocks. *Cell* 96, 271-290.

Dunlap, J.C. 2006. Proteins in the *Neurospora* circadian clockworks. *J. Biol. Chem.* 281, 28489-28493.

Elliott, C.G. 1994. Reproduction in fungi: Genetical and physiological aspects. Chapman &

Hall, London.

Fankhauser, C., Chory, J. 1997. Light control of plant development. *Ann. Rev. Cell Dev. Biol.* 13, 203-229.

Ferreira, A.V.B., Saupe, S., Glass, N.L. 1996. Transcriptional analysis of the *mtA* idiomorph of *Neurospora crassa* identifies two genes in addition to *mtA-1*. *Mol. Gen. Genet.* 250, 767-774.

Fischer, R. 1999. Nuclear movement in filamentous fungi. *FEMS Microbiol. Rev.* 23, 39-68.

Franklin, K.A., Davis, S.J., Stoddart, W.M., Vierstra, R.D., Whitelam, G.C. 2003. Mutant analyses define multiple roles for phytochrome C in *Arabidopsis* photomorphogenesis. *The Plant Cell*, 15, 1981–1989.

Franchi, L., Fulci, V., Macino, G. 2005. Protein kinase C modulates light responses in *Neurospora* by regulating the blue light photoreceptor WC-1. *Mol. Microbiol.* 56, 334-345.

Freitag, M.F., Hickey, P.C., Raju, N.B., Selker, E.U., Read, N.D. 2004. GFP as a tool to analyze the organization, dynamics and function of nuclei and microtubules in *Neurospora crassa. Fungal Genet. Biol.* 41, 897-910.

Froehlich, A.C., Liu, Y., Loros, J.J., Dunlap, J.C. 2002. White Collar-1, a circadian blue light photoreceptor, binding to *frequency* promoter. *Science* 297, 815-819.

Froehlich, A.C., Loros, J.J., Dunlap, J.C. 2003. Rhythmic binding of a WHITE COLLAR-containing complex to the frequency promoter is inhibited by FREQUENCY. *Proc. Natl. Acad. Sci. U.S.A.* 100, 5914–5919.

Froehlich, A.C., Noh, B., Vierstra, R.D., Loros, J., Dunlap, J.C. 2005. Genetic and molecular analysis of phytochromes from the filamentous fungus *Neurospora crassa*. *Eukaryot. Cell*, 4, 2140–2152.

Fuchs, F., Westermann, B. 2005. Role of Unc104/KIF1-related motor proteins in mitochondrial transport in *Neurospora crassa. Mol. Biol. Cell* 16, 153–161.

Furuya, M. 1993. Phytochromes-their molecular species, gene families, and functions, *Annu. Rev. Plant Physiol. Plant Mol. Biol.* 44, 617-645.

Galagan, J.E., Calvo, S.E., Borkovlch, K.A., Selker, E.U., Read, N.D., Jaffe, D., FitzHugh, W., Ma, L.-J., Smirnov, S., Purcell, S., Rehman, B., Elkins, T., Engels, R., Wang, S., Nielsen, C.B., Butler, J., Endrizzi, M., Qui, D., Ianakiev, P., Bell-Pedersen, D., Nelson, M.A., Werner-Washburne, M., Selitrennikoff, C.P., Kinsey, J.A., Braun, E.L., Zelter, A., Schulte,U., Kothe, G.O., Jedd, G., Mewes, W., Staben, C., Marcotte, E., Greenberg, D., Roy, A., Foley, K., Naylor, J., Stange-Thomann, N., Barrett, R., Gnerre, S., Kamal, M., Kamvysselis, M., Mauceli, E., Bielke, C., Rudd, S., Frishman, D., Krystofova, S., Rasmussen, C., Metzenberg, R.L., Perkins, D.D., Kroken, S., Cogoni, C., Macino, G., Catcheside, D., Li, W., Pratt, R.J., Osmani, S.A., DeSouza, C.P.C., Glass, L., Orbach, M.J., Berglund, J.A., Voelker, R., Yarden, O., Plamann, M., Seiler, S., Dunlap, J.,

Radford, A., Aramayo, R., Natvig, D.O., Alex, L.A., Mannhaupt, G., Ebbole, D.J., Freitag, M., Paulsen, I., Sachs, M.S., Lander, E.S., Nusbaum, C., Birren, B. 2003. The genome sequence of the filamentous fungus *Neurospora crassa*. *Nature* 422, 859-868.

Gill, S.R., Schroer, T.A., Szilak, I., Steuer, E.R., Sheetz, M.P. Cleveland, D.W. 1991. Dynactin, a conserved, ubiquitously expressed component of an activator of vesicle motility mediated by cytoplasmic dynein. *J. Cell Biol.* 115, 1639-1650.

Glass, N.L., Staben, C. 1990. Genetic control of mating in *Neurospora crassa*. *Semin. Dev. Biol.* 1, 177–184.

Glass, N.L., Kuldau, G.A. 1992. Mating type and vegetative incompatibility in filamentous ascomycetes. *Annu. Rev. Phytopathol.* 30, 201-24.

Glass, N.L., Nelson, M.A. 1994. Mating-type genes in mycelial ascomycetes. In The Mycota. Brambl, R., Marzluf, G.A. (eds.), Vol. I, pp. 295-306.

Glass, N.L., Jacobson, D.J., Shiu, P.K.T. 2000. The genetics of hyphal fusion and vegetative incompatibility in filamentous ascomycete fungi. *Annu. Rev. Genet.* 34, 165–86.

Glass, N.L., Kaneko, I. 2003. Fatal attraction: Nonself recognition and heterokaryon incompatibility in filamentous fungi. *Eukaryot. Cell* 2, 1-8.

Grummt, M., Pistor, S., Lottspeich, F., Schliwa, M. 1998. Cloning and functional expression of a 'fast' fungal kinesin. *FEBS lett.* 427, 79-84.

Gyula, P., Schäfer, E., Nagy, F. 2003. Light perception and signalling in higher plants. *Curr. Opin. Plant Biol.* 6, 446–452.

Hahn, J., Strauss, H.M., Landgraf, F.T., Gimenèz, H.F., Lochnit, G., Schmieder, P., Hughes, J. 2006. Probing protein–chromophore interactions in Cph1 phytochrome by mutagenesis. *FEBS J.* 273, 1415–1429.

Harding, R.W., Turner, R.V. 1981. Photoregulation of the carotenoid biosynthetic pathway in *albino* and *white collar* mutants of *Neurospora crassa*. *Plant Physiol.* 68: 745-749.

Harding, R.W., Melles, S. 1983. Genetic analysis of phototropism of *Neurospora crassa* perithecial beaks using white collar and albino mutants. *Plant Physiol.* 72, 996-1000.

Harris, S.D., Read, N.D., Roberson, R.W., Shaw, B, Seiler, S., Plamann, M., Momany, M. 2005. Polarisome meets Spitzenkörper: microscopy, genetics, and genomics converge. *Eukaryot. Cell* 4, 225-229.

Heintzen, C., Loros, J.J., Dunlap, J.C. 2001. The PAS protein VIVID defines a clock-associated feedback loop that represses light input, modulates gating and regulates clock resetting. *Cell* 104, 453–464.

Hennig, L., Stoddart, W.M., Dieterle, M., Whitelam, G.C., Schäfer, E. 2002 Phytochrome E controls light-induced germination of *Arabidopsis*. *Plant Physiol.*. 128, 194–200.

Hughes, J., Lamparter, T., Mittmann, F., Hartmann, E., Gärtner, W., Wilde, A., Börner, T. 1997. A prokaryotic phytochrome. *Nature* 386, 663.

Idnurm, A., Howlett, B.J. 2001. Characterization of an opsin gene from the ascomycete

Leptosphaeria maculans. *Genome* 44, 167-171.

Inoué, S., Salmon, E.D. 1995. Force generation by microtubule assembly/disassembly in mitosis and related movements. *Mol. Biol. Cell.* 6:1619–1640.

Jacobson, D.J., Powell, A.J., Dettman, J.R., Saenz, G.S., Barton, M.M., Hiltz, M.D., Dvorachek, W.H.Jr., Glass, N.L., Taylor, J.W., Natvig, D.O. 2004. *Neurospora* in temperate forests of western North America. *Mycologia* 96, 66–74.

Johnson, T.E. 1976. Analysis of pattern formation in *Neurospora* perithecial development using genetic mosaics. *Dev. Biol.* 54, 23-36.

Kallipolitou, A., Deluca, D., Majdic, U., Lakamper, S., Moroder, L., Schliwa, M., Woehike, G. 2001. Unusual properties of the fungal conventional kinesin neck domain from *Neurospora crassa*. *EMBO J.* 20, 6226-6235.

Karniol, B., Verstra, R.D. 2003. The pair of bacteriophytochromes from Agrobacterium tumefaciens are histidine kinases with opposing photobiological properties. *Proc. Natl. Acad. Sci. U.S.A.* 100, 2807-2812.

Kim, H., Metzenberg, R.L., Nelson, M.A. 2002. Multiple functions of *mfa-1*, a putative pheromone precursor gene of *Neurospora crassa*. *Eukaryot. Cell* 1, 987-999.

Kim, H., Nelson, M.A. 2005. Molecular and functional analyses of *poi-2*, a novel gene highly expressed in sexual and perithecial tissues of *Neurospora crassa*. *Eukaryot. Cell* 4, 900-910.

Lauter, F.R., Russo, V.E.A. 1991. Blue light induction of conidiation-specific genes in *Neurospora crassa*. *Nucleic Acids Res.* 19, 6883–6886.

Lenz, J.H., Schuchardt, I., Straube, A., Steinberg, G. 2006. A dynein loading zone for retrograde endosome motility at microtubule plus-ends. *EMBO J.* 25, 2275-2286.

Lewis, M.T., Feldman, J.F. 1996. Evolution of the frequency (frq) clock locus in ascomycete fungi. *Mol. Biol. Evol.* 13, 1233-1241.

Li, W.Z., Chinnappa, C.C. 2004. Isolation and characterization of PHYC gene from *Stellaria longipes*: differential expression regulated by different red/far-red light rations and photoperiods. *Planta* 220, 18-30.

Loros, J.J., Dunlap, J.C. 2001. Genetic and molecular analysis of circadian rhythms in *Neurospora*. *Annu. Rev. Physiol.* 63,757–794.

Maheshwari, R. 1999. Microconidia of *Neurospora crassa*. *Fungal Genet. Biol.* 26, 1-18.

Martinez-Garcia, J.F., Huq, E., Quail, P.H. 2000. Direct targeting of light signals to a promoter element-bound transcription factor. *Science* 288, 859–863.

McNelly-Ingle, C.A., Frost, L.C. 1965. The effect of temperature on the production of perithecia by *Neurospora crassa*. *J. Gen. Microbiol.* 39, 33-42.

Metzenberg, R.L., Glass, N.L. 1990. Mating type and mating strategies in *Neurospora*. *BioEssays* 12, 53-59.

Michán, S., Lledías, F., Hansberg, W. 2003. Asexual development is increased in

Neurospora crassa cat-3-null mutant strains. *Eukaryot. Cell* 2, 798–808

Minke, P.F., Lee, I.H., Plamann, M. 1999a. Microscopic analysis of *Neurospora ropy* mutants defective in nuclear distribution. *Fungal Genet. Biol.* 28, 55-67.

Minke, P.F., Lee, I.H., Tinsley, J.H., Bruno, K.S., Plamann, M. 1999b. *Neurospora crassa ro-10* and *ro-11* genes encode novel proteins required for nuclear distribution. *Mol. Microbiol.* 32, 1065-1076.

Miller, R.K., Heller, K.K., Frisèn, L., Wallack, D.L., Loayza, D., Gammie, A.E., Rose, M.D. 1998. The kinesin-related proteins, Kip2p and Kip3p, function differently in nuclear migration in yeast. *Mol. Biol. Cell* 9, 2051-2068.

Monte, E., Alonso, J.M., Ecker, J.R., Zhang, Y., Li, X., Young, J., Austin-Phillips, S., Quail, P.H. 2003. Isolation and characterization of phyC mutants in *Arabidopsis* reveals complex crosstalk between phytochrome signaling pathways. *Plant Cell* 15, 1962-1980.

Montgomery, B.L., Lagarias, J.C. 2002. Phytochrome ancestry: Sensors of bilins and light. *Trends Plant Sci.* 7, 357-66.

Mukerji, K.G., Verma, V., Gupta, R. 1983. Biology of sexual reproduction in some ascomycetes. *Phytomorphology* 33, 107-122.

Nelson, M.A., Metzenberg, R.L. 1992. Sexual development genes of *Neurospora crassa*. *Genetics* 132, 149-162.

Nelson, M.A. 1996. Mating systems in ascomycetes: a romp in the sac. *Trends Genet.* 12, 69-74.

Ni, M., Tepperman, J.M., Quail, P.H. 1999. Binding of phytochrome B to its nuclear signalling partner PIF3 is reversibly induced by light. *Nature* 400, 781–784

O'Shea, S.F., Chaure, P.T., Halsall, J.R., Olesnicky, N.S., Leibbrandt, A., Connerton, I.F., Casselton, L.A. 1998. A large pheromone and receptor gene complex determines multiple *B* mating-type specificities in *Coprinus cinereus*. *Genetics* 148, 1081–1090.

Oka, Y., Matsushita, T., Mochizuki, N., Suzuki, T., Tokutomi, S., Nagatani, A. 2004. Functional analysis of a 450–amino acid N-terminal fragment of phytochrome B in *Arabidopsis*. *Plant Cell* 16, 2104–2116.

Paschal, B.M., Vallee, R.B. 1987. Retrograde transport by the microtubule-associated protein MAP 1C. *Nature* 330, 181-183.

Perkins, D.D., Margolin, B.S., Selker, E.U. Haedo, S.D. 1997. Occurence of repeat induced point mutation in long segmental duplications of *Neurospora*. *Genetics*, 147, 125–136.

Plamann, M., Minke, P.F., Tinsley, J.H., Bruno, K.S. 1994. Cytoplasmic dynein and actin-related protein Arp1 are required for normal nuclear distribution in filamentous fungi. *J. Cell Biol.* 127, 139-149.

Pöggeler, S., Kück, U. 2000. Comparative analysis of the mating-type loci from *Neurospora crassa* and *Sordaria macrospora*: identification of novel transcribed ORFs. *Mol. Gen. Genet.* 263, 292-301.

Pöggeler, S., Kück, U. 2001. Identification of transcriptionally expressed pheromone receptor genes in filamentous ascomycetes. *Gene* 280, 9–17.

Prigozhina, N.L., Walker, R.A., Oakley, C.E., Oakley, B.R. 2001 γ-Tubulin and the C-terminal motor domain kinesin-like protein, KLPA, function in the establishment of spindle bipolarity in *Aspergillus nidulans*. *Mol. Biol. Cell* 12, 3161– 3174.

Purschwitz, J., Müller, S., Kastner, C., Fischer, R. 2006. Seeing the rainbow: light sensing in fungi. *Curr. Opin. Microbiol.* 9, 566–571.

Quail, P.H., Boylan, M.T., Parks, B.M., Short, T.W., Xu, Y., Wagner, D. 1995. Phytochromes: photosensory perception and signal transduction. *Science* 268, 675– 80.

Raju, N.B., Newmeyer, D. 1977. Giant ascospores and abnormal croziers in a mutant of *Neurospora crassa*. *Exp. Mycol.* 1, 152-165.

Read, N.D. 1983. A scanning electron microscopic study of the external features of perithecium development in *Sordaria humana*. *Can. J. Bot.* 61, 3217-3229.

Read, N.D. 1994. Cellular nature and multicellular morphogenesis in higher fungi, p. 251–269. *In* D. S. Ingram and A. Hudson (ed.), Shape and form in plants and fungi. Academic Press, Ltd., London, United Kingdom.

Read, N.D., Beckett, A. 1996. Ascus and ascospore morphogenesis. *Mycol. Res.* 100, 1281-1314.

Reinsch, S., Gonczy, P. 1998. Mechanisms of nuclear positioning. *J. Cell Sci.* 111, 2283–2295.

Riquelme, M., Reynaga-Peña, C.G., Gierz, G., Bartnicki-García, S. 1998. What determines growth direction in fungal hyphae? *Fungal Genet. Biol.* 24, 101-109.

Riquelme, M., Roberson, R.W., McDaniel, D.P., Bartnicki-García, S. 2002. The effects of ropy-1 mutation on cytoplasmic organization and intracellular motility in mature hyphae of *Neurospora crassa*. *Fungal Genet. Biol.* 37, 171–179.

Sargent, M.L. Briggs, W.R. 1967. The effects of light on a circadian rhythm of conidiation in *Neurospora*. *Plant Physiol.* 42, 1504-1510.

Saupe, S.J., Stenburg, L., Shiu, K.T., Griffiths, A.J., Glass, N.L. 1996. The molecular nature of mutations in the mt A-1 gene of the *Neurospora crassa* A idiomorph and their relation to mating-type function. *Mol. Gen. Genet.* 250, 115-12.

Saupe S.J., Glass, N.L. 1997. Allelic specificity at the *het-c* heterokaryon incompatibility locus of *Neurospora crassa* is determined by a highly variable domain. *Genetics* 146, 1299–1309.

Schneider-Poetsch, H.A.W. 1992. Signal transduction by phytochrome: phytochromes have a module related to the transmitter modules of bacterial sensor proteins. *Photochem. Photobiol.* 56, 839–846.

Schwerdtfeger, C., Linden, H. 2001. Blue light adaptation and desensitization of light signal transduction in *Neurospora crassa*. *Mol. Microbiol.* 39, 1080–1087.

Schwerdtfeger, C., Linden, H. 2003. VIVID is a flavoprotein and serves as a fungal blue light photoreceptor for photoadaptation. *EMBO J.* 22, 4846-4855.

Seiler, S., Plamann, M. 2003. The genetic basis of cellular morphogenesis in the filamentous fungus *Neurospora crassa Mol. Biol. Cell* 14, 4352–4364.

Seiler, S., Plamann, M., Schliwa, M. 1999. Kinesin and dynein mutants provide novel insights into the roles of vesicle traffic during cell morphogenesis in *Neurospora. Curr. Biol.* 9, 779-785.

Seale, T. 1973. Life cycle of *Neurospora crassa* viewed by scanning electron microscopy. *J. Bacterol.* 113, 1015-1025.

Sharma, R. 2001. Phytochrome: A serine kinase illuminates the nucleus! *Curr. Science* 80, 178-188.

Shiu, P.K.T., Glass, N.L. 2000. Cell and nuclear recognition mechanisms mediated by mating type in filamentous ascomycetes. *Curr. Opin. Microbiol.* 3, 183-188

Smith, H. 1999. Tripping the light fantastic. *Nature* 400, 710-713.

Somers, D.E., Sharrock, R.A., Tepperman, J.M., Quail, P.H. 1991. The *hy3* long hypocotyl mutant of *Arabidopsis* is deficient in phytochrome B. *Plant Cell* 3, 1263– 74.

Somers, D.E., Devlin, P.F., Kay, S.A. 1998. Phytochromes and cryptochromes in the entrainment of the *Arabidopsis* circadian clock. *Science* 282, 1488–90

Springer, M.L., Yanofsky, C. 1989. A morphological and genetic analysis of conidiophore development in *Neurospora crassa. Genes Devel.* 3, 559-571.

Springer, M.L. 1993. Genetic control of fungal differentiation: the three sporulation pathways of *Neurospora crassa. Bioessays* 15, 365–374.

Stanewsky, R., Kaneko, M., Emery, P., Beretta, B., Wager-Smith, K., Kay, S.A., Rosbash, M., Hall, J.C. 1998. The *cry*^{b} mutation identifies cryptochrome as a circadian photoreceptor in *Drosophila. Cell* 95, 681-692.

Stein, L.D., Bao, Z., Blasiar, D., Blumenthal, T., Brent, M.R., Chen, N., Chinwalla, A., Clarke, L., Clee, C., Coghlan, A., Coulson, A., D'Eustachio, P., Fitch, D.H.A., Fulton, L.A., Fulton, R.E., Griffiths-Jones, S., Harris, T.W., Hillier, L.W., Kamath, R., Kuwabara, P.E., Mardis, E.R., Marra, M.A., Miner, T.L., Minx, P., Mullikin, J.C., Plumb, R.W., Rogers, J., Schein, J.E., Sohrmann, M., Spieth, J., Stajich, J.E., Wei, C., Willey, D., Wilson, R.K., Durbin, R., Waterston, R.H. 2003. The genome sequence of *Caenorhabditis briggsae*: A platform for comparative genomics. *PLoS Biol.* 1, 166-192.

Steinberg, G. Schliwa, M. 1995. The Neurospora organelle motor: a distant relative of conventional kinesin with unconventional properties. *Mol. Biol. Cell* 6, 1605-1618.

Steinberg, G. 2006. Preparing the way: Fungal motors in microtubule organization. *Trends Microbiol.* 15, 14-21.

Steinberg, G. 2007. Hyphal Growth: a Tale of Motors, Lipids, and the Spitzenkörper. *Eukaryot Cell.* 6, 351–360.

Strauss, H.M., Hughes, J., Schmieder, P. 2005. Heteronuclear solution-state NMR studies of the chromophore in cyanobacterial phytochrome Cph1. *Biochemistry* 44, 8244–8250.

Tasler, R., Moises, T., Frankenberg-Dinkel, N. 2005. Biochemical and spectroscopic characterization of the bacterial phytochrome of *Pseudomonas aeruginosa*. *FEBS J.* 272, 1927-1936.

Thresher, R., Hotz Vitaterna, M., Miyamoto, Y., Kazantsev, A., Hsu, D., Petit, C., Selby, C., Dawut, L., Smithies, O., Takahashi, J., Sancar, A. 1998. Role of mouse cryptochrome bluelight photoreceptor in circadian responses. *Science* 282, 1490-1494.

Trinci, A.P.J. 1984. Regulation of hyphal branching and hyphal orientation, p. 23–52. *In* D. H. Jennings and A. D. M. Rayner (ed.), The ecology and physiology of the fungal mycelium. Cambridge University Press, Cambridge, United Kingdom.

Turian, G., Bianchi, D.E. 1972. Conidiation in *Neurospora*. *Bot. Rev.* 38, 119–154.

Vaillancourt, L.J., Raudaskoski, M., Specht, C.A., Raper, C.A. 1997 Multiple genes encoding pheromones and a pheromone receptor define the B ß1 mating-type specificity in *Schizophyllum commune*. *Genetics* 146: 541–551.

Vallee, R.B., Wall, J.S., Paschal, B.M., Shpetner, H.S. 1988. Microtubule-associated protein 1C from brain is a two-headed cytosolic dynein. *Nature* 332, 561-563.

Vierula, P.J., Mais, J.M. 1997. A gene required for nuclear migration in *Neurospora crassa* codes for a protein with cystein-rich, LIM/RING-like domains. *Mol. Microbiol.* 24, 331-340.

Viswanath-reddy, M., Turian, G. 1975. Physiological change during protoperithecial differentiation in *Neurospora tetrasperma*. *Physiol. Plant.* 35, 166-174.

Weber, I., Gruber, C., Steinberg, G. 2003. A class-V myosin required for mating, hyphal growth, and pathogenicity in the dimorphic plant pathogen *Ustilago maydis*. *Plant Cell*, 15, 2826-2842.

Wendland, J., Vaillancourt, L.J., Hengner, J., Lengeler, K.B., Laddison, K.J., Specht, C.A., Raper, C.A., Kothe, E. 1995. The mating-type locus B-alpha-1 of *Schizophyllum commune* contains a pheromone receptor gene and putative pheromone genes. *EMBO J.* 14: 5271–5278.

Wu, J., Glass, N.L. 2001. Identification of specificity determinants and generation of alleles with novel specificity at the *het-c* heterokaryon incompatibility locus of *Neurospora crassa*. *Mol. Cell Biol.* 21, 1045-1057.

Wu, S.H., Lagarias, J.C. 2000. Defining the bilin lyase domain: lessons from the extended phytochrome superfamily. *Biochemistry* 39, 13487-13495.

Yamamoto, A., Hiraoka, Y. 2003. Cytoplasmic dynein in fungi: insights from nuclear migration. *J. Cell Sci.* 116, 4501-4512.

Yang, H.-Q., Tang, R.-H., Cashmore, A.R. 2001. The signaling mechanism of *Arabidopsis* CRY1 involves direct interaction with COP1. *Plant Cell*, 13, 2573–2587.

Yang, Q., Poole, S.I., Borkovich, K.A. 2002. A G-protein subunit required for sexual and vegetative development and maintenance of normal G protein levels in *Neurospora crassa*. *Eukaryot. Cell* 1, 378–390.

CHAPTER 2

Materials and methods

2.1 Chemicals

Unless otherwise stated, chemicals were purchased from Sigma Chemical Company (Sigma-Aldrich Co. Ltd., Dorset, UK).

2.2 *Neurospora crassa* strains

Neurospora crassa strains, including wild type and knockout mutant strains used in this study are listed in Table 2.1-2.5. Unless otherwise indicated strains were obtained from the Fungal Genetics Stock Center (FGSC) (http://www.fgsc.net/). All knock out (KO) mutants were generated from the 74a (FGSC 4200) strains.

Table 2.1 *Neurospora crassa* wild type strains

Strain name*	FGSC strain #	Edinburgh strain #	Genotype**	Source
74a-ORS-6a (74*a*)	4200	12	wild type *mat a*	FGSC
74-OR23-1A (74*A*)	2489	13	wild type *mat A*	FGSC

*, Last letter of strain name refers to mating-type background

**, The wild-type strain of *N. crassa* used as the "reference" or "type" strain is the Oak Ridge-derived St. Lawrence strain 74-OR23-1A. 74 ORS-6a was the product of six recurrent backcrosses to 74-OR23-1VA (Kafer, 1982), beginning with ORSa. The ORSa strain was itself the product of seven recurrent backcrosses to 74-OR23-1A, beginning with 74 OR8-1a (Mylyk *et al.*, 1974). The only function of the prefix "74-" is to show that all of these OR strains are alike in having been derived from backcrosses to ST74A or its *mat A* descendents. It has therefore been deemed unnecessary and has often been omitted from numbers designating the OR wild-type strains (Perkins, 2003).

Table 2.2 Photoreceptor mutants

Strain name*	FGSC strain #	Edinburgh strain #	Genotype**	Source
Δ*wc-1a*	11711	61	*NCU02356::hyg mat a*	FGSC
Δ*wc-1A*	11712	62	*NCU02356::hyg mat A*	FGSC
Δ*phy-1a*	11235	63	*NCU04834::hyg mat a*	FGSC
Δ*phy-1A*	11236	64	*NCU04834::hyg mat A*	FGSC
Δ*phy-2a*	11240	65	*NCU05790::hyg mat a*	FGSC
Δ*phy-2A*	11241	66	*NCU05790::hyg mat A*	FGSC
Δ*orp-1a*	11552	67	*NCU01735::hyg mat a*	FGSC
Δ*orp-1A*	11553	68	*NCU01735::hyg mat A*	FGSC
frqa	2671	69	*frq;bd*† *mat a*	FGSC
frqA	2670	70	*frq;bd*† *mat A*	FGSC
Δ*cry-1a*	12981	71	*NCU00582::hyg mat a*	FGSC
Δ*cry-1A*	12982	72	*NCU00582::hyg mat A*	FGSC

*, Last letter of strain name refers to mating-type background.

**, All the strains in this table are derived from 74A or 74a wild type.

†, *band*, an allele enabling clear visualization of circadian regulated spore formation (conidial banding) (Sargent & Woodward, 1969).

Table 2.3 Sex pheromone and sex pheromone receptor mutants

Strain name*	Edinburgh strain #	Genotype**	Source
Δ*pre-1a*	73	*pre1::hyg mat a*	K. Borkovich, University of California, Riverside
Δ*pre-1A*	74	*pre1::hyg mat A*	K. Borkovich, University of California, Riverside
Δ*pre-2a*	75	*pre2::hyg mat a*	K. Borkovich, University of California, Riverside
Δ*pre-2A*	76	*pre2::hyg mat A*	K. Borkovich, University of California, Riverside
Δ*ccg-4a*	77	*ccg4::hyg mat a*	K. Borkovich, University of California, Riverside
Δ*ccg-4A*	78	*ccg4::hyg mat A*	K. Borkovich, University of California, Riverside
Δ*mfa-1a*	79	*mfa1::hyg mat a*	K. Borkovich, University of California, Riverside
Δ*mfa-1A*	80	*mfa1::hyg mat A*	K. Borkovich, University of California, Riverside

*, Last letter of strain name refers to mating-type background

**, All the strains in this table are derived from 74A or 74a wild type.

Table 2.4 Motor proteins and motor protein related mutants

Strain name*	FGSC strain #	Edinburgh strain #	Genotype†	Source
Δ*kip-2a*	11374	81	*NCU02626::hyg mat a*	FGSC
Δ*myo-5A***	11442	82	*NCU01440::hyg mat A*	FGSC
Δ*myo-2a***	11485	83	*NCU00551::hyg mat a*	FGSC
Δ*myo-1a***	11611	84	*NCU02111::hyg mat a*	FGSC
Δ*kin-2a*	11722	85	*NCU06733::hyg mat a*	FGSC
Δ*ro-11a*	11946	86	*NCU08566::hyg mat a*	FGSC
Δ*ro-11A*	11947	87	*NCU08566::hyg mat A*	FGSC
Δ*dyn-2a*	12006	88	*NCU02610::hyg mat a*	FGSC
Δ*dyn-2A*	12007	89	*NCU02610::hyg mat A*	FGSC
Δ*dlca*	12008	90	*NCU03882::hyg mat a*	FGSC
Δ*dlcA*	12009	91	*NCU03882::hyg mat A*	FGSC
Δ*dyn-27a*	12010	92	*NCU04043::hyg mat a*	FGSC
Δ*dyn-27A*	12011	93	*NCU04043::hyg mat A*	FGSC

Δ*dica*	12014	94	*NCU09142::hyg mat a*	FGSC
Δ*dicA*	12015	95	*NCU09142::hyg mat A*	FGSC
Δ*kar-3a*	12046	96	*NCU04581::hyg mat a*	FGSC

*, Last letter of strain name refers to mating-type background.

**, The number followed the name of myosin mutant is indicated as different classes of myosins, Δ*myo-1*, class I myosin, Δ*myo-2*, class II myosin, Δ*myo-5*, class V myosin.

†, All the strains in this table are derived from 74A or 74a wild type.

Table 2.5 Expressing fluorescence proteins strains

Strain name*	**Edinburgh strain #**	**Genotype****	**Source**
N2283*a*	1	*his-3+::pccg1-hH1+-sgfp mat a*	M. Freitag, Oregon State University
N2282*A*	97	*his-3+::pccg1-hH1+-sgfp mat A*	M. Freitag, Oregon State University
ro-1a (H1-GFP)	98	*his-3$^+$::pccg1-hH1+-sgfp; ro-1 mat a*	M. Freitag, Oregon State University
ro-2a (H1-GFP)	99	*his-3$^+$::pccg1-hH1+-sgfp; ro-2 mat a*	M. Freitag, Oregon State University
ro-3 (H1-GFP)	100	*his-3$^+$::pccg1-hH1+-sgfp; ro-3 mat a*	M. Freitag, Oregon State University
N2505*a*	7	*rid his3$^+$::Bml+gfp; mat a*	M. Freitag, Oregon State University
N2944*A*	103	*rid his3$^+$::rfp$^+$ mat A*	M. Freitag, Oregon State University
N2946*a*	104	*rid his3$^+$::rfp$^+$ mat a*	M. Freitag, Oregon State University
TMF619-1*A*	105	*his3$^+$::gfp$^+$ mat A*	M. Freitag, Oregon State University
TMF620-1*a*	106	*rid his3$^+$::gfp$^+$ mat a*	M. Freitag, Oregon State University

*, Last letter of strain name refers to mating-type background.

**, All the strains in this table are derived from 74A or 74a wild type.

2.3 Culture media

The culture media used were: Vogel's medium (Vogel, 1956), synthetic crossing medium (Westergaard & Mitchell, 1947) and water agar.

Solid Vogel's medium was prepared according to the recipe in Table 2.8. Liquid Vogel's medium followed the same recipe, excluding the agar. Vogel's medium was prepared from a 50 x stock solution (Table 2.6 and Table 2.7) that contained trace elements (Table 2.8) and biotin (Table 2.9).

Agar (Oxoid agar No. 3, www.oxoid.com) was used at an increased concentration of 2% (w/v) to produce a firmer gel, encouraging growth to be limited to one plane on the agar surface, which is more suitable for light microscopy. Agar media were prepared in 300 ml batches contained in 500 ml flasks, and sterilised by autoclaving for 15-30 min at 121 °C. They were then either allowed to set for storage, or when cooled to 50 °C poured into plastic Petri dishes (8.5 cm diam., Greiner Bio-One, www.greinerbioone.com) or made up as slants in plastic tubes (3 ml agar in 15 ml Greiner tubes, allowed to set at > 45°, Greiner Bio-One, www.greinerbioone.com) with plastic screw caps. If stored, the agar was melted by microwaving with the 650 W microwave set at medium power for 10-15 min, swirling every 3 min, then allowed to cool to 50 °C in a water bath before pouring.

When preparing the Vogel's agar medium, with hygromycin (Calbiochem, EMD Biosciences, Inc. La Jolla, CA), the Vogel's medium was cooled to 50 °C in a water bath and then the hygromycin was added into the medium at a final concentration 150 µg/ml and poured into plastic Petri dishes immediately. The agar plates were left in the biological safety cabinet (Heraeus Instruments Ltd., Germany) to cool and become solid for 30 min before storing them in the refrigerator at 4 °C.

Once poured, plates and tubes were normally stored in the dark, at room temperature to prevent condensation, and used within 1 month. Liquid media (for microscopy purposes and dilution of dyes or inhibitors) were prepared in 100 ml batches using the same recipes,

but excluding the agar, and stored in 10 ml aliquots in plastic tubes (15 ml Greiner tubes) in the refrigerator at 4 °C. The liquid media were allowed to warm to room temperature before use.

Synthetic crossing medium was prepared from a 2x stock solution. The unautoclaved stock (Tables 2.10 and 2.11) was stored 4 °C with 2 ml/l chloroform as a preservative. Sucrose (2%) and agar (2%) were added before autoclaving. There was normally some cloudiness from precipitation after autoclaving. Water agar medium (Table 2.12) was made up with distilled water.

Table 2.6 Vogel's sucrose minimal medium.

Component	Quantity
*Vogels 50× stock solution	20 ml
Sucrose	20 g
Agar	20 g
dH_2O	1 l

*see Table 2.7

Table 2.7 Composition of Vogel's 50x stock solution (stored at 4 °C).

Component	Quantity per litre dH_2O
$Na_3Citrate•2H_2O$	126.7 g
KH_2PO_4	250.0 g
NH_4NO_3	100.0 g
$MgSO_4•7H_2O$	10.0 g
$CaCl_2•2H_2O$	5.0 g
Trace elements solution*	5 ml stock
Biotin solution**	5 ml stock
Chloroform	2-3 ml

*see Table 2.8, **see Table 2.9

Table 2.8 Composition of Vogel's trace elements stock solution (stored at 4 °C).

Component	Quantity per litre dH_2O
Citric acid•$1H_2O$	5 g
$ZnSO_4•7H_2O$	5 g

$Fe(NH_4)_2SO_4 \cdot 7H_20$	1 g
$CuSO_4 \cdot 5H_2O$	0.25 g
$MnSO_4 \cdot 1H_2O$*	0.05 g
H_2BO_4	0.05 g
$Na_2MoO_4 \cdot 2H_20$	0.05 g

Table 2.9 Composition of biotin stock solution for Vogel's (stored at 4 °C).

Component	**Content per litre of 50 % ethanol**
d-biotin	50 mg

Table 2.10 Synthetic crossing (SC) medium

Component	Quantity
$KNO_3(NaNO_3)$	1.0 g
KH_2PO_4	1.0 g
$MgSO4 \cdot 7H_2O$	1.0 g
NaCl	0.1 g
$CaCl_2$	0.1 g
d-biotin	0.5 mg
Trace element solution*	see Table 2.13
Sucrose	20 g
Agar	20 g
dH_2O	1 l

Table 2.11 Composition of SC trace elements stock solution (stored at 4 °C)

Component	**Quantity per litre dH_2O**
H_2BO_4	0.01 mg
$CuSO_4 \cdot 5H_2O$	0.1 mg
$Fe(NH_4)_2SO_4 \cdot 7H_20$	0.2 mg
$Na_2MoO_4 \cdot 2H_20$	0.02 mg
$ZnSO_4 \cdot 7H_2O$	2.0 mg

Table 2.12 Water agar

Component	Quantity
Agar	20 g
dH_2O	1 l

2.4 Culture conditions

Neurospora crassa strains were inoculated onto SC medium and water agar plates (section 2.3), and grown at: (1) 24 °C under continuous light to induce protoperithecia, or (2) 35 °C in the dark on Vogel's medium (section 2.3) for 2 days then moved to continuous light at 25 °C, for conidial production. For culturing the knockout mutant stains, the Vogel's medium with hygromycin (at a final concentration of 150 μg/ml) was used to maintain the knockout (KO) genotype. The plates were sealed with Parafilm (www.parafilm.com) before being placed in the incubator. To enable faster or healthy growth for producing protoperithecia, Parafilm was replaced with Micropore tape (3M, www.3m.com), enabling better aeration, and for containment the plate was placed within a larger plastic Petri dish (14 cm diam., Nunc, www.nuncbrand.com).

2.5 *Neurospora crassa* storage

Agar slants were inoculated and allowed to grow at 25 °C for 7 days in continuous light by which time significant conidiation had occurred. These slants were then refrigerated at 4 °C and used for up to 4 weeks. Additionally similar slants were frozen at -20 °C as a backup for several years. To recover the cultures an inoculating loop was used to remove spores and transfer them into liquid media or onto slants.

For long term storage, slants consisted of 2 ml solid Vogel's medium. If KO mutants were being stored, the Vogel's medium was prepared with hygromycin (150 μg/ml)) in a sterile 75 x 12 mm glass tubes (Disposable culture tubes, borosilicate glass, Thermo Fisher

Scientific Inc., USA www.fishersci.com) and sealed with a cotton wool bung (Robinson Healthcare Ltd., Chesterfield, UK) and metal cap. Flasks were inoculated and grown for 2 days at 35 °C in the dark and then for 5 days at room temperature in natural light until maximum conidiation had occurred. The slants were sealed with Parafilm and stored at -20 °C.

2.6 Genomic analyses

2.6.1 BLAST search analysis

BLAST searches (Altschul *et al.*, 1990; 1997) were used to identify homologues of known proteins in sequenced genome of assigned genes and corresponding putative proteins.

BLAST searches were performed in the following order:

1. Proteins involved in nuclear or organelle movement and position, and photoreceptors were identified in *Aspergillus nidulans, S. cerevisiae* and *Ustilago maydis* by a literature search.
2. The sequences of the proteins identified were obtained from the NCBI website (http://www.ncbi.nlm.nih.gov/) or Broad Institute (predicted protein sequences) website (http://www.broad.mit.edu/).
3. With these sequences, a BLAST search for proteins (pBLAST, default settings, Blosum62 matrix) was performed on sequenced filamentous fungal genomes (http://www.genome.wi.mit.edu/annotation/fungi/). The hypothetical proteins found were blasted against the NCBI and *A. thaliana* (http://www.ncbi.nlm.nih.gov/BLAST/Genome/ara.html) genome databases for both *N. crassa* and *Magnaporthe oryzae*.

2.6.2 Conserved domain analysis

Conserved domain searches were carried out using RPSBLAST (http://www.ncbi.nlm.nih.gov/Structure/) to further strengthen evidence for protein function (Marchler-Bauer & Bryant, 2004). Databases were searched with the following reach tools: CDD (v2.02), COG (v1.00), Pfam (v11.0) and Smart (v4.0).

2.6.3 Multiple alignments

Clustal W alignments (Higgins *et al.,* 1994) of budding yeast proteins and the *N. crassa* putative homologues were performed with BioEdit (Hall, 1999).

2.6.4 Phylogenetic analyses

DNA sequences were aligned using the multiple alignment program CLUSTAL W (Higgins *et al.,* 1994). Neighbour-joining (NJ) trees (Saitou & Nei, 1987) based on phytochrome genes were constructed with Kimura's (Kimura, 1980) two-parameter distance using the program PAUP*, version 4.0b10 (Swofford, 2002). Heuristic tree searches were executed utilizing the tree-bisection-reconnection (TBR) branch-swapping algorithm with random sequence analysis. The bootstrap values were obtained from 1000 replications of NJ analyses.

2.7 Live-cell imaging and sample preparation

For experiments requiring the *N. crassa* trichogyne assay (section 2.7.7) or conidial sex tube induction (section 2.9), a female culture was grown on SC agar medium (section 2.3) at 25 °C under continuous light for 7 days. 10 ml of distilled water was then added to the female culture and repeatedly several times of sucked-up and flushed out gently by pipette. This water (mainly containing conidia of the female culture) was discarded. This process of adding and discarding 5 ml of distilled water was repeated three times. After this

procedure almost 95 % of the conidia from the female culture were removed. The inverted agar block method was employed for microscopic imaging (section 2.7.1).

2.7.1 Inverted agar block method

The inverted agar block culture method (Hickey *et al.*, 2005; Fig 2.1). Using a sterile scalpel, a block of agar measuring ~ 2 cm x 2 cm was excised from a female culture bearing protoperithecia. The agar block was then inverted and transferred onto a droplet of water containing conidia (1 x 10^6 per ml) of opposite mating type on a large (48 x 64 mm # 1.5, R.A. Lamb, www.ralamb.co.uk) cleaned glass cover slip cleaned up by 70% ethanol (Fig. 2.1). The sample was placed on the microscope stage and allowed more than 30 min to recover and resume normal growth. When examining a sample over extended time periods, drying could be a problem. To prevent this, the base of a plastic Petri dish, with a hole cut through the centre so as not to perturb sample illumination, and containing a damp piece of filter paper, was placed over the sample on the microscope stage. From time to time the liquid media was also refreshed from the side using a pipette.

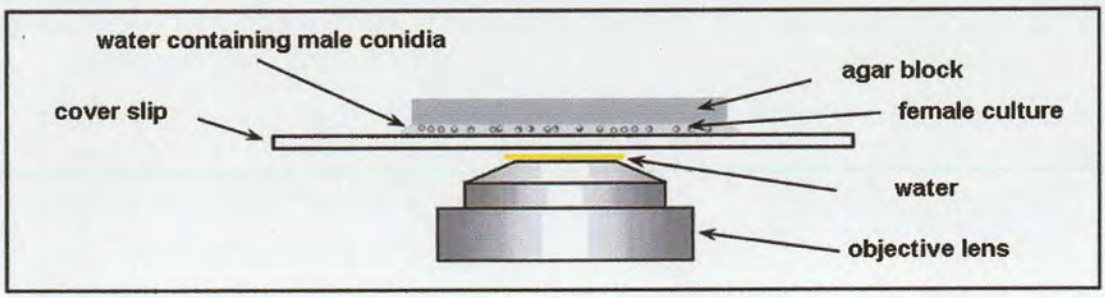

Figure 2.1 Inverted agar block culture method (adapted from Hickey *et al.*, 2005).

2.7.2. Liquid culture

Liquid culture techniques were used for experiments in which conidial sex tubes (CSTs) were induced with synthetic sex pheromone in water (section 2.9.2). A 1 x 10^5

conidia ml^{-1} suspension was prepared (section 2.4) and 300 µl droplets of the conidial suspension were placed into eight well slide culture chambers (Nalge Nunc International, www.nalgenunc.com). Serial dilutions of the sex pheromones (from 51.2 µg/ml to 25 ng/ml) were applied to the eight well slide culture chambers.

2.7.3 FM4-64 staining

Sample preparation and microscopic analysis after FM4-64 staining was performed as described in Hickey *et al.* (2002) except that FM4-64 was added to samples after they had been monitored on the microscope stage. FM4-64 (16 mM stock concentration; 10 µM working concentration) was diluted in liquid synthetic crossing medium (section 2.3) or water.

The procedure for preparing the FM4-64 solution was as follows:

1. Remove vial of FM4-64 from freezer and allow thawing (keep from exposure to light by wrapping in foil).
2. Add 10 µl of DMSO and ensure all the FM4-64 is dissolved, taking special care to ensure there is no dye on the sides of the vial.
3. Divide the contents of a fresh bottle into 1 ml aliquots in sterile tubes. Close the tubes tightly and store at -20 °C. Use each aliquot only once and then discard.
4. Prepare five Eppendorf tubes with 400 µl of H_2O.
5. Into each Eppendorf tube add 2 µl of the dye/DMSO and shake on whirlimixer (Fisher Scientific, Loughborough, UK) for 5 sec.
6. Wrap in foil and refrigerate as stock.

2.7.4. Sample preparation for cytoskeletal inhibitor studies

Two cytoskeletal inhibitors were made up as stock solutions in DMSO and working concentrations were prepared (Table 2.15) after dilution in SC medium or water (section

2.3). Benomyl and Latrunculin B were first dissolved in DMSO (see section 2.7.3). The inhibitors were applied 12 h after adding the opposite mating-type male conidia to a 5 days old female culture. Thirty min after applying the inhibitors, the nuclear behaviour in the conidia and trichogynes was recorded. Perithecial formation was assayed 2 days after adding the inhibitors to 5 days old female cultures.

Table 2.13 Inhibitors used for live-cell imaging

Compound type of chemical	Stock concentration	Working concentration	Target
benomyl	50 mg/ml	10 µg/ml	Microtubule
Latrunculin B	10 mM	20 µM	actin

2.7.5. Confocal laser scanning microscopy

Confocal laser scanning microscopy was performed using a BioRad Radiance 2100 system, mounted on a Nikon TE2000U Eclipse inverted microscope using a 60 x (1.2 NA) water immersion plan apochromat objective (Nikon, Kingston-upon-Thames, UK). Images of GFP and FM4-64 labelling were captured simultaneously for both GFP and FM4-64, using 488 nm excitation with an argon laser. Fluorescence emission was collected between 500 and 520 nm for GFP and FITC and above 620 nm for FM4-64. Samples were imaged using a plan apo 60 x water immersion (NA 1.2) objective. A laser power of 10% with a scan speed of 166 lines per sec was used.

Confocal images were captured with Lasersharp 2000 software (v. 5.1; BioRad Microscience). Image analysis and editing was done with Image J (v. 1.34) and Paintshop Pro software (v. 7; Jasc, Inc.).

2.7.6. Wide-field fluorescence microscopy

Wide-field fluorescence microscopy was performed using a Nikon TE2000, with a TILL monochromator light source (TILL Photonics GmbH, Munich, Germany). Wide-field microscopy images were captured using a Hamamatsu Orca camera (Hamamatsu Photonics UK Ltd., Welwyn Garden City, Hertfordshire, UK) driven by Simple PCI software (Compix Inc., Imaging Systems, Sewickley, USA) and further analysed with Image J (vers. 1.34).

2.7.7. Trichogyne homing assay

Chemotropic interactions between trichogynes and conidia of opposite mating type were analysed using the following procedures:

1. *Neurospora crassa* strains were inoculated onto SC medium (section 2.3) and grown at 25 °C under continuous light for 7 days.
2. 10 ml of distilled water was added to a 7 day old female culture and sucked up and ejected from a pipette three times and finally sucked up, to remove as many as possible conidia as possible from the culture surface.
3. Conidia of opposite mating type (used as male fertilizing agents) were collected from 4- to 5-day-old cultures on Vogel's agar medium and suspended in distilled water using the same technique as used to remove conidia from the female culture (see [2] above). The conidial suspension, which also contained hyphal fragments, was filtered through miracloth (Calbiochem).
4. In all experiments, unless stated otherwise, conidia were used at a concentration of 1 x 10^5 per ml. The conidial concentration was adjusted using a haemocytometer (Neubauer Improved 0.0625 mm^2, Superior – Marienfeld, Germany).
5. The inverted agar block culture method was used (see section 2.7.1) for the trichogyne assay. Trichogyne orientation and growth were monitored and photographed using bright field or differential interference contrast optics with a 60 x (N. A. 1.2) water

immersion plan apo objective on an inverted TE2000E microscope (Nikon, Kingston-Upon-Thames, United Kingdom). Observations were made 10-15 h after application of macroconidia (see section 2.7.6). For monitoring the nuclear behaviour during trichogyne-conidium interactions, the H1-GFP nuclear labelled strains (Table 2.7) were used and imaged by confocal microscopy with a 60 x (N. A. 1.2) water immersion plan apo objective on an inverted TE2000U microscope (Nikon, Kingston-Upon-Thames, United Kingdom) (see section 2.7.5). Again observations were made 10-15 h after application of macroconidia.

2.8 Low-temperature electron microscopy (Read & Jeffree, 1991)

Conidia were incubated at 24 °C on sterile sheets uncoated cellophane overlying solid water agar medium (section 2.3) for 7 days to form protoperithecia. 8 h after adding 1 x 10^5 conidia per ml of opposite mating type incubated at 24 °C, the cellophane was cut into 5-15 mm rectangles and attached to the surface of a cryospecimen carrier (Gatan, Oxford, United Kingdom) with a film of Tissue-Tek OCT compound (Sakura Finetek, Torrance, Calif.) as an adhesive. Cryofixation was performed by plunging the sample mounted onto the specimen carrier into subcooled liquid nitrogen. The specimen carrier was then transferred under low vacuum to the cold stage of a 4700II field emission scanning electron microscope (Hitachi, Wokingham, United Kingdom). The microscope cold stage was warmed to -80 °C whilst under continuous visual observation until ice contamination on the sample surface had been removed by sublimation. The specimen was subsequently cooled to below -119 °C, returned to the specimen stage of the Gatan Alto 2400 cryopreparation system at ~ -180 °C, and coated with ~10 nm of 60:40 gold-palladium alloy (Testbourne Ltd., Basingstoke, United Kingdom) in an argon gas atmosphere. The coated specimen was finally examined in the SEM at ~ -160 °C with a beam accelerating voltage of 2 kV, a beam current of 10 μA, and working distances of 12 to 15 mm. Digital images were captured at a resolution of

2,560 by 1,919 pixels using the lower secondary electron detector.

2.9 Experiments on conidial sex tubes

Two different origins, light-born and dark-born, of conidia were collected. Light-born conidia were collected from the culture which grown at 25 °C for 7 days in continuous light on Vogel's medium plates. Dark-born conidia used for these experiments were prepared from dark grown cultures. *N. crassa* was inoculated on to Vogel's medium plates and the plates were covered with aluminum foil and incubated in 35 °C for 7 days. Conidial production was very poor without light and the cultures were white in colour because they lacked carotenoids.

2.9.1 Preparation of conidia for conidial sex tube induction and live-cell imaging

Conidial sex tubes (CSTs) were induced by either (1) adding macroconidia to a protoperithecial culture of opposite mating type (method 1 below) or (2) germinating isolated macroconidia in the presence of the appropriate concentration of the synthetic CCG-4 (Bobrowicz *et al.,* 2002) or the truncated synthetic MFa-1 pheromone (Kim *et al.,* 2002) (method 2 below).

Method 1 (Fig. 2.2)

1. *Neurospora crassa* strains were inoculated onto SC medium (section 2.3) and grown at 25 °C under continuous light for 7 days. 10 ml of distilled water was added to the 7 day old female culture and sucked up and ejected from a pipette three times, and finally sucked up, to remove as many conidia as possible from the culture surface. A 2 x 2 cm of agar block bearing protoperithecia was cut out of the culture. Conidia from the opposite mating type (used as male fertilizing agent) were collected from 4- to 5-day-old cultures on Vogel's agar medium and suspended in distilled water.

2. For imaging unstained specimens and for quantifying of CSTs, 100-µl drops of conidial suspensions (mostly comprising of macroconidia) were added to 900 µl distilled water and placed on a 48 x 64 mm coverglass (No. 1.5, Raymond A Lamb, Ltd.).
3. The inverted agar block method of preparation (Hickey *et al.*, 2005) (Fig 2.1) was used for imaging. A 30 x 30 mm agar block bearing protoperithecia was placed over the droplet of conidial suspension. Wheat germ agglutinin (WGA) (50 µM) or Pokeweed lectin-FITC (5 µg/ml) dyes were added to the sample for 20 min.
4. For high resolution imaging, the stained samples were examined at room temperature by confocal microscopy with a 60 x (N.A. 1.2) water immersion plan apo objective using blue excitation (section 2.7.5). For CST quantitation, wide-field fluorescence microscopy (section 2.7.6) was used. If for quantitation the nuclear number in CSTs then followed the next two steps
5. The CSTs were collected 8 h after application of the macroconidia by using a scalpel to cut a square hole (5 x 5 mm) in the centre of the agar and employing a 200-µl pipette to suck up the liquid medium containing CSTs.
6. Confocal laser scanning microscopy (section 2.7.5) was used to image the nuclear labelled strain which was expressing H1-GFP. The number of H1-GFP fluorescing nuclei in CSTs was quantified.

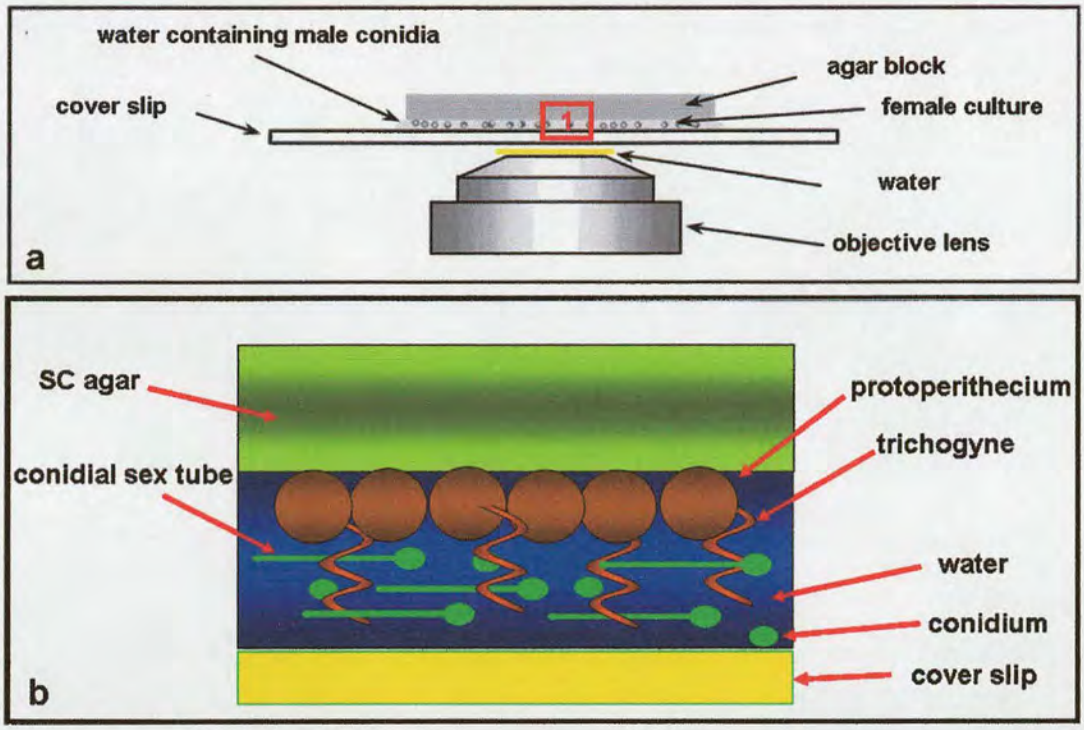

Figure 2.2 The set up for conidial sex tube experimentation on the microscope stage. An enlargement of shown in (a) to show more the detail of CST experiment set up. The inverted agar block cultural method (Hickey *et al.*, 2005; Fig. 2.1).

Method 2 (Fig. 2.3)

1. A 1 x 10^5 ml^{-1} conidial suspension in water was prepared and 300 µl droplets of this suspension were placed into eight well slide culture chambers (Nalge Nunc International, www.nalgenunc.com) (also see section 2.7.2).
2. A serial dilution of synthetic sex pheromone (section 2.7.2) from 51.2 µg/ml to 25 ng/ml was prepared and added to each well in the eight well slide culture chambers.
3. Samples were incubated at 25 °C in continuous light for 8 h.
4. Wheat germ agglutinin (WGA) (50 µM) was added to the sample for 20 min and then examined at room temperature
5. Wide-field fluorescence microscopy (section 2.7.6) was used to take images of CSTs to determine the percentage CST formation.
6. Confocal laser scanning microscopy (section 2.7.5) was used to image the nuclear labelled strain which was expressing H1-GFP. The number of nuclei in the CSTs was

quantified.

7. The software SigmaPlot (v. 10.0, Systat Software, Inc., London, UK) was used for analysis of CST quantification data.

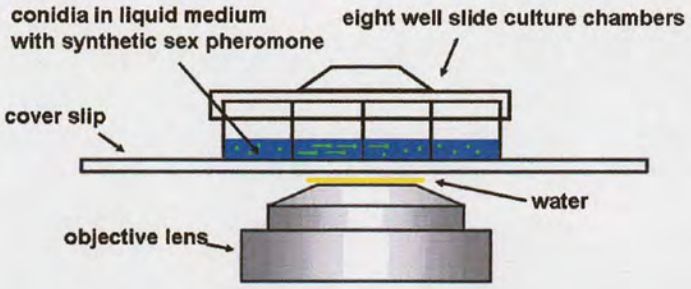

Figure 2.3 The set up for conidial sex tube experimentation on the microscope stage using eight well slide culture chambers.

2.9.2 Synthetic sex pheromone MFa-1 and CCG-4

The *N. crassa* sex pheromones (Table 2.16) were synthesized by Sigma-Genosys (Sigma-Genosys Co. Ltd., Dorset, England). They were frozen as 200 µg/ml (with PBS) and aliquots stored at -20 °C.

Table 2.14 Synthesized sex pheromone of *N. crassa*

Name	Protein sequence	Description
MFa-1	MPSTAASTKVPQT TMNFNGYCVVM	MFa-1 is the sex pheromone from the *mat a* wild type strain with the CAAX motif (in red). C is cysteine, A is aliphatic, and X is one of many residues.
MFa-1D	MPSTAASTKVPQT TMNFNGY	MFa-1D is MFa-1 without the COOH-terminal CAAX motif. In *S. cerevisiae,* biogenesis of the equivalent Mfa-1 precursor proceeds via a distinctive multistep pathway that involves COOH-terminal modification, NH2-terminal proteolysis, and a nonclassical export mechanism. Many steps of a-factor biogenesis occur in association with membranes.
CCG-4	QWCRIHGQSCW	CCG-4 is the sex pheromone from the *mat A* wild type strain

2.9.3 Photobiology experiments

For the photobiology experiments, specialized temperature-controlled (Snijders Scientific B.V. Ltd., The Netherlands) cabinets containing different LED light arrays were used. The LED light sources and interference filters used in this study are listed in Table 2.17.

Table 2.15 LED light sources and interference filters used for photobiology experiments

filter	wave length	photon fluence rate*	type of light
FarRed	757 nm ± 20nm.	30.0 μM m^2 s^{-1}	LED
Red	660 nm ± 10 nm	5.0 μM m^2 s^{-1}	LED
Green	530 nm ± 10 nm	4.5 μM m^2 s^{-1}	interference filter
Blue	480 nm ± 10 nm	6.0 μM m^2 s^{-1}	interference filter

*fluence rates were measured with a radiometer (Q201 PAR Radiometer, Macam photometrics Ltd., Scotland)

A second method used interference filters to provide light of different wavelengths (Table 2.17). The experimental set up is shown in Fig 2.4. For experiments using isolated macroconidia that were treated with synthetic sex pheromone (section 2.9.2) to induce CSTs, the macroconidia were harvested from culture grown in complete darkness. They were then prepared for protoperithecial experiments in a dark room using night goggles (CAMO Surveillance Equipment, Ireland) which operate with a 800 nm infrared light source.

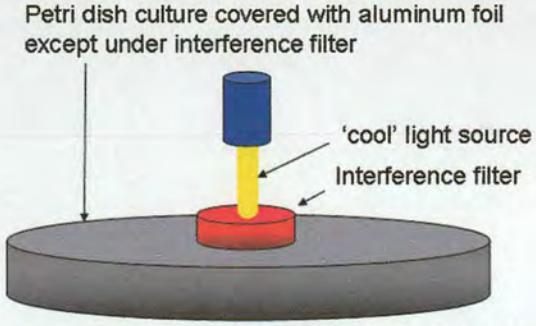

Fig 2.4 Photobiological assay set up. The "cool" light source was from a fibre-optic light source (Flexilux 150HL Universal, Micro Instruments (Oxford) Ltd, UK) fitted with a 150 W bulb giving a light output of ~350 μmol m^{-2} sec^{-2} photosynthetically active radiation.

2.9.4 Imaging conidial sex tube phototropisms

For imaging CST phototropisms, 1 ml droplets of conidial suspensions at a concentration 1 x 10^5 ml^{-1} were placed on a 48 x 64 mm cover slip. A 30 x 30 mm block of water agar bearing protoperithecia was placed over the conidial suspension and the whole set up placed in a small dark box with a small hole (Fig 2.5). The sample was exposed to lateral light provided by a Universal Flexilux 150 HL light source, which was transmitted through a hole in the side of small dark box. Samples were irradiated in this way for 16 h then examined at room temperature using brightfield or differential interference contrast optics with a 20 x objective on an inverted TE1900E microscope (Nikon, Kingston-Upon-Thames, United Kingdom).

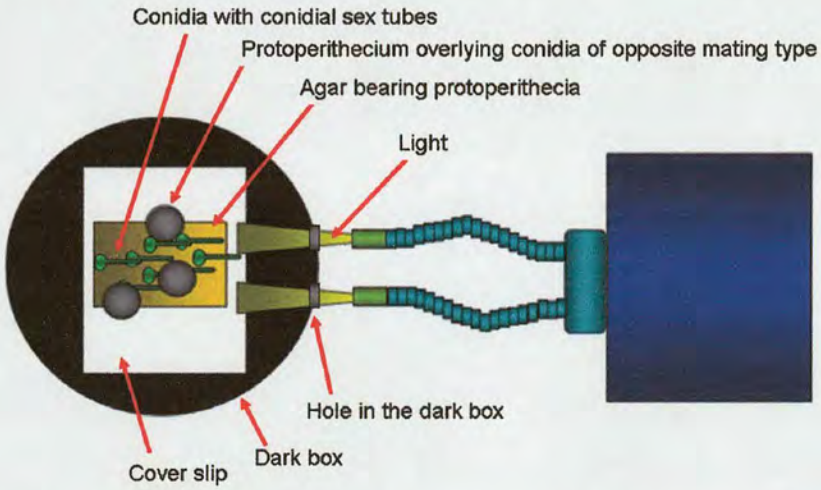

Figure 2.5 The experimental set up to induce conidial sex tube phototropisms. The dark box is a Petri dish daubed with black ink (BEROL, UK) and covered with black paper then covered aluminum foil outside. Not to scale.

2.10 Digital image processing and animations

Confocal images were captured using Lasersharp software (v. 5.2 and v. 6.0; Bio-Rad, now Zeiss, www.zeiss.co.uk), and were initially viewed using Image J (v. 1.34) before further processing.

Widefield microscopy images were captured using a Hamamatsu Orca camera (Hamamatsu Photonics UK Ltd., Welwyn Garden City, Hertfordshire, UK) driven by

Simple PCI software (Compix Inc., Imaging Systems, Sewickley, USA).

The number of perithecia produced in a plate culture was determined by capturing an image of the culture using Nikon digital camera coolpix 950 (Nikon, Edinburgh, Scotland) and quantifying the number of 'particles' (i.e. perithecia) using analyze particles function under analyze tool in imageJ (freeware; http://rsb.info.nih.gov/ij/)

Further processing was carried out with Paintshop Pro (v. 7 and v. 8; JASC Software, now Corel, www.corel.com), ImageJ and SimplePCI (Compix Inc. Imaging Systems, www.cimaging.net). Time-courses of images were edited and built up into animation movies (.avi and .mpg files) using Animation Shop (v. 3; JASC Software, now Corel, www.corel.com), Photoshop (v. 7.0 Adobe, www.adobe.com) and ImageJ (freeware; http://rsb.info.nih.gov/ij/). ImageJ was used to quantify protoperithecial and perithecial number in plate cultures by detecting the protoperithecia and perithecia as dark spots in the images captured. To quantify the protoperithecial number in the plate cultures, the conidia needed to be removed from the culture surface by the method described in section 2.9.1, method 1 and the captured images needed to be contrast enhanced to enhance the dark protoperithecial spots using Photoshop (Adobe Systems Incorporated, London, UK)

References

Altschul, S.F., Gish, W., Miller, W., Myers, E.W., Lipman, D.J. 1990. Basic local alignment search tool. *J. Mol. Biol.* 215, 403-410.

Altschul, S.F., Madden, T.L., Schaffer, A.A., Zhang, J., Zhang, Z., Miller, W., Lipman, D.J. 1997. Gapped BLAST and PSI-BLAST: a new generation of protein database search programs. *Nucleic Acids Res.* 25, 3389-3402.

Bobrowicz, P., Pawlak, R., Correa, A., Bell-Pedersen, D., Ebbole, D.J. 2002. The *Neurospora crassa* pheromone precursor genes are regulated by the mating-type locus and the circadian clock. *Mol. Microbiol.* 45, 795-804.

Hall, T.A. 1999. BioEdit: a user-friendly biological sequence alignment editor and analysis program for Windows 95/98/NT. *Nucl. Acids Symp. Ser.* 41, 95–98.

Higgins D.; Thompson J.; Gibson T.; Thompson J.D.; Higgins D.G.; Gibson T.J. 1994. CLUSTAL W: Improving the sensitivity of progressive multiple sequence alignment through sequence weighting, position-specific gap penalties and weight matrix choice. *Nucleic Acids Res. 22*, 4673-4680.

Hickey, P.C., Jacobson, D.J., Read, N.D., Glass, N.L. 2002. Imaging hyphal fusion in *Neurospora crassa. Fungal Genet. Biol.* 37, 109-119.

Hickey, P.C., Swift, S.M., Roca, M.G., Read, N.D. 2005. Live-cell imaging of filamentous fungi using vital fluorescent dyes. In *Methods in Microbiology. Vol. 34. Microbial Imaging* (ed. By T. Savidge C. Pothoulakis), pp. 63-87. Elsevier: Amsterdam.

Kafer, E. 1982. Backcrossed mutant strains which produce consistent map distances and negligible interference. *Neurospora Newslett.* 29, 41-44.

Kim, H., Metzenberg, R.L., Nelson, M.A. 2002. Multiple functions of *mfa-1*, a putative pheromone precursor gene of *Neurospora crassa*. *Eukaryot. Cell* 1, 987-999.

Kimura, M. 1980. A simple method for estimating evolutionary rates of base substitutions through comparative studies of nucleotide sequences. *J. Mol. Evol.* 16, 111-120.

Marchler-Bauer, A., Bryant, S.H. 2004. CD-Search: protein domain annotations on the fly. *Nucleic Acids Res.* 32, 327-331.

Mylyk, O.M., Barry, E.G., Galeazzi, D.R. 1974. New isogenic wild types in *N. crassa*. *Neurospora Newslett.* 21, 24.

Perkins, D.D. 2004. Wild type *Neurospora crassa* strains preferred for use as standards. *Fungal Genet. Newsl.* 51, 7-8.

Read, N.D., Jeffree, C.E. 1991. Low-temperature scanning electron microscopy in biology. *J. Microscopy* 161, 59-72.

Saitou, N., Nei, M. 1987. The neighbor-joining method: A new method for reconstructing phylogenetic trees. *Mol. Biol. Evol.* 4, 406-425.

Sargent, M.L., Woodward, D.O. 1969. Genetic determinants of circadian rhythmicity in Neurospora. *J. Bacteriol.* 97, 861–866.

Staben, C., Jensen, B., Singer, M., Pollock, J., Schechtman, M., Kinsey, J., Selker, E. 1989. Use of a bacterial hygromycin B resistance gene as a dominant selectable marker in *Neurospora crassa* transformation. *Fungal Genet. Newsl.* 36, 79-81.

Swofford, D. L. 2000. PAUP*. Phylogenetic analysis using parsimony (*and other methods), version 4; Sinauer Associates: Sunderland, MA.

Westergaard, M., Mitchell, H.K. 1947. *Neurospora* V. A synthetic medium favoring sexual reproduction. *Amer. J. Bot.* 34, 573–577.

CHAPTER 3

Male and female interactions during mating

3.1 Introduction

Mating in *Neurospora crassa* typically involves a trichogyne hypha growing out from the ascogonium within a protoperithecium (the female structure) towards a conidium (the male cell) of opposite mating type (Backus, 1939; Bistis, 1981). A trichogyne often branches and grows chemotropically towards sex pheromone emitted by the conidium. On making contact with the conidium, the trichogyne usually wraps round the conidium prior to fusing with it (Backus, 1939). Macroconidia, arthroconidia and microconidia most commonly act as male fertilizing agents (Davis, 2000; Nelson & Metzenberg, 1992). After cell fusion, one or more male nuclei migrate through the trichogyne to the ascogonium (Davis, 2000; Sansome, 1947). The nuclei subsequently paired up and formed dikaryotic ascogenous hyphae. The formation of the dikaryon is thought to stimulate the transition from protoperithecial to the perithecial stage. The protoperithecium is normally fertilized by

a single conidial nucleus, although mixed male parentage and mixed female parentage is occasionally encountered (Johnson, 1976). Nevertheless, very little is known about the behaviour of the male and female nuclei during the whole process of mating in *N. crassa* or, for that matter, other filamentous fungi.

The mating of *N. crassa* is regulated by two different idiomorphs at the *mat* locus: *mat A* and *mat a*. The *mat A* idiomorph contains three genes, *mat A-1*, *mat A-2* and *mat A-3,* whilst only one gene, *mat a-1*, is found at the *mat a* idiomorph (section 1.4). The *mat A-1* and *mat a-1* genes regulate the recognition of male and female strains (Saupe & Glass, 1997; Wu & Glass, 2001; Glass & Kaneko, 2003).

Conidia release the CCG-4 pheromone from *mat A* and MFa-1 pheromone from *mat a* (Bobrowicz *et al.,* 2002; Kim *et al.,* 2002) and there bind to and activate the cognate sex pheromone receptors, PRE-1 of *mat A* and PRE-2 of *mat a* (Kim & Borkovich, 2004), on trichogyne surface (Bistis, 1981).The mating factor *ccg-4* gene (which is similar to α-factor gene [*MFα*] in *Saccharomyces cerevisiae*) encodes a precursor containing multiple repeats of the pheromone peptide sequence bordered by Kex2 protease processing sites. The mating factor *mfa-1* gene (which is similar to a-factor gene [*MFa*] in *S. cerevisiae*) encodes a short peptide with a C-terminal CAAX motif (C, cysteine; A, aliphatic; X, any amino acid residue). The mature MFa-1 is highly hydrophobic due to prenylation (lipitation) at the cysteine residue, while the mature CCG-4 is hydrophilic and unmodified (Kim & Borkovich, 2006; Borowicz *et al.,* 2002; Kim *et al.,* 2002).

The aims of the experimental research described in this chapter were to:

1. Show how the female trichogyne responds chemotropically, and how it physically interacts with the male macroconidium during mating.
2. Analyse the importance of sex pheromones and pheromone receptors from the male and female partners during mating.
3. Analyse the behaviour of male and female nuclei within trichogyne during mating.

4. Determine whether nuclear division is arrested during the conidium-trichogyne interaction.
5. Show whether male nuclei from different conidia can be involved in the formation of a single perithecium.
6. Determine whether the protoperithecial wall can be derived from hyphae of both mating types.

These aims were fulfilled by using confocal live-cell imaging of strains in which nuclei had been labelled with H1-GFP, and by using low-temperature scanning electron microscopy, and mutants lacking sex pheromone or sex pheromone receptors.

3.2 Results

3.2.1 Protoperithecial development is induced by either low nitrogen or low nutrient containing media

Protoperithecia started to form on solid SC medium (section 2.3), and on water agar (section 2.3), 2 and 5 days, respectively, after inoculation with a conidial suspension and incubation at 25 °C in constant light. Trichogynes grew out from the protoperithecia in search of conidia of opposite mating type. Perithecia with ostiolate necks developed 3 days and 2 days, after spreading conidia of opposite mating type over 7 day and 5 day old cultures possessing protoperithecia on water agar and SC medium, respectively. By contrast, on the commonly used Vogel's medium (section 2.3) minimal medium supplemented with a sugar (section 2.3) or on rich complete media (section 2.3), protoperithecia and perithecia either are not produced or are produced in very low numbers.

3.2.2 Trichogynes home towards conidia

The chemotropic behaviour of individual trichogynes was observed by covering water agar bearing protoperithecia by adding drops of a macroconidial suspension from a donor

culture of the opposite mating type to it (section 2.7.7). In contrast to the vegetative hyphal growth rate which was 5-20 μm/min on the microscope stage at room temperature (20-25 °C), trichogynes grew very slowly (0.25-0.63 μm/min) out from protoperithecia under the same conditions. Trichogynes grew chemotropically, with a characteristic 'wiggly' growth pattern, towards conidia of opposite mating type (Fig. 3.1) and formed multiple septa. The septa formed during the trichogyne growth. The first septum usually formed ~ 50 μm behind the point where a trichogyne fused to conidium. Within 2.5 h of adding macroconidia of opposite mating type, the trichogynes began to grow towards the conidia and fusion took place approximately 3 h later. Figure 3.2 shows an image of a protoperithecium with trichogynes homing towards conidia. After making contact with a conidium, the trichogyne normally coiled around it (Fig. 3.3A). A macroconidium sometimes fused with a trichogyne tip but more frequently fused with a region just behind the trichogyne tip (not shown). After fusion with a macroconidium, a trichogyne sometimes underwent branching and these branches were also often found to grow for considerable distances towards another conidium of opposite mating type. The presence of a macroconidium also often induced a trichogyne in its vicinity to branch, especially in regions > 50 μm back from the trichogyne tip (data not shown).

Very short trichogyne branches or pegs (~ 2 μm in length) were sometimes induced < 30 μm of trichogyne tips in the presence of conidia of the opposite mating type (Figs. 3.3B and 3.3C).

In some cases (I recorded at least 30 cases), a single macroconidium attracted all trichogynes within its vicinity (e.g., in Fig. 3.4 10 trichogynes were attracted by one single macroconidium). An interesting observation commonly made was that a trichogyne was often not attracted to the closest macroconidium of opposite mating type (data not shown).

The membrane-selective dye, FM4-64, labels vesicles within the Spitzenkörper of growing vegetative hyphae of *N. crassa* (Fischer-Parton *et al.*, 2000; Hickey *et al.*, 2005). I

was unable to detect a stained Spitzenkörper-like structure in the tips of growing trichogynes (data not shown).

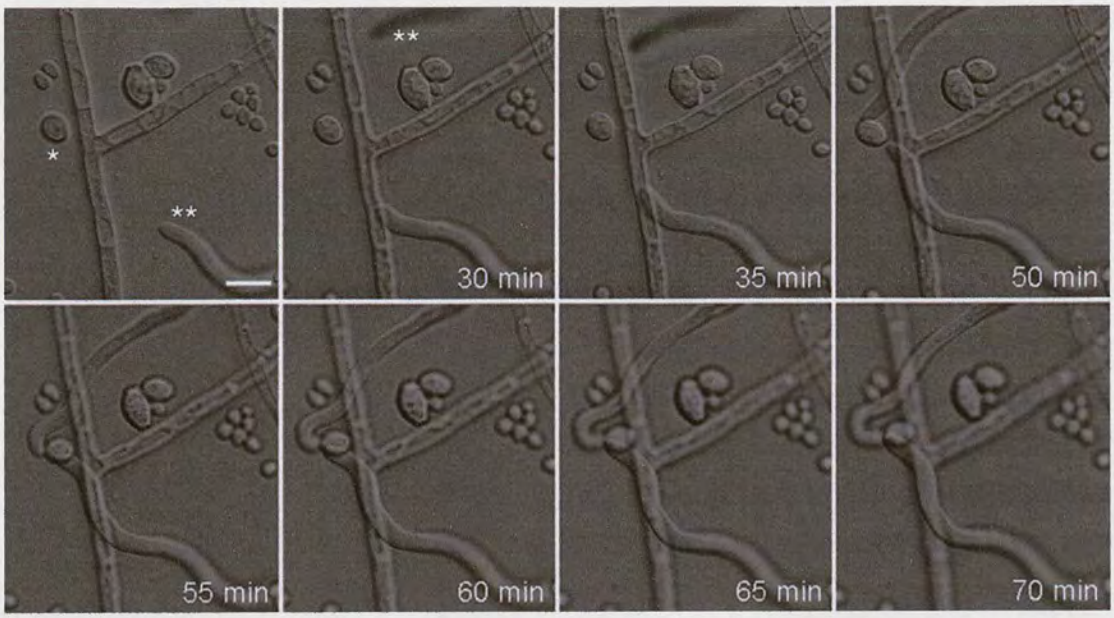

Figure 3.1 Two trichogynes (**) (74a) homing with a 'wiggly' growth pattern towards a macroconidium (*) (74A). Trichogynes respond to a pheromone emitted by conidia of the opposite mating type. Also see movie 3.1. Bar = 10 µm.

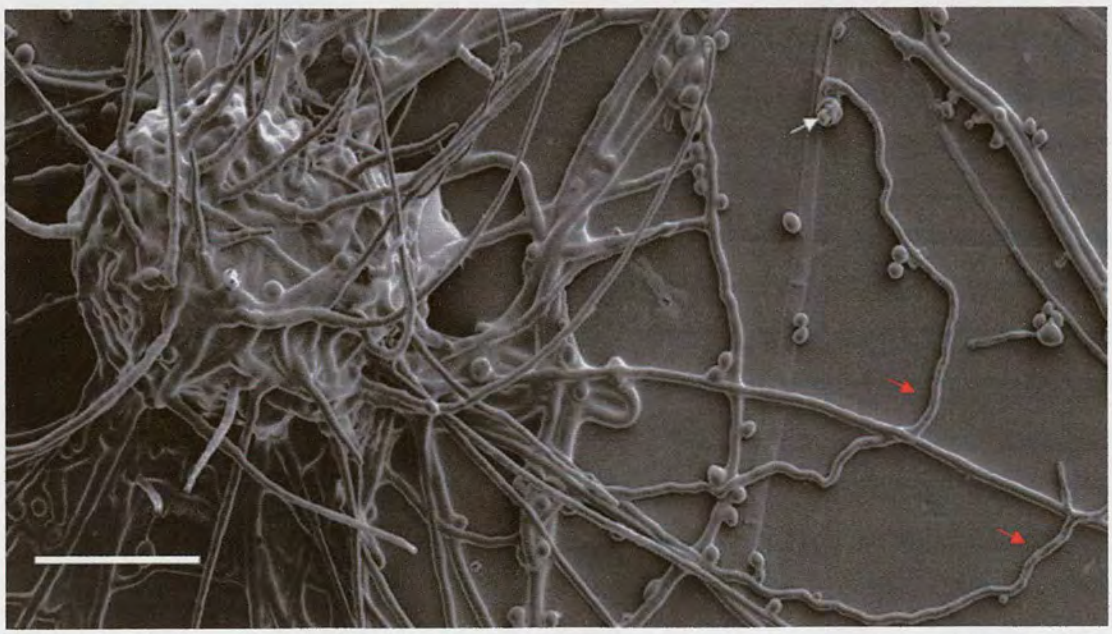

Figure 3.2 Protoperithecium with trichogynes (red arrows) (74a) and male conidium (white arrow) (74A). 14 h after male conidia were added to a 7-day old culture with young protoperithecia formed on water agar. Bar = 50 µm.

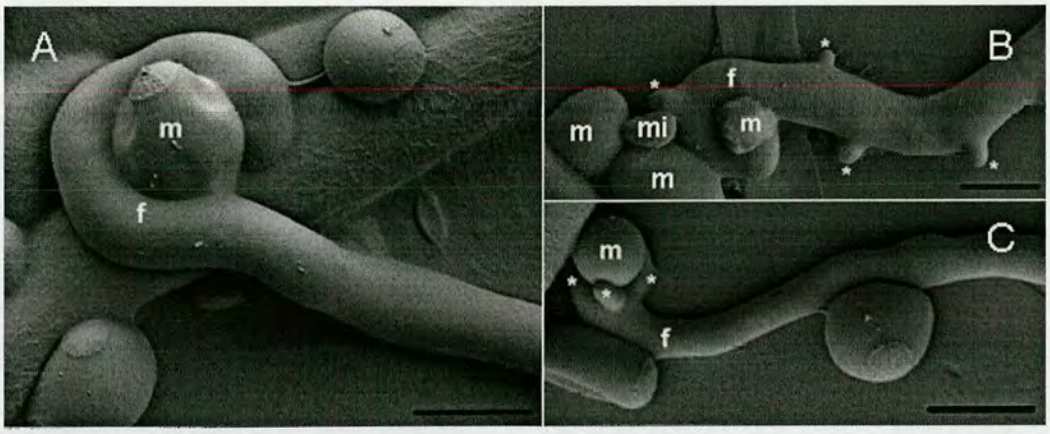

Figure 3.3 Trichogyne-conidium interactions (74a used as female and 74A used as male). **A**. A trichogyne coiled around a macroconidium. **B**. A trichogyne with several short subapical branches (*) and associated macroconidia and a macroconidium. **C**. A trichogyne with three short subapical branches in the tip region which have formed immediately adjacent to the male macroconidium. f, female trichogyne. m, macroconidium. mi, microconidium. * short trichogyne branches. Bar = 5 µm.

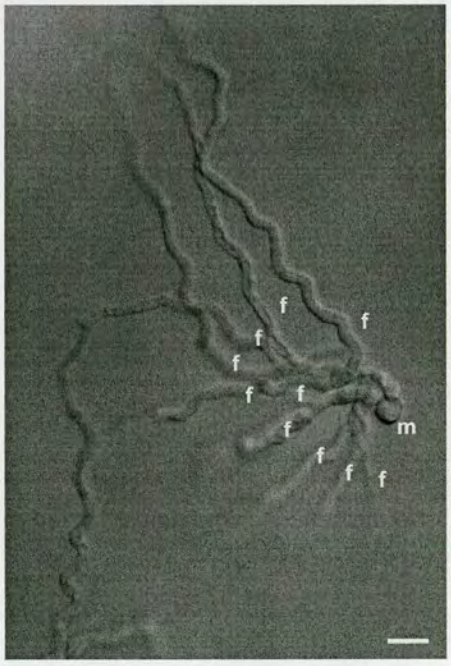

Figure 3.4 Ten trichogynes (74a) that have homed towards a single macroconidium (74A). m, single macroconidium. f, female trichogynes. Bar = 10 µm.

3.2.3 Trichogynes interacting with conidia sometimes formed hyphal aggregates

Although male nuclei normally passed through into the trichogynes after fusing with them, this was not always the case (e.g., Figs. 3.5A and 3.5B). When the male nuclei did not

pass through into the trichogyne, it commonly continued to grow around the conidium for another 48 h to form a hyphal aggregate that was of a similar size to protoperithecium (< 50 μm in diameter). Within 2 days, however, the hyphal compartments with these hyphal aggregates underwent cell death. If individual hyphal aggregate were cut out from the agar surface with a needle and transplanted to fresh SC medium (section 2.3), they continued to grow and enlarge for up to two more days before they died.

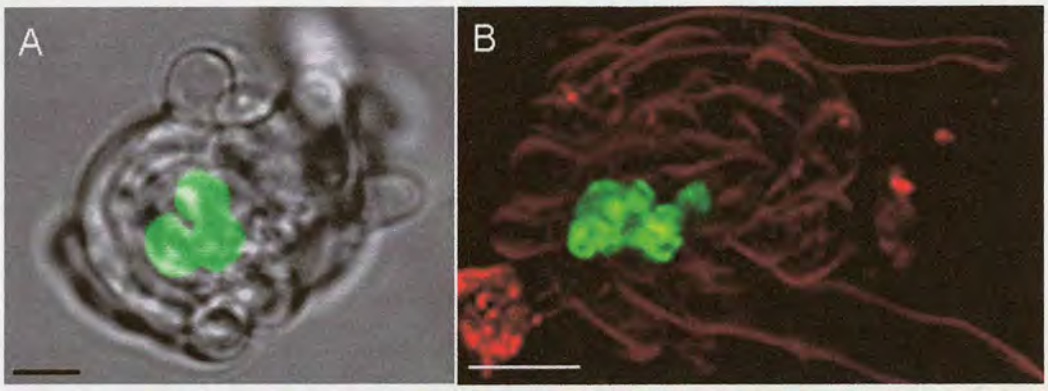

Figure 3.5 Trichogyne coiled and aggregated around a macroconidium. Both **A** and **B** show an interacting trichogyne and macroconidium 30 h after adding conidia to the female culture. Although the trichogynes have coiled around the conidia, the male nuclei (green) have not passed through to the female trichogyne. The male nuclei were labelled with H1-GFP. The macroconidia and trichogynes were strained with the membrane-selective dye FM4-64. Bar = 5 μm. In (**A**) 74a was used as the female and 74A used as the male. In (**B**) 74A was used as the female and 74a used as the male.

3.2.4 Cognate sex pheromones and pheromone receptors are important for mating and normal perithecial development

Sex pheromones from male conidia (CCG-4 and MFa-1 from *mat A* and *mat a*, respectively, Bobrowicz *et al.*, 2002; Kim *et al.*, 2002) and sex pheromone receptors (PRE-1 and PRE-2 from *mat A* and *mat a*, respectively, Kim & Borkovich, 2004) are crucial for mating (Table 3.1). Pheromone lacking Δ*mfa-1 mat a* or Δ*ccg-4 mat A* strains used as males when applied to 74*A* and 74*a* wild type females, respectively (marked as red in Table 3.1), induced protoperithecia to develop into perithecia but they lacked asci and ascospores. These fruitbodies have been termed 'barren perithecia' (Raju & Perkins, 1978). Less than

1% of protoperithecia (74A or 74a) further developed into perithecia in the absence of sex pheromone from the opposite mating type partner, but these perithecia lacked asci (i.e. were "barren"). Interestingly, female deletion mutants lacking PRE-1, MFa-1 or CCG-4 in 74a, or female deletion mutants lacking MFa-1 and CCG-4 in 74A, underwent no perithecial development when crossed with pheromone-lacking male mutants (Table 3.1). This suggests that the PRE-1 pheromone receptor form 74a and the pheromones MFa-1 and CCG-4 from females of both mating type (74A and 74a) are important in the development of protoperithecia into full fertile perithecia.

3.2.5 Mitotic division is blocked following trichogyne-conidium fusion

Depending on the length of the trichogyne it took a few hours for a macroconidial nucleus to reach the ascogonium after the macroconidium had fused with a trichogyne. Extensive (> 25 cases of 74a as female and 74A as male; and > 25 cases of 74A as female and 74a as male) imaging of male strains expressing nuclear target H1-GFP indicated that no incoming male nuclei divided in the macroconidium during the 7 h before fusion or in the trichogyne within 5 h after fusion. Normally, during macroconidial germination, nuclear division starts to occur within a few hours after the macroconidia have been hydrated with growth medium at 22 °C (Serna & Stadler, 1978). All nuclei in a macroconidium passed through into the trichogyne if fusion occurred. Individual protoperithecia produced multiple trichogynes and all of these trichogynes could home towards different macroconidia. In addition, trichogynes from different protoperithecia often grew towards a single conidium.

Table 3.1 Outcome of the mating of sex pheromone and sex pheromone receptor mutants

female \ male	74 *A*	74 *a*	Δ*pre-1 A*	Δ*pre-1 a*	Δ*pre-2 A*	Δ*pre-2 a*	Δ*mfa-1 A*	Δ*mfa-1 a*	Δ*ccg-4 A*	Δ*ccg-4 a*
74 *A*	-	+[a]	-	+[a]	-	+[b]	-	+[b,d]	-	+[a]
74 *a*	+[a]	-	+[a]	-	+[a]	-	+[a]	-	+[c,d]	-
Δ*pre-1 A*	-	-	-	-	-	-	-	-	-	-
Δ*pre-1 a*	+[a]	-	+[a]	-	+[a]	-	+[a]	-	-	-
Δ*pre-2 A*	-	+[a]	-	+[a]	-	+[a]	-	+[c,d]	-	+[b]
Δ*pre-2 a*	-	-	-	-	-	-	-	-	-	-
Δ*mfa-1 A*	-	+[a]	-	+[a]	-	+[a]	-	-	-	+[a]
Δ*mfa-1 a*	+[a]	-	+[a]	-	+[a]	-	+[a]	-	-	-
Δ*ccg-4 A*	-	+[a]	-	+[a]	-	+[a]	-	-	-	+[a]
Δ*ccg-4 a*	+[a]	-	+[a]	-	+[b]	-	+[a]	-	-	-

+, protoperithecia enlarge and darken after fertilization; -, no perithecial development; [a], 24 h after adding male conidia; [b], 48 h after adding male conidia; [c], 72 h after adding male conidia; [d], barren perithecia (perithecia possessing necks but no asci).

3.2.6 Male nuclei from different conidia can be involved in fertilizing a single protoperithecium

Following fusion between multinucleate macroconidium and female trichogynes, more than one male nucleus past through the female trichogyne to the ascogonium in the protoperithecium. A mixed population of macroconidia (one expressing nuclear targeted H1-GFP, the other expressing cytoplasm targeted RFP) were add in a 1:1 ratio to a female (lacking nuclear or cytoplasm labelling) and the resulting ascus contents in the perithecia were examined. Figure 3.6A shows that both GFP and RFP labelled different ascospores in a single ascus (4 ascospores exhibited green fluorescence and 4 ascospores showed red fluorescence). These results indicated that at least two male nuclei from different conidia had migrated to the ascogonium and participated in fertilization. Less than 1% of the asci resulted from different male nuclei pairing up, fusing and undergoing meiosis; most (i.e. > 99%) of the other asci resulted from a male and a female nucleus pairing up, fusing and undergoing meiosis.

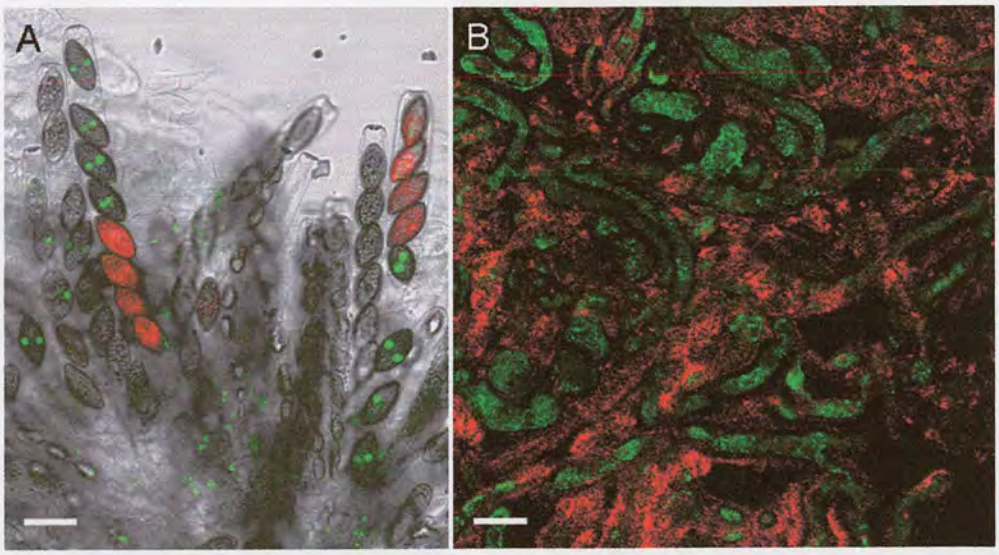

Figure 3.6 Asci containing ascospores and perithecial wall hyphae. **A**. Asci containing ascospores, some of which are labelled with nuclear H1-GFP (with 74A background) and others with cytoplasmic RFP (with 74A background). These results show that more than one conidium was involved in the fertilization which resulted in the formation of these ascospores. Bar = 30 μm. **B**. Perithecial wall contain cytoplasmic GFP labelled 74*A* (green) and cytoplasmic RFP labelled 74*a* (red) derived from hyphae of different mating types. Bar = 10 μm.

3.2.7 Hyphae of both mating types can aggregate together to form protoperithecial wall tissue

The perithecial wall has been reported as being derived from the female parent (Johnson, 1976). This was tested by using a different culture method from that used above. Instead, strains of opposite mating type (*mat A* with cytoplasmic expressing GFP and *mat a* with cytoplasmic expressing RFP) were inoculated on opposite sites of a Petri dish containing SC medium.

When the perithecial walls of the perithecia formed down the middle between the two converged colonies were examined by confocal microscopy, some of the perithecia (~ 1%) were found to contain both labels (Fig. 3.6B). This demonstrates that perithecial walls from hyphae can originate from both mating types. No perithecial wall cells that contained the cytoplasmic expressing GFP and cytoplasmic expressing RFP, and which would have

appeared yellow when co-localized, were observed (Fig. 3.6B). This suggested that hyphal fusion resulting in cytoplasmic containing does not occur or occurs rarely between hyphae that aggregate to form the perithecial wall.

3.2.8 Female nuclei are immobilized, round up and clump together after fusion

Figure 3.7 shows how the female nuclear behaviour within the trichogyne changes following fusion with a macroconidium. These changes in nuclear behaviour occurred 1.5-2.5 h after fusion and involved the female nuclei becoming immobilized, rounding up and clumped together (Fig. 3.7). Furthermore, as indicated in section 3.2.5, they did not undergo nuclear division once in this post-fusion phase. At least 50 cases were recorded and showed the same phenomena.

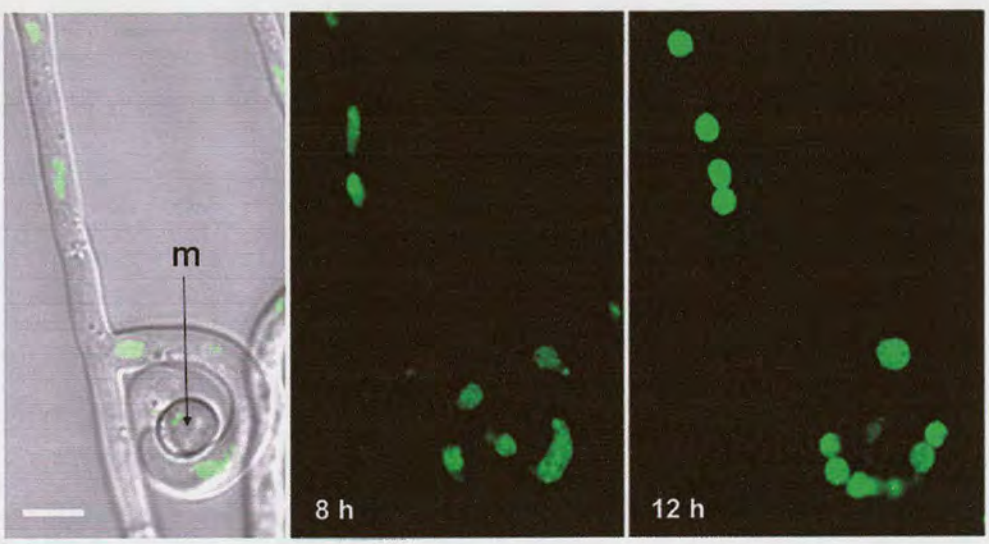

Figure 3.7 Changes in female nuclear behaviour within the trichogyne (74a background) following fusion with a macroconidium (74A). The female nuclei in the trichogyne were labelled with H1-GFP. Brightfield and confocal images at 8 h (before fusion) and 12 h (after fusion) following the addition of conidia of opposite mating type. Labelled nuclei are shown in a trichogyne branch coiled around a macroconidium (m). Note that before fusion the female nuclei are commonly pear-shaped and very mobile. After fusion they became immobilized, round up and clump together. Bar = 10 μm.

3.2.9 Only male nuclei migrate through the trichogyne towards the ascogonium

Commonly 9-10 h after a trichogyne made contact with a macroconidium of opposite mating type, the male nuclei started to migrate from the macroconidium towards the ascogonium (Fig. 3.8). The male nuclei exhibit very fast movement through the trichogyne, the fastest nuclear velocity recorded in this study was ~ 45 μm per min (Fig. 3.8) and the average nuclear velocity was ~40 - 45 μm per min (n = 5).

Feature of male nuclear movement were: (1) male nuclei always moved unidirectionally towards the ascogonium (movies 3.2 and 3.3), (2) the multiple male nuclei from a macroconidium moved down the trichogyne sequentially, (3) all the male nuclei left a macroconidium and migrated down the trichogyne, (4) male nuclei exhibited an 'inchworm-type' of movement, which involved them having a repeated elongated and then condensed morphology. At all times the morphologies of the male nuclei were very distinctive and could be readily distinguished from the spherical female nuclei (Figs. 3.8 and 3.9). Sometimes the male nuclei were very elongated (< 50 μm in length).

The pattern of inchworm-like movement of two male nuclei over a 12.5 min period is shown in Fig. 3.8C. The nuclei were normally condensed when they passed through septal pores, or in the region of septal pores, and were elongated when moving between adjacent septa.

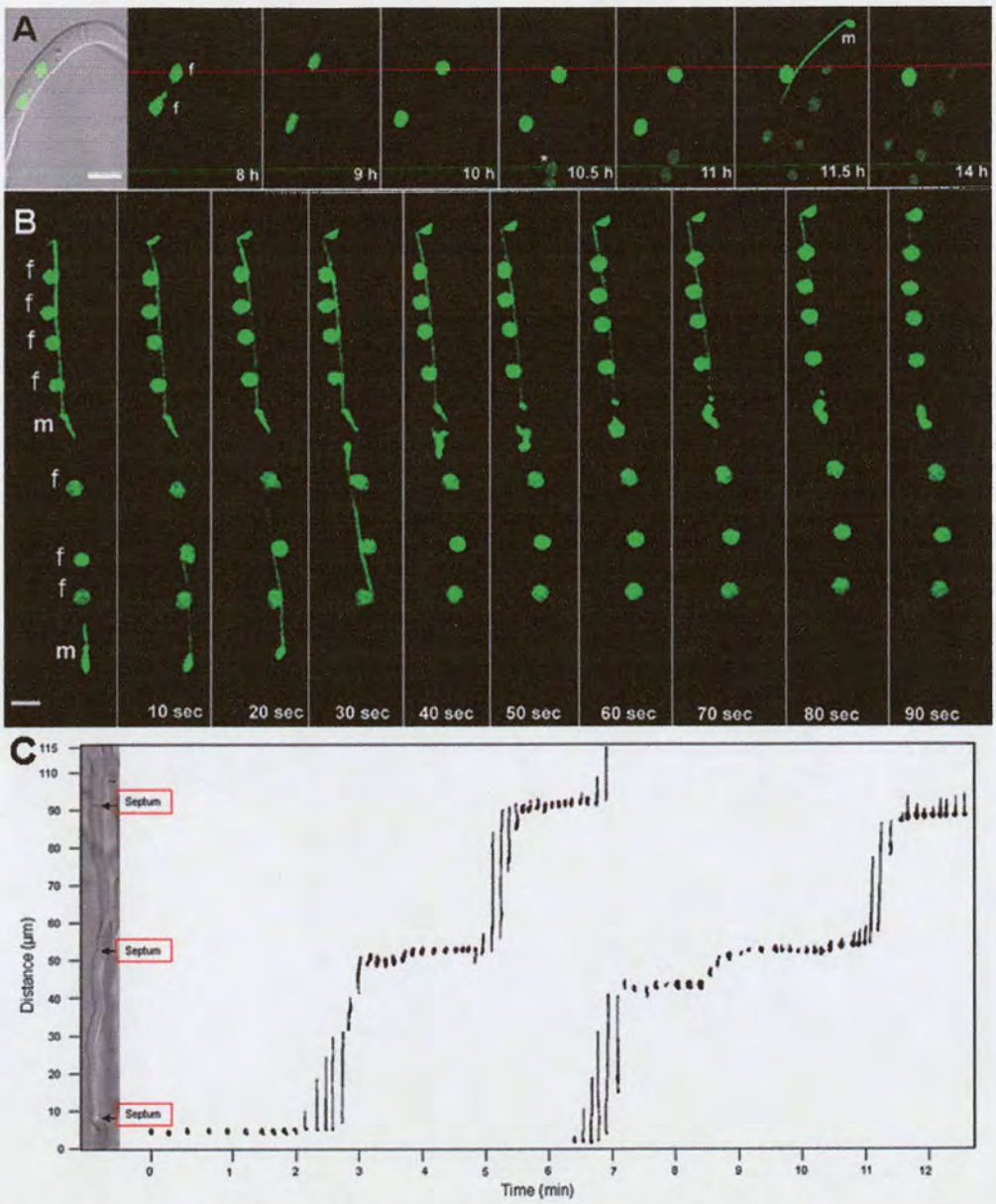

Figure 3.8 Time course of male nuclear movement through female trichogynes in which both male and female nuclei are labelled with H1-GFP. **A**. Conidium-trichogyne fusion occurred 9-10 h after adding conidia of opposite mating type. A highly elongated male nucleus can be seen at the 11.5 h time point. f, female nuclei (74a background); m, male nuclei (74A background). *, nuclei in other a growing hypha. Bar = 10 µm. **B**. Two male nuclei (74a background) moving through the trichogyne (74A background) past the immobilized, round female nuclei. Note that the male nuclei exhibit an inchworm-like type of movement having repeated elongated and then condensed morphologies. Bar = 5 µm. **C**. The pattern of male nuclear movement in the trichogyne. The characteristics of male nuclear movement were that they: (1) exhibited an 'inchworm-like' movement, (2) moved unidirectionally towards the ascogonium, (3) they became condensed and stopped at/close to the septa, (4) they elongated later moving between septa, and (5) moved sequentially through the trichogyne

3.3 Discussion

Mating in *N. crassa* is a process involving male-female cell interactions and this is regulated by cognate sex pheromone and receptors (Bobrowicz *et al.,* 2002; Kim & Borkovich, 2004; Mayrhofer & Pöggeler 2005). In this chapter, conidium-trichogyne and male–female nuclear interactions were investigated. In addition, the contribution of male parental nuclei to the asci and perithecial wall were examined. Observations were also made on the formation of hyphal aggregates formed when trichogynes coiled around macroconidium but did not fuse with them.

3.3.1 Trichogyne morphogenesis is regulated by pheromone released from conidia

A single protoperithecium can produce more than one trichogyne. The pattern of trichogyne growth is influenced by conidia of opposite mating type which produce peptide pheromones (Bobrowicz *et al.*, 2002; Kim *et al.,* 2002; Pöggeler & Kück, 2000) to attract the trichogyne and also act as male fertilizing agents. Before male fertilizing agents (i.e. conidia) have been added to the female culture, it was very difficult to distinguish trichogynes from other hyphae (i.e. fringe hyphae, Read, 1983) arising from the protoperithecial surface However, once the female trichogynes responded to male conidia, they took on very distinctive 'wiggly' growth appearance.

I showed that more than one trichogyne can be attracted to a single macroconidium. However, I did not obtain any evidence for more than one trichogynes fusing with a single macroconidium. The different trichogynes from a single protoperithecium were found to be simultaneously attracted to different macroconidia, and nuclei from more than one conidium could contribute the asci within a single perithecium. Genetic evidence has been previously reported for this phenomenon in *N. crassa* (Sansome, 1947; Davis, 2000)

A detailed microscopic characterization of the process of trichogyne growth towards a

conidium in *N. crassa* strongly indicated release of a diffusible chemoattractant pheromone from macroconidia of opposite mating type. Previous experimentation on this phenomenon has only been done with microconidia as the male fertilizing agents (Bistis, 1981, 1983, 1986), and my observations with using macroconidia as the male fertilizing agents were consistent with these published results.

Trichogyne branching could be induced by the close proximity of macroconidia and trichogyne branches often fused with macroconidia. Fusion between a trichogyne and macroconidium occurred not only at the trichogyne tip but also at any subapical location along the length of the trichogyne or trichogyne branch. This suggests that pheromone receptors may be located in the plasma membrane along the whole length of the trichogyne. Another possibility, however, is that the close proximity of a conidium may actually induce the localization of pheromone receptors in the trichogyne plasma membrane in the region close to the conidium. Analysis of the factors responsible for trichogyne chemoattraction suggested that the chemoattractants secreted by *mat A* and *mat a* strains differ in their chemical properties because the chemoattractants produced by the *A* strain was much more effective than that produced by the *mat a* strain (Bistis, 1983). Now, we know that these differences probably relate to the fact that each mating type produces a different peptide sex pheromone (Bobrowicz *et al.,* 2002; Kim *et al.*, 2002; Pöggeler & Kück, 2000). An interesting observation of mine was that trichogyne did not always fuse with the closest macroconidium of opposite mating type. How trichogynes select a single macroconidium from numerous conidia is unclear but it suggests that not all macroconidia of opposite mating type are releasing the same amount of sex pheromone.

I failed to label a Spitzenkörper-like structure in the tips of growing trichogynes using the membrane-selective FM4-64, as has been reported for growing vegetative hyphae (Fischer-Parton *et al.,* 2000; Hickey *et al.,* 2005). After staining with FM4-64, Spitzenkörper have also been shown to play an important role during hyphal fusion in mature colonies, and

persist after the fusion hyphae have made contact and a fusion pore has been formed (Hickey *et al.,* 2002; Read & Roca, 2006). However, the apical accumulation of vesicles has not been identified in conidial anastomosis tubes (CATs) during fusion. Neither have Spitzenkörper been observed in young germ tubes of *N. crassa* (Araujo-Palomares *et al.,* 2007). The reason why a apical vesicle cluster is not labelled with FM4-64 in trichogynes, CATs or germ tubes may be because they are very small compared with fusion hyphae in the mature colony. Furthermore, since all three of these specialized hyphae grow very slowly thus may possess fewer vesicles in their tips growing compared with growing vegetative hyphae.

3.3.2 Male and female nuclei exhibit different behaviour following fusion

After a trichogyne and conidium fused, the female trichogyne nuclei were immobilized, rounded up and tended to clump together, whilst all of the male conidial nuclei became very mobile and rapidly moved past the female nuclei through the trichogyne towards the female ascogonium. The male nuclei exhibited a characteristic inchworm-like pattern of movement which, to my knowledge, has not been described in fungi before. Although the *mat a-1* and *mat A-1* genes are both required for mating identity, postfertilization functions, and vegetative incompatibility (Saupe & Glass, 1997), these genes or other genes at the mating-type locus may also be involved in the regulation of the contrasting behaviour of the male and female nuclei following trichogyne-conidium fusion. Nevertheless, how the different nuclei are recognized and what mechanisms are involved, is unclear. It seems likely, however, that this will involve the regulation of the activity of cytoskeletal motor proteins (i.e. dynein, kinesin and/or myosin; see section 1.6).

3.3.3 Male nuclei from different conidia can be involved in sexual reproduction

Figure 3.6 shows two different male nuclei labelled with different fluorescent proteins in a single ascus (4 ascospores with green and 4 ascospores with red fluorescence). These male

nuclei were derived from two different conidia. To my knowledge, this phenomenon has not been described previously in *N. crassa*. There are two explanations for this phenomenon: (1) *Self-fertilization* (selfing) has occurred. In the closely related coprophilous species, *Sordaria brevicollis,* which is normally heterothallic, selfing (homothallism) has been also observed (Robertson *et al.,* 1998). A similar situation has additionally been observed in the basidiomycete human pathogen *Cryptococcus neoformans* (Lin *et al.,* 2005). My results may provide the first evidence showing that *N. crassa* can undergo sexual reproduction in one mating type (*mat A*). (2) *Mating-type switching* has occurred. There is no evidence for mating-type switching in *N. crassa*, as found in *Saccharomyces cerevisiae* (Perkins, 1987). To distinguish between (1) and (2), the mating types of the individual ascospores from asci containing the two different male nuclei would need to be determined. If (1) had occurred, all the ascospores in an ascus should be the same mating type; if (2) had occurred, 50% should be *A* and 50% *a* mating types.

3.3.5 Nuclear division was inhibited at the beginning of trichogyne homing

In *S. cerevisiae,* the cell cycle is arrested in the G1 phase during mating (McKinney & Cross, 1995). In my study, a similar phenomenon was observed. I was unable to obtain any evidence of conidial nuclei entering trichogynes or female nuclei already located in trichogyne undergoing division. Nuclear division is re-initiated in the ascogonium (Thompson-Coffe & Zickler, 1994). The mechanisms of nuclear division inhibition in the early stages of sexual reproduction in *N. crassa* may be similar to *S. cerevisiae* in which pheromone stimulated MAP kinase signalling is involved (Schrick *et al.,* 1997).

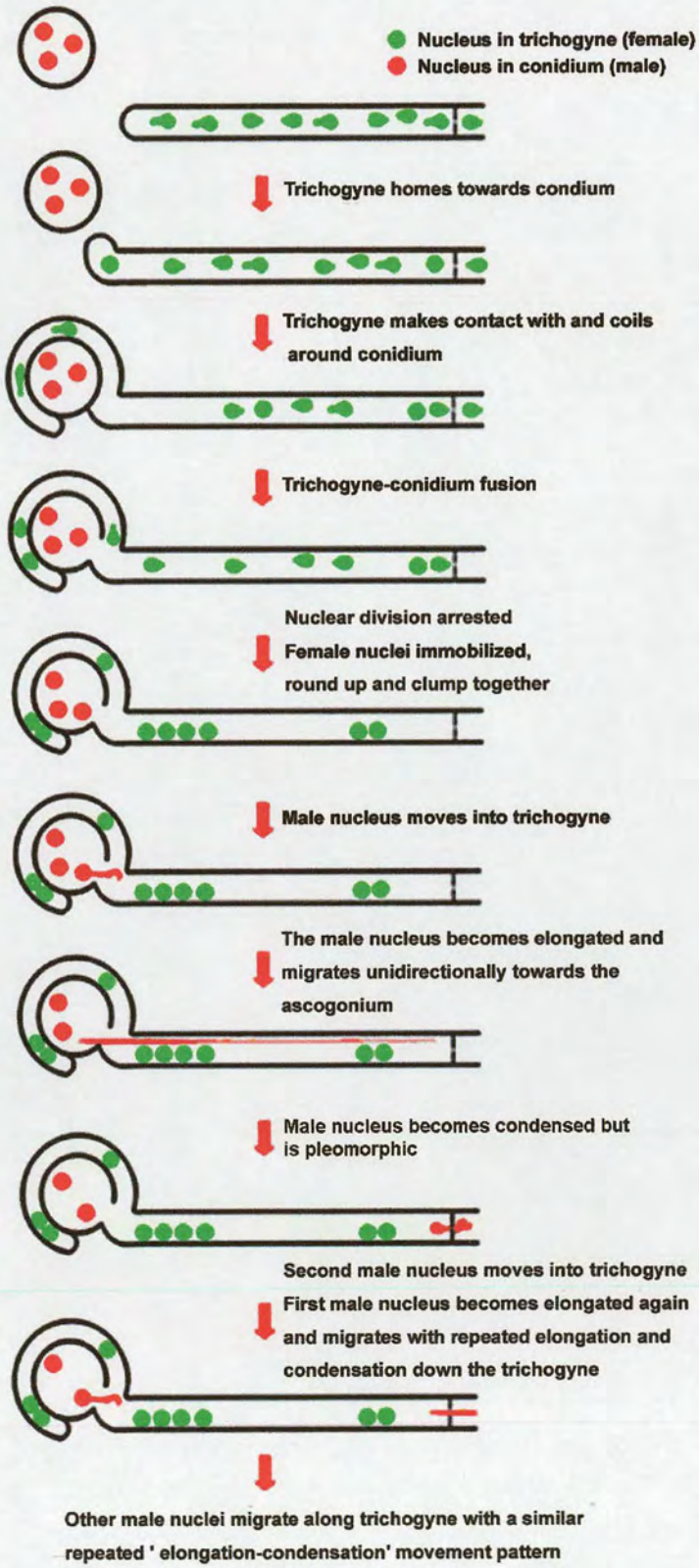

Figure 3.9 Different stages involved in the process of trichogyne-conidium interactions. Also see movie 3.4.

3.5 Summary

1. Within 2.5 h of adding macroconidia to the opposite mating type, trichogynes began to grow towards conidia and fusion took place after approximately an additional 3 h later. A macroconidium sometimes fused with a trichogyne tip but more frequently fused with a region just behind the trichogyne tip.
2. Sex pheromones from male macroconidia (CCG-4 and MFa-1 from mat *A* and mat *a*, respectively) and sex pheromone receptors (PRE-1 and PRE-2 from mat *A* and mat *a*, respectively) on female trichogynes are required for mating.
3. Following conidium-trichogyne fusion, the female nuclei became immobilized, rounded up and clumped together (Fig. 3.9).
4. Following conidium-trichogyne fusion, all of the male nuclei moved unidirectionally and sequentially to the ascogonium with an inchworm-like, repeated elongation and condensation pattern of movement (Fig. 3.9).
5. Male and female nuclei underwent nuclear arrest following macroconidium-trichogyne fusion.
6. Perithecial wall hyphae can be derived from both mating types.

References

Araujo-Palomares, C.L., Castro-Longoria, E., Riquelme, M. 2007. Ontogeny of the Spitzenkörper in germlings of *Neurospora crassa*. *Fungal Genet. Biol.* 44, 492-503.

Backus, M.P. 1939. The mechanics of conidial fertilization in *Neurospora sitophila*. *Bull. Torrey Botan. Club*. 66, 63-76.

Bistis, G.N. 1981. Chemotropic interactions between trichogyenes and conidia of opposite mating type in *Neurospora crassa*. *Mycologia* 73, 959-975.

Bistis, G.N. 1983. Evidence for diffusible, mating-type-specific trichogyne attractants in *Neurospora crassa*. *Experimental Mycol.* 7, 292-295.

Bistis, G.N. 1996. Trichogynes and fertilization in uni- and bimating-type colonies of *Neurospora tetrasperma*. *Fungal Genet. Biol.* 20, 93-98.

Bobrowicz, P., Pawlak, R., Correa, A., Bell-Pedersen, D., Ebbole, D.J. 2002. The *Neurospora crassa* pheromone precursor genes are regulated by the mating-type locus and the circadian clock. *Mol. Microbiol.* 45, 795-804.

Davis, R.H. 2000. *Neurospora*: contributions of a model organism. Oxford University Press, New York.

Fischer-Parton, S., Parton, R.M., Hickey, P.C., Dijksterhuis, J., Atkinson, H.A., Read, N.D. 2000. Confocal microscopy of FM4-64 as a tool for analysing endocytosis and vesicle trafficking in living fungal hyphae, *J. Microsc.* 198, 246–259.

Glass, N.L. Kaneko, I. 2003. Fatal attraction: nonself recognition and heterokaryon incompatibility in filamentous fungi. *Eukaryot. Cell*, 2, 1-8.

Hickey, P.C., Jacobson, D.J., Read, N.D., Glass, N.L. 2002. Imaging hyphal fusion in *Neurospora crassa*. *Fungal Genet. Biol.* 37, 109-119.

Hickey, P.C., Swift, S.M., Roca, M.G., Read, N.D. 2005. Live-cell imaging of filamentous fungi using vital fluorescent dyes. In *Methods in Microbiology. Vol. 34. Microbial Imaging* (ed. By T. Savidge C. Pothoulakis) , pp. 63-87. Elsevier: Amsterdam.

Johnson, T.E. 1976. Analysis of pattern formation in *Neurospora* perithecial development using genetic mosaics. *Dev. Biol.* 54, 23-36.

Kim, H., Metzenberg, R.L., Nelson, M.A. 2002. Multiple functions of *mfa-1*, a putative pheromone precursor gene of *Neurospora crassa*. *Eukaryot. Cell*, 1, 987–999.

Kim, H., Borkovich, K.A. 2004. A pheromone receptor gene, *pre-1*, is essential for mating-type-specific directional growth and fusion of trichogynes and female fertility in *Neurospora crassa*. *Mol. Microbiol.* 52, 1781-1798.

Kim, H., Borkovich, K.A. 2006. Pheromones are essential for male fertility and sufficient to direct chemotropic polarized growth of trichogynes during mating in *Neurospora crassa*. *Eukaryot. Cell* 5, 544-554.

Lin, X., Hull, C.M., Heitman, J. 2005. Sexual reproduction between partners of the same mating type in *Cryptococcus neoformans*. *Nature* 434, 1017-1021.

Mayrhofer, S., Pöggeler, S. 2005. Functional characterization of an α–factor-like *Sordaria macrospora* peptide pheromone and analysis of its interaction with its cognate receptor in *Saccharomyces cerevisiae. Eukaryot. Cell* 4, 661–672.

McKinney, J.D., Cross, F.R. 1995. *FAR1* and the G1 phase specificity of cell-cycle arrest by mating factor in *Saccharomyces cerevisiae. Mol. Cell Biol.* 15, 2509–2516.

Nelson, M.A., Metzenberg, R.L. 1992. Sexual development genes of *Neurospora crassa. Genetics* 132, 149-162.

Perkins, D.D. 1987. Mating-type switching in filamentous ascomycetes. *Genetics* 115, 215-216.

Pöggeler, S., Kück, U. 2000. Comparative analysis of the mating-type loci from *Neurospora crassa* and *Sordaria macrospora*: identification of novel transcribed ORFs. *Mol. Gen. Genet.* 263, 292-301.

Raju, N.B., Perkins, D.D. 1978. Barren perithecia in *Neurospora crassa. Can. J. Genet. Cytol.* 20, 41-59.

Read, N.D. 1983. A scanning electron microscopic study of the external features of perithecium development in *Sordaria humana. Can. J. Bot.* 61, 3217-3229.

Read, N.D., Roca, M.G. 2006. Vegetative Hyphal Fusion in Filamentous Fungi, pp 87-98. *In* F. Baluska, D. Volkmann and P. W. Barlow (ed.), Cell-Cell Channels, Landes Bioscience. Georgetown, Tx.

Robertson, S.J., Bond, D.J. Read, N.D. 1998. Homothallism and heterothallism in *Sordaria brevicollis. Mycol. Res.* 102, 1215–1223.

Sansome, E.R. 1947. The use of heterokaryons to determine the origin of the ascogenous nuclei in *Neurospora crassa. Genetica* 24, 59-64.

Saupe S.J., Glass, N.L. 1997. Allelic specificity at the *het-c* heterokaryon incompatibility locus of *Neurospora crassa* is determined by a highly variable domain. *Genetics* 146, 1299–1309.

Schrick, K., Garvik, B., Hartwell, L.H. 1997. Mating in *Saccharomyces cerevisiae*: the role of the pheromone signal transduction pathway in the chemotropic response to pheromone. *Genetics* 147, 19–32.

Serna, L., Stadler, D. 1978. Nuclear division cycle in germinating conidia of *Neurospora crassa. J. Bacteriol* 136, 341-351.

Thompson-Coffe, C., Zickler, D. 1994. How the cytoskeleton recognizes and sorts nuclei of opposite mating type during the sexual cycle in filamentous ascomycetes. *Dev. Biol.* 165, 275-271.

Wu, J., Glass, N.L. 2001. Identification of specificity determinants and generation of alleles with novel specificity at the *het-c* heterokaryon incompatibility locus of *Neurospora crassa. Mol. Cell Biol.* 21, 1045-1057.

CHAPTER 4

A new cell type produced by macroconidia that is involved in sexual reproduction

4.1 Introduction

Neurospora crassa is a multicellular organism in which 28 morphologically distinct cell types have been recognized. Twenty-four of these cell types are associated with mating and the development of protoperithecia and perithecia (Bistis *et al.,* 2003). Three different types of conidia (microconidia, macroconidia and arthroconidia) have been described as male fertilization agents (Davis, 2000; Nelson & Metzenberg, 1992). Up until recently, these conidia were believed to produce only one type of hypha, the germ tube, which is involved in colony establishment. Two years ago, Roca *et al.*, (2005) described a new type of hypha produced by conidia which they called the conidial anastomosis tube (CAT), and which is involved in fusing conidial germlings. In this chapter I described a third type of hypha produced by conidia, the conidial sex tube (CST).

The aims of the experimental research described in this chapter were to:

1. Identify the characteristics of CSTs, and how they can be distinguished from germ tubes and CATs.
2. Show that the CST is involved in mating and can act as a male fertilizing agent.
3. Show that sex pheromones and receptors are involved in CST production.

These aims were fulfilled by using confocal live-cell imaging of strains in which nuclei had been labelled with H1-GFP or H1-RFP, or the cell wall stained with wheat germ agglutinin (WGA) labelled with fluoresceinisothiocynate (FITC). In addition, high resolution low-temperature scanning electron microscopy was used to image cell surfaces at high magnification, and mutants lacking sex pheromone or sex pheromone receptors were analyzed for CST formation.

4.2 Results

4.2.1 The conidial sex tube is a new cell type produced by macroconidia

During mating, it was often observed that trichogynes were attracted to what initially seemed to be germ tubes emerging from conidia (Fig. 4.1). Growth extension of these hyphae often stopped when trichogynes were approaching them (Movie 4.1-4.4). The trichogynes were found to fuse with this hypha and labelling the nuclei of the male strain with H1-GFP showed that male nuclei passed through into the trichogyne (Fig. 4.2). These hyphae only emerged from macroconidia of opposite mating type to the female strain. Hyphae were never observed to emerge from microconidia within 8 h of conidia being added to a female culture.

At this stage we concluded the following about this hypha: (1) it is involved in the mating process, (2) it is only formed when the opposite mating type are present, (3) it acts as a male fertilizing agent, and (4) it is produced by macroconidia, but not microconidia. This preliminary evidence indicated that this was a new type of hypha produced by conidia and we

decided to call it the **Conidial Sex Tube (CST)**. Further characterization of CSTs was restricted to those produced by macroconidia.

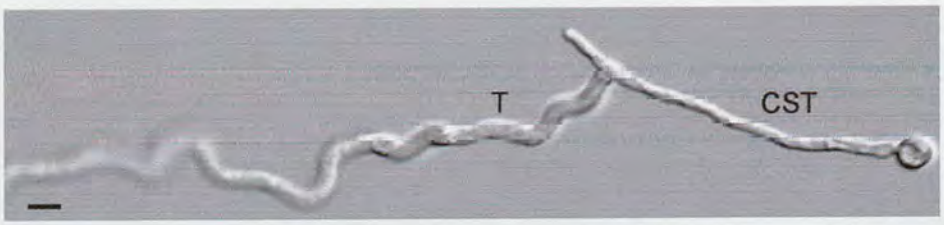

Figure 4.1 A trichogyne (T, 74a) that has homed towards and made (74A) contact with a CST. Bar = 5 μm.

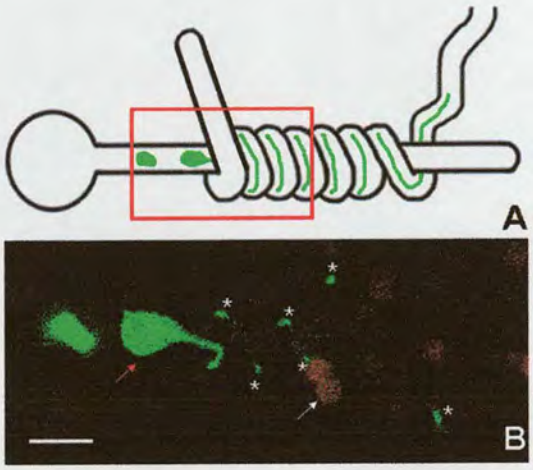

Figure 4.2 Nuclei from the CST (74A) pass through into the trichogyne (74a). **A**. Diagram showing a male nucleus passing through into a trichogyne from a CST and elongating inside the coiled trichogyne. This is a reconstruction drawn from confocal imaging; the image in (B) is a single confocal image showing an optical section through the region indicated in red. **B**. Confocal image showing that one of the male nuclei from the CST that has elongated inside the trichogyne. The rest of the elongated region of the male nucleus can only be seen in cross section (asterisks). The red arrow indicates the male nucleus (in green and labelled with H1-GFP; red arrow); the white arrow indicates the female nuclei (in red and labelled with H1-RFP; white arrow) in the trichogyne. Bar = 2 μm.

4.2.2 Conidial sex tubes are a morphologically and physiologically distinct cell type

Female trichogynes of opposite mating type were found to wrap around CSTs (Figs. 4.2A and 4.3A-D). Compared with germ tubes (Fig. 4.4A) and CATs (Fig. 4.4B), CSTs had the following combination of distinguishing characteristics (Figs. 4.4C and D): (1) they are

thin (2.5-3.5 μm) (germ tubes (4-7 μm) are thicker), (2) they can be long (CATs are short), (3) they mostly grow straight (germ tubes tend not to), (4) they are unbranched (germ tubes branch), (5) commonly septate (CATs never undergo septation), (6) they exhibit no chemotropism to other cell types (germ tubes tend to avoid each other whilst CATs grow towards each other) and (7) they do not fuse with each other (compare Figs. 4.4A and B with C and D).

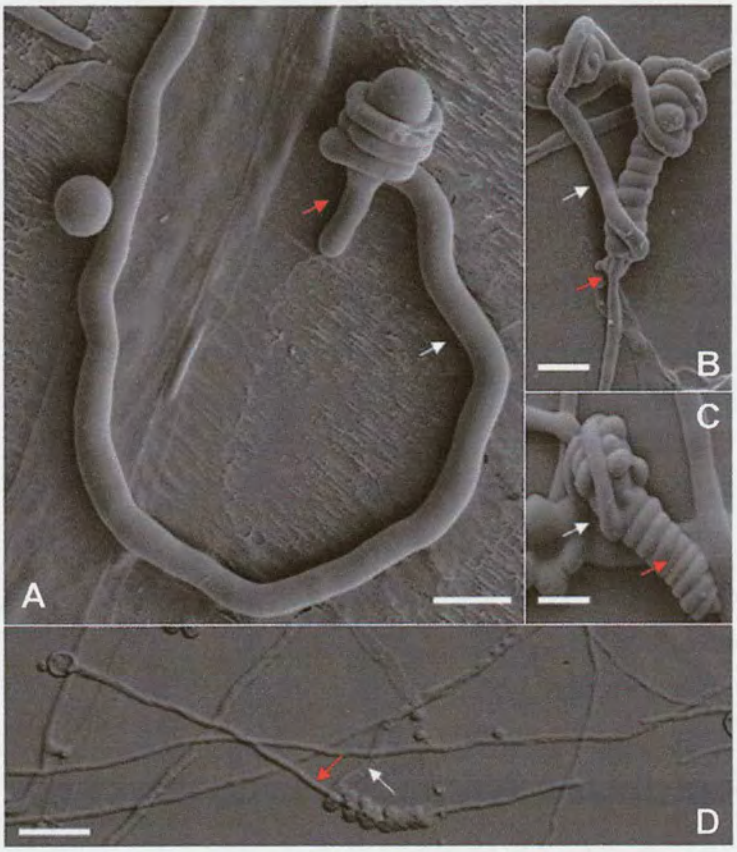

Figure 4.3 Conidial sex tubes (74A) with trichogynes of opposite mating type (74a) wrapped around them. **A-C**. SEMs showing trichogynes wrapped around CSTs. Bars = 10 μm; **D**. DIC image of a trichogyne wrapped around a very long CST. Bar = 30 μm. Red arrows indicate CSTs and white arrows indicate trichogynes.

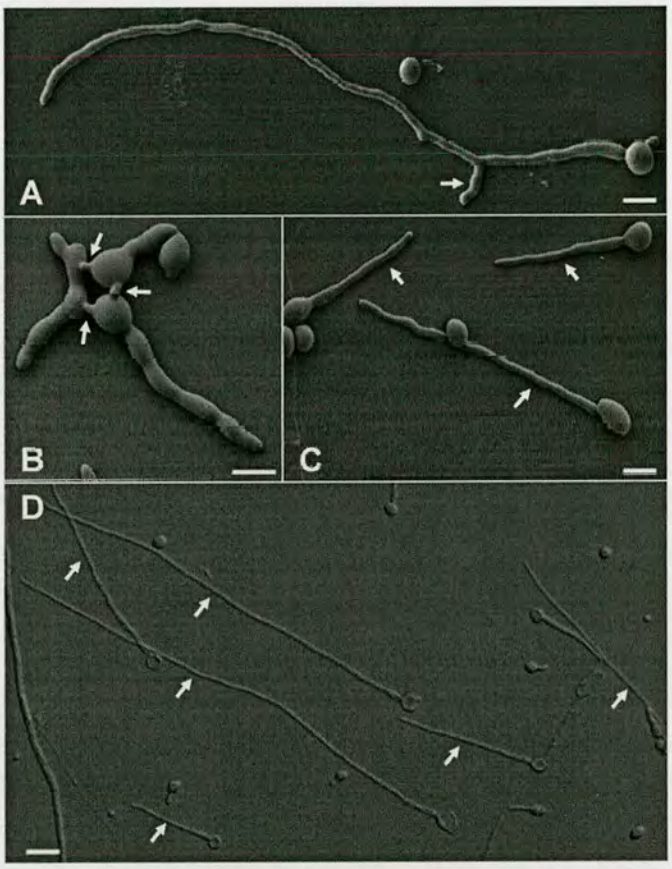

Figure 4.4 SEMs and DIC image of three different types of hyphae produced by macroconidia (74A). **A**. SEM of a conidial germ tube on water agar 10 h after inoculation. The white arrow indicates the germ tube branch. **B**. SEM of macroconidia fused together by CATs 10 h after inoculation. The white arrows indicate three fused CATs; **C**. SEM of CSTs 10 h after inoculation on water agar. The white arrows indicate the CSTs. Bar = 10 μm (in **A**, **B** and **C**). **D**. DIC image of CSTs 15 h after inoculation. The white arrows indicate long CSTs formed from macroconidia. Bar = 30 μm.

4.2.3 Conidial sex tube induction requires the presence of protoperithecia of opposite mating type

Conidial sex tube induction requires the presence of protoperithecia of opposite mating type. Figure 4.5A shows that when macroconidia of *mat A* (male) were added to a female *mat a* culture bearing protoperithecia and incubated for 6 h, the macroconidia formed CSTs. The same result was obtained when the male was *mat a* and the female was *mat A* (not shown). Figure 4.5B shows that when macroconidia (male) of *mat A* were added to a female *mat A*

culture bearing protoperithecia and incubated for 6 h, they did not germinate (similar results were obtained when *mat a* macroconidia were added to *mat a* protoperithecia, data not shown).

Figures 4.5C and D shows that when macroconidia (male) of either the same mating type or the opposite mating type of a *ro-1* female culture (section 5.2), and incubated for 6 h, they did not germinate. The *ro-1* mutant is defective in dynein (section 5.2) and does not produce protoperithecia (section 5.2).

The amount of CST production for each of the treatments shown in Fig. 4.5 is shown in Fig. 4.6. Normally 40-60% of macroconidia produced CSTs 6 h after inoculation in the presence of the opposite mating type bearing protoperithecia.

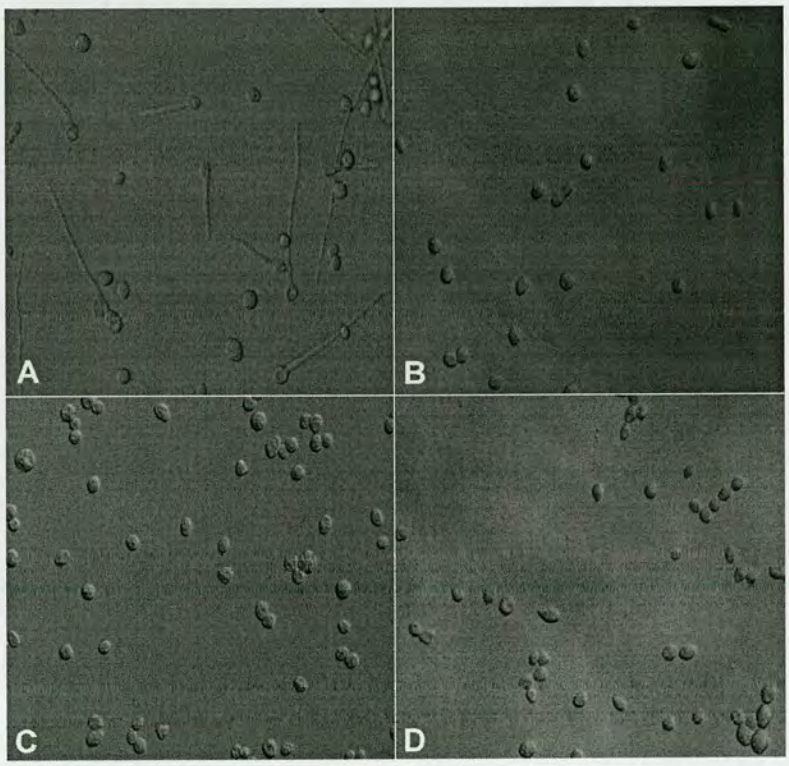

Figure 4.5 Conidial sex tubes are only induced in the presence of a culture of opposite mating bearing protoperithecia. **A**. DIC image of CST (74A + 74a); **B**. DIC image of ungerminated conidia (74A + 74A); **C**. DIC image of ungerminated conidia (74A + ro-1 female sterile *mat A* [74A background]); **D**. DIC image of ungerminated conidia (74a + ro-1 female sterile *mat A* [74A background)). Bar = 30 μm.

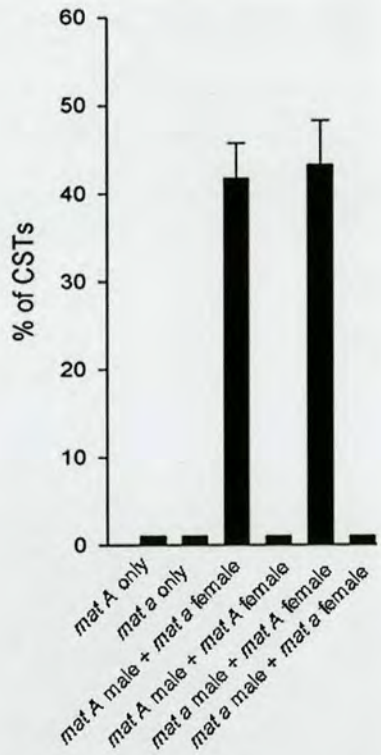

Figure 4.6 Quantitation of CST formation by macroconidia after adding macroconidia to solid Vogel's medium on their own, after adding macroconidia to female cultures bearing protoperithecia of opposite mating type, or after adding macroconidia to female cultures of the same mating type. All cultures were incubated for 6 h. CSTs were identified by being thin, straight, unbranched and not staining with fluorescently labelled wheat germ agglutinin. % of CSTs indicates the percentage of macroconidia which produce CSTs from the total number of macroconidia. The error bars indicate standard errors of the mean. The wild type strains used were 74A and 74a.

4.2.4 Conidial sex tube induction requires sex pheromones and pheromone receptors

Trichogynes are attracted and grow chemotropically towards CSTs but CSTs do not grow towards trichogynes. More than one trichogyne can home towards a single CST (Figs. 4.7A-C) but trichogynes never responded chemotropically to germ tubes or vegetative hyphae. Conidial sex tubes can form < 3 septa. Nuclei from different regions between these septa were observed to pass through into different trichogynes. CST growth only occurred during the first 4-8 h after adding a male conidial suspension to a 7 day old culture of opposite mating type

bearing protoperithecia. Four hours after adding male conidia, trichogynes started to grow chemotropically towards CSTs. After making contact with them, the trichogynes coiled around the CSTs (Figs. 4.3A-D) and fused with them.

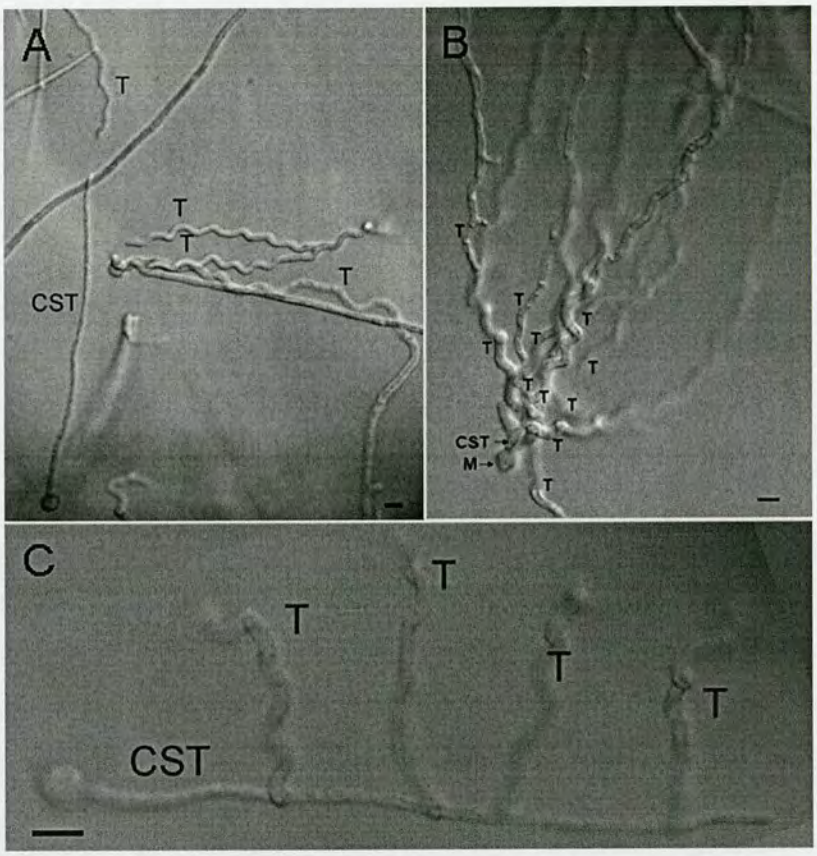

Figure 4.7 Multiple trichogynes are attracted by a single CST. **A**. Four trichogynes (74a) that are homing towards a single CST (74A). **B**. At least 11 trichogynes (74A) that have been attracted towards a single CST (74a). **C**. Four trichogynes (74A) that have been attracted to different points along the length of a single CST (74a). CST, conidial sex tube. M, macroconidium. T, trichogyne. Bars = 10 μm.

The percentage of CSTs produced by sex pheromone (Δ*ccg-4* and Δ*mfa-1*) and sex pheromone receptors mutants (Δ*pre-1* and Δ*pre-2*) were both greatly reduced (~5-10% compared with ~55% in the wild type), when used as a male in a cross with a female and assayed for 8 h (Fig. 4.8). These results indicate that the normal level of CST induction requires the conidia to produce both sex pheromones and pheromone receptors.

After 6 h at 25 °C, 10-20% of macroconidia formed germ tubes in water (in Vogel's

medium 95-100% of macroconidia form germ tubes). When the synthetic pheromone, MFa-1 (which is normally expressed by the *mat a* strain) was added to *mat A* macroconidia in water, macroconidial germination seemed to be completely inhibited at concentrations > 25 ng/ml (Fig. 4.9). At higher concentration of MFa-1 (6.4-25.6 μg/ml), hyphae with the characteristics of CSTs were formed (i.e. they were long, thin, unbranched and exhibited no chemoattraction to each other). The sex pheromone receptor mutant, Δ*pre-1 mat A*, did not respond to this concentration of synthetic MFa-1 pheromone (Fig. 4.9). Interestingly, when the concentration of MFa-1 was > 51.2 μg/ml, CST formation was not induced (Fig. 4.9).

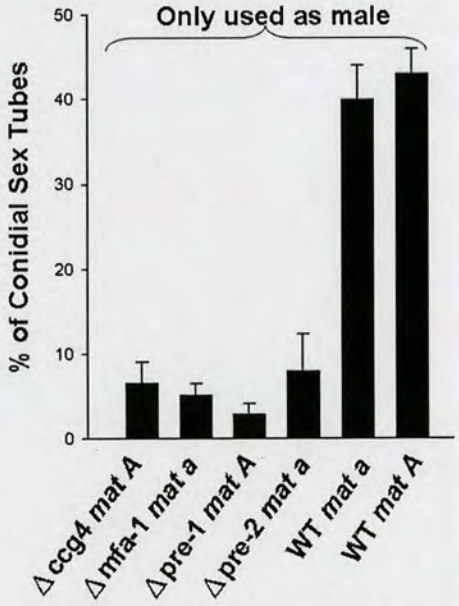

Figure 4.8 Histogram showing quantitation of CST formation in the wild type, and in pheromone (Δ*ccg4* and Δ*mfa-1*) and pheromone receptor (Δ*pre-1* and Δ*pre-2*) mutants when used as the male with wild type female cultures of the opposite mating type. % of Conidial Sex Tubes indicates the percentage of macroconidia which produce CSTs from total number of macroconidia. The error bars indicate standard errors of the mean. The wild type strains used were 74A and 74a.

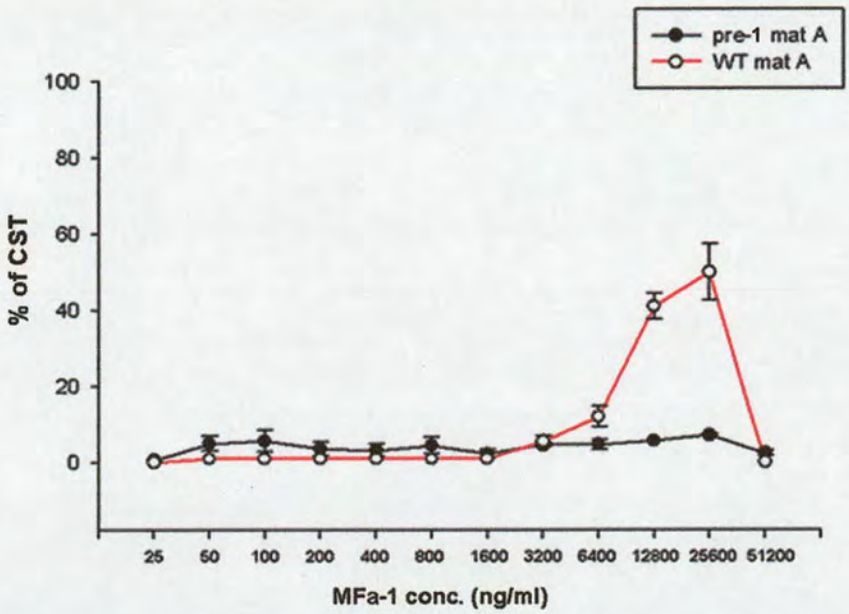

Figure 4.9 Response of wild type and *Δpre-1 mat A* conidia to synthetic sex pheromone MFa-1. Germ tube and CAT formation were inhibited by the pheromone; CST production was stimulated by 3.2-25.6 μg/ml MFa-1 pheromone. % of CSTs indicates the percentage of macroconidia which produce CSTs from the total number of macroconidia. The error bars indicate standard errors of the mean. The wild type strain used was 74A.

4.2.5 Conidial sex tube formation is conidial density dependent

Figure 4.10 showed that CST formation is weakly conidial density dependent and the optimal conidial concentration to produce maximally CSTs was ~10^5 per ml. In contrast, CAT formation was strongly conidial density dependent (optimal conidial density is 10^6 per ml, Roca *et al.*, 2005) and germ tube formation was conidial density independent (Fig. 4.10). Conidial sex tube, germ tube and CAT formation were all inhibited at 10^7 conidia per ml (Fig. 4.10).

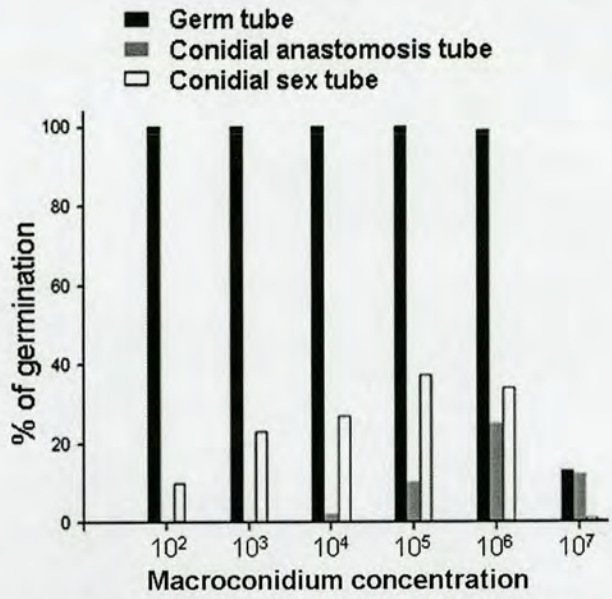

Figure 4.10 Histogram showing the influence of macroconidium concentration on CST, germ tube and CAT formation by the 74A wild type strain. CST formation was performed in SC medium (section 2.3) at 25 °C and quantified after 6 h and germ tube and CAT formation were performed in Vogel's medium (section 2.3) at 35 °C and quantified after 6 h. Data on CAT formation was kindly provided by Dr. M. Gabriela Roca, (University of Edinburgh). % of germination indicates the percentage of macroconidia which germinated from the total number of macroconidia.

4.2.6 The conidial sex tube surface texture is different from other cell types

The surface textures of conidial sex tubes, dry macroconidia (released from their conidiophores), hydrated macroconidia (attached to their conidiophores), germ tubes and CATs were examined in the frozen hydrated state by low-temperature scanning electron microscopy (Fig. 4.11). The surface texture of the CSTs resembled to same extent, the rodlet patterning of the surface of dry macroconidia (Beever & Dempsey, 1978), but possible the 'rodlet' patterning on the CST surface was less marked. The surface texture of hydrated macroconidia was granular, whilst that of germ tubes and CATs was smooth (Fig. 4.11). To determine if CSTs had a different surface chemistry to that of germ tubes, the staining characteristics of the following fluorescently labelled lectins were examined: Concanavalin A lectin (Con A), *Bandeiraea simplicifoliabs* lectin (BSL), *Lens culinaris* agglutinin (LCA),

Lycopersicon esculentum agglutinin (LEA), *Phaseolus limensis* agglutinin (PLA), *Pisum sativum* agglutinin (PSA), Pokeweed agglutinin (PWN), *Tetragonolobus purpureas* agglutinin (TPA) and wheat germ agglutinin (WGA). Only two lectins, WGA and Pokeweed lectin (PWN) showed differential staining of the CSTs *vs.* germ tubes, and only stained germ tubes (Fig. 4.12). Both lectins are selective for N-acetylglucosamine (and thus labelled chitin) which would thus appear to be on the surface of germ tubes but not CSTs (Fujii *et al.,* 2004; Monsigny *et al.,* 1980).

A mutant defective in the *eas* gene that encodes a hydrophobin protein that is responsible for the rodlet patterning on macroconidial surface (Beever & Dempsey, 1978) was found not to produce CSTs (data not shown). This supports the view that the rodlet-like patterning seen in Fig. 4.11A is produced by hydrophobins and that this hydrophobin is required for CST formation.

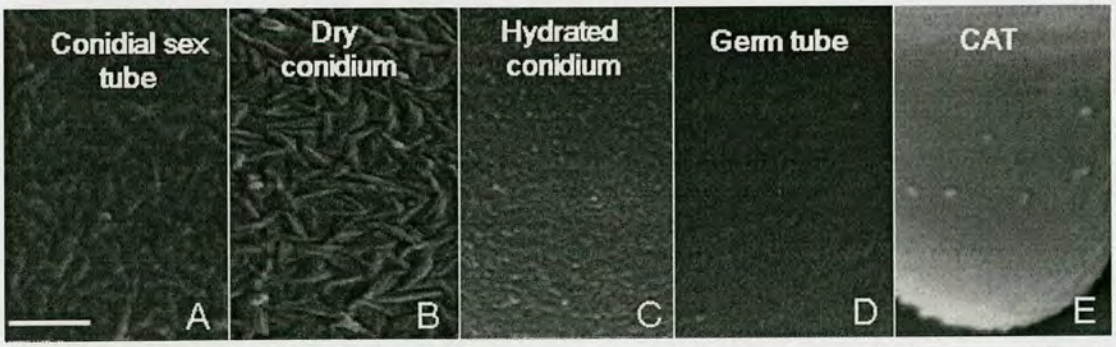

Figure 4.11 High resolution SEMs of surface texture of cells. **A**. Surface texture of a CST. **B**. surface texture of a dry conidium (released from its conidiophore). **C**. Surface texture of a hydrated conidium (still attached to its conidiophore). **D**. Surface texture of a germ tube. **E**. Surface texture of a CAT. Bar = 0.5 µm. The wild type strain used was 74A.

Table 4.1 Compilation of the lectins used in this study

Abbreviation	Name	Plant source	Binding sugar
WGA	Wheat germ agglutinin	Wheat (*Triticum vulgare*)	N-acetylglucosamine
PWA	Pokeweed agglutinin	Pokeweed (*Phytolacca americana*)	N-acetylglucosamine

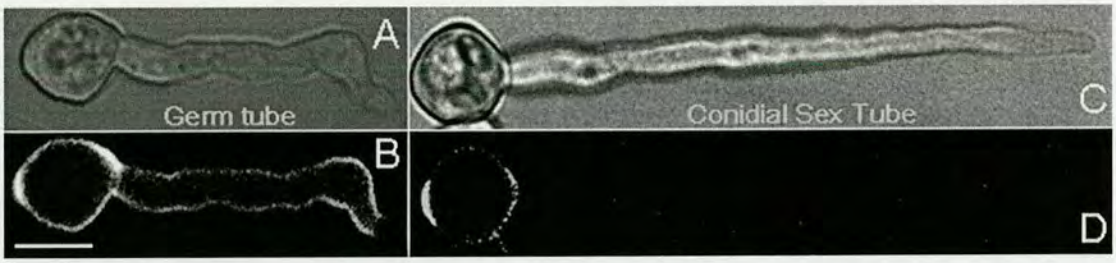

Figure 4.12 Staining of a CST and germ tube with WGA-FITC. **A**. Brightfield image of a germ tube. **B**. Confocal image of the same germ tube shown in A with WGA-FITC. The surfaces of the macroconidium and germ tube are stained. **C**. Brightfield image of a CST. **D**. Confocal image of the same CST shown in **C** showing that WGA-FITC has stained the macroconidium but not the CST. Bar = 5 μm. The wild type strain used was 74A.

4.2.7 Cell cycle arrest occurs in conidial sex tubes

Conidial sex tubes and germ tubes were produced in *mat A* and *mat a* strains expressing H1-GFP to visualize their nuclei. Macroconidia are multinucleate and contain 2-6 nuclei (Davis, 2000). Quantitation of the number of nuclei present at 0 h and 6 h in macroconidia and germ tubes (*mat A*), and after 8 h in CSTs (*mat A*♂+ *mat a*♀) indicated that CSTs possessed less than 6 nuclei whilst the number of nuclei in germ tubes was greatly increased (Fig. 4.13), indicating that cell cycle arrest had occurred in the CSTs. Furthermore, nuclei undergoing mitosis in germ tubes were frequently observed whilst mitotic nuclei in CSTs were never found.

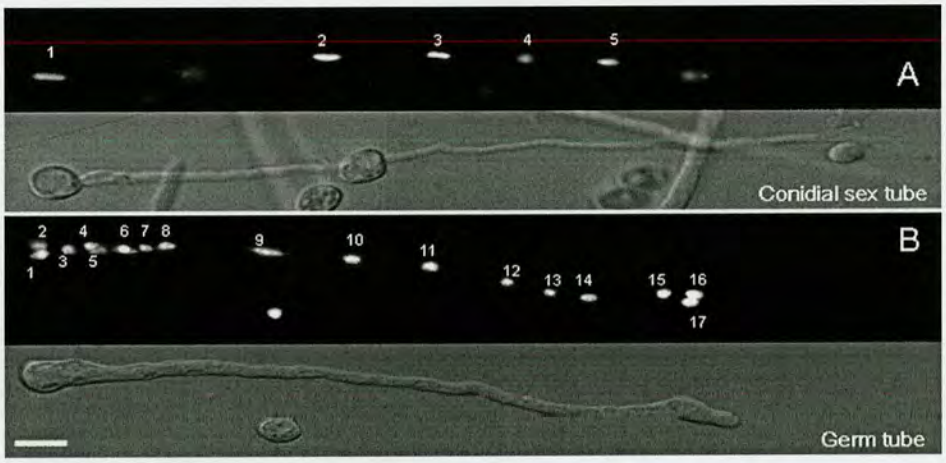

Figure 4.13 Confocal and complimentary brightfield images of a H1-GFP labelled strain of a CST and a germ tube of similar length. **A**. CST containing 5 nuclei. **B**. Germ tube containing 17 nuclei. Bar = 15 µm. The wild type strain used was 74A.

4.3 Discussion

4.3.1 The discovery of a new cell type produced by male conidia

My study has demonstrated for the first time that the hypha (conidial sex tube) produced from macroconidia (but not microconidia) in the presence of pheromone of opposite mating type (and produced by protoperithecia) is a novel new cell type. Under these conditions, germ tube and CAT formation are inhibited. Bistis (1981) did not observe CSTs in his studies on mating in *N. crassa,* probably because he exclusively used *microconidia* as male fertilization agents. In my study, I have primarily used macroconidia as male fertilization agents. Backus (1939) working on *Neurospora sitophila,* showed that trichogynes homing towards "germinated conidia" (Fig. 4.14) which are very similar in appearance to the CSTs derived from macroconidia described here. Furthermore, he stated that "germinated conidia can bring about fertilization as effectively and promptly as can ungerminated conidia" but did not suggest that the germinated conidia may have produced hyphae that were not germ tubes.

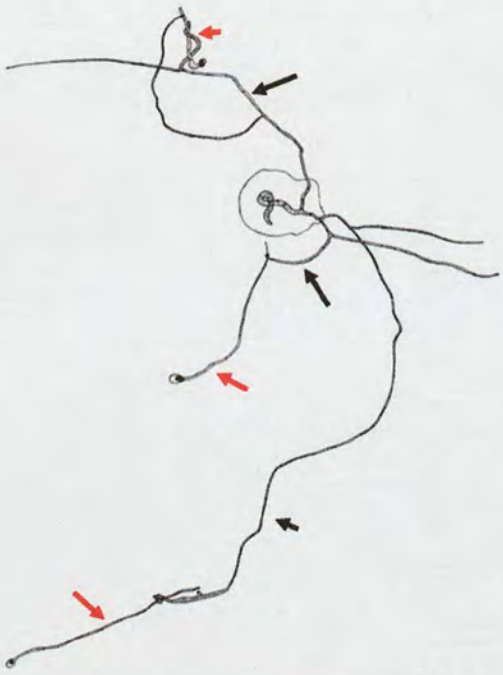

Figure 4.14 Trichogynes homing towards 'germinated macroconidia' in *Neurospora sitophila*. Black arrowheads indicated trichogynes and red arrowheads indicate the '*germinated macroconidia*' (copied and modified from Backus, 1939).

4.3.2 Key features of conidial sex tubes

I have shown that CSTs can be clearly distinguished from germ tubes and CATs, by having the following combination of attributes. They: (1) are thin (thinner than germ tubes but wider than CATs), (2) are long (can be longer than unbranched germ tubes and are much longer than CATs), (3) grow straight (germ tubes tend not to be straight), (4) are unbranched (germ tubes under go branching), (5) do not exhibit positive or negative chemotropic responses towards or away from CSTs or other hyphae (CATs home toward each other whilst germ tubes tend to avoid each other), (6) are produced by macroconidia but not microconidia (microconidia can produce both germ tubes and CATs), (7) are septate (CATs lack septa), (8) lack chitin on their surfaces (in contrast to both germ tubes and CATs), (9) possess a different surface texture to germ tubes and CATs which may be composed of hydrophobin rodlets

(germ tubes and CATs have a smooth surface texture), (10) undergo cell cycle arrest (in contrast to germ tubes), and (11) are produced in a cell density dependent manner (in contrast to germ tubes).

In addition, the arrest of nuclear division in CSTs probably results from sex pheromone signalling as occurs in the budding yeast during mating. However, as in budding yeast, cells continue to grow even through nuclear division has been inhibited (Madden & Snyder, 1998).

4.3.3 Factors which induce and inhibit conidial sex tube induction

Normal conidial germination involving germ tube and CAT formation occurs in the presence of nutrients in *N. crassa* (Schmit & Brody, 1976), although I showed that a 10-20% of macroconidia can form germ tubes in water. Germ tubes are involved in colony establishment whilst CATs function in fusing conidial germlings in the young developing colony (Roca *et al.*, 2005). Conidial sex tubes, on the other hand, form normally in water but require the presence of the opposite mating type to be produced (in my experiments I only tested the synthetic pheromone MFa-1 with *mat A* male cultures, in detail). I also found that both a low concentration (50 ng/ml) and a high concentration (25.6 μg/ml) of the synthetic CCG-4 pheromone induced CST formation in the wild type 74 *mat a* strain (data not shown). Because more experiments would be required to analyse the significance of these results, I did not include these preliminary findings on the effects of synthetic CCG-4 on CST induction in my thesis.

Neurospora crassa produces two different pheromones, MFa-1 (which is hydrophobic) from *mat a* and CCG-4 (which is hydrophilic) from *mat A,* It is not clear why *N. crassa* produces two distinct hydrophobic and hydrophilic pheromones. However, Kim et al. (2002) postulated that MFa-1 may have an additional role in cementing together the hyphae which form the perithecial wall. The hydrophobic nature of MFa-1 requires prenylation which may

involve a second peptide (Kim *et al.,* 2002). An analogous situation may occur in *S. cerevisiae*, where a second peptide (a-factor related peptide) is produced from the pro-a-factor and is involved in cell-cell adhesion (Chen *et al.,* 1997).

In budding yeast, a-factor (which is similar to MFa-1 in *N. crassa*) needs to be prenylated to be fully functional during mating. However, unprenylated a-factor was found to still function in mating but its pheromone activity was reduced ~ 1,000-fold (Caldwell *et al.,* 1994). The synthetic MFa-1 pheromone I used was unprenylated and had a hydroxyl group at its C-terminal which made it hydrophilic.

Conidial sex tube formation was conidial density dependent suggesting that induction may also involve a form of quorum sensing (i.e. a mechanism whereby cells sense their cell density by releasing signal molecules into the environment, Miller & Bassler, 2001). This suggests that there may be signal molecules produced by macroconidia that also play a role in CST induction. The observation that ~3-8% of mutants lacking pheromone receptors (Δ*pre-1 mat A* and Δ*pre-2 mat a*) formed CSTs when used as the male and crossed with wild type female cultures, supports this view.

Spores of many fungi germinate poorly, if at all, at high spore concentrations and this is due to diffusible self-inhibitors produced by the fungi themselves (Macko & Staples, 1973). Germ tube, CAT and CST formation were inhibited by this unknown self-inhibitor in *N. crassa*, when high concentrations of the conidia (> 10^7/ml) were used.

4.3.4 Germ tube and CAT formation are inhibited by pheromone

My results showed that germ tube and CAT formation were inhibited when cultures bearing protoperithecia were present. This was not mating-type dependent. The inhibition of conidial germination by the presence of a previously formed mycelium has also been reported by Bistis (1981). These results suggested that both sex pheromones of both mating types can

cause the inhibition.

4.3.5 Active signalling by the male cell during mating but why?

Previous studies on mating in *N. crassa* have focused on the female response of trichogyne to the male conidium but no attention has been paid to the response of the conidium to the trichogyne. This is probably because no morphological changes occur to the male ungerminated conidium during mating. I have produced the first evidence that a male cell can actively respond to the female in *N. crassa* by forming a CST. This induction seems to due to the sensing of sex pheromone produced by protoperithecia of opposite mating type. In budding yeast, when pheromones are produced, cells of opposite mating types become polarized and grow toward to their partner (Madden & Snyder, 1998). However, in *N. crassa* the only cells that respond chemotropically to sex pheromone are trichogynes (Bistis, 1981); the CSTs do not grow towards trichogynes.

The question then is why do macroconidia produce CSTs given that these conidia when ungerminated can probably attract and fused with trichogynes to effect fertilization? The only hypothesis I can suggest is that by being longer and having a much higher surface area to volume ratio, which perhaps results in the release of more sex pheromone, CST may be more effective at attracting trichogynes than ungerminated conidia.

4.4 Summary

1. Conidia undergo three developmental pathways resulting in the production of germ tubes, CATs and CSTs (Fig. 4.15).
2. The CST is a new cell type, which is morphologically and physiologically different and under separate genetic control, from the other two types of hyphae (germ tubes and CATs) produced by conidia.

3. Conidial sex tubes are actively induced by sex pheromone of the opposite mating type.

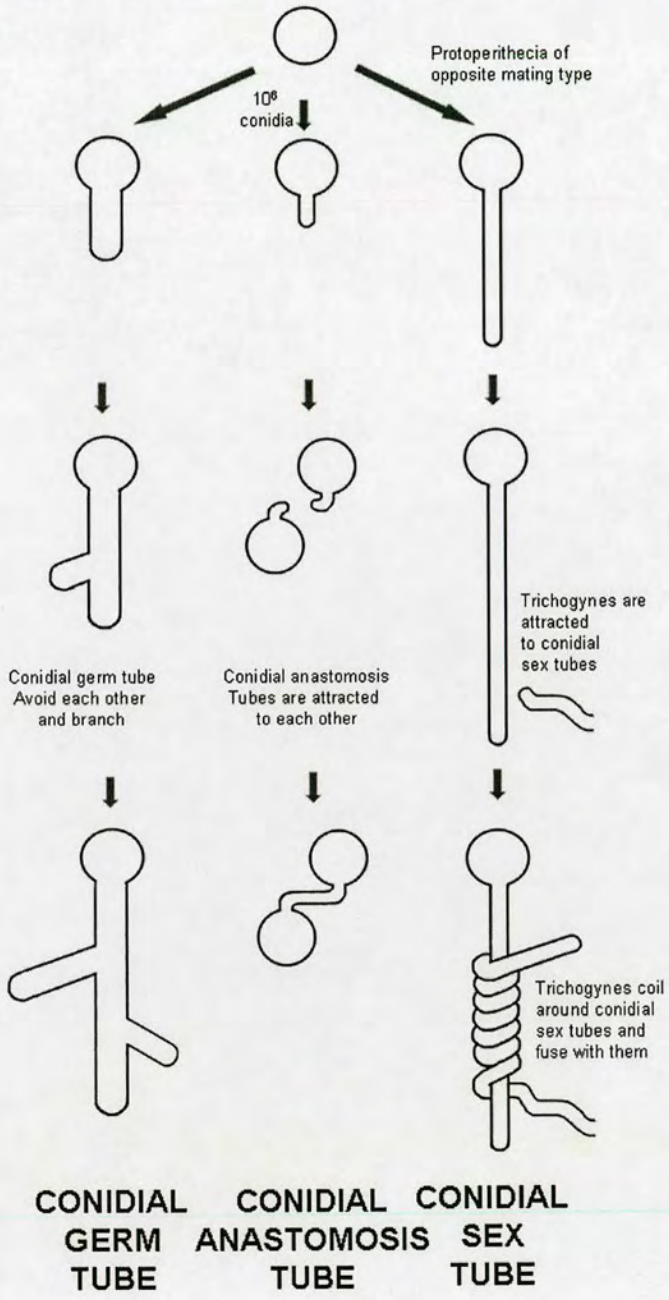

Figure 4.15 Macroconidial germination can result in three developmental pathways leading to three different types of specialized hyphae (the conidial germ tube, conidial anastomosis tube and conidial sex tube).

References

Backus, M.P. 1939. The mechanics of conidial fertilization in *Neurospora sitophila. Bull. Torrey Botan. Club*. 66, 63-76.

Beever, R.E., Dempsey, G.P. 1978. Function of rodlets on the surface of fungal spores. *Nature* 272, 608-610.

Bistis, G.N. 1981. Chemotropic interactions between trichogynes and conidia of opposite mating type in *Neurospora crassa. Mycologia* 73, 959-975.

Bistis, G.N., Perkins, D.D., Read, N.D. 2003. Cell types of *Neurospora crassa. Fungal Genet. Newsl.* 50, 17–19.

Caldwell, G.A., Wang, S.H., Xue, C.B., Jiang, Y., Lu, H.F., Naider, F., Becker, J.M. 1994. Molecular determinants of bioactivity of the *Saccharomyces cerevisiae* lipopeptide mating pheromone. *J. Biol. Chem.* 269, 19817-19825.

Chen, P., Choi, J.D., Wang, R., Cotter, R.J., Michaelis, S. 1997. A novel a-factor-related peptide of *Saccharomyces cerevisiae* that exits the cell by a Ste6p-independent mechanism. *Mol. Biol. Cell* 8, 1273-1291.

Davis, R.H. 2000. *Neurospora*: contributions of a model organism. Oxford University Press, New York.

Fujii, T., Hayashida, M., Hamasu, M., Ishiguroc, M., Hata, Y. 2004. Structures of two lectins from the roots of pokeweed (*Phytolacca americana*). *Acta Cryst.* D60, 665-673.

Kim, H., Metzenberg, R.L., Nelson, M.A. 2002. Multiple functions of *mfa-1*, a putative pheromone precursor gene of *Neurospora crassa. Eukaryot. Cell*, 1, 987–999.

Macko, V., Staples, R.C., Gershon, H., Renwick, J.A.A. 1970. Self-inhibitor of bean rust uredospores: Methyl 3,4-dimethoxycinnamate. *Science* 170, 539–540.

Madden, K., Snyder, M. 1998. Cell polarity and morphogenesis in budding yeast. *Ann. Rev. Microbiol.* 52, 687-744.

Miller M B, Bassler, B. L. 2001. Quorum sensing in bacteria. *Ann Rev Microbiol.* 55, 165-199.

Monsigny, M., Roche, A.C., Sene, C., Maget-Dana, R., Delmotte, F. 1980. Sugars-lectin interactions: how does wheat germ agglutinin bind sialoglycoconjugates, *Eur. J. Biochem.* 104, 147–152.

Nelson, M.A., Metzenberg, R.L. 1992. Sexual development genes of *Neurospora crassa. Genetics* 132, 149-162.

Roca, M.G., Arlt, J., Jeffree, C.E., Read, N.D. 2005. Cell biology of conidial anastomosis tubes in *Neurospora crassa. Eukaryot. Cell*, 4, 911-919.

Schmit, J.C., Brody, S. 1976. Biochemical genetics of *Neurospora crassa* conidial germination. *Bacteriol. Rev.* 40, 1-41.

CHAPTER 5

Influence of motor proteins and cytoskeleton on nuclear behaviour during mating

5.1 Introduction

Nuclear migration in *N. crassa* is cytoplasmic microtubule dependent (Minke *et al.*, 2000) and is regulated by the microtubule-associated motor proteins, dynein (Plamann *et al.*, 1994; Bruno *et al.*, 1996; Minke *et al.*, 1999a,b) and the kinesins (Seiler *et al.*, 1997). There is one dynein and ten kinesins in *N. crassa* (section 1.6.2 and section 1.6.3). The dynein is a multi-subunit protein complex and composed of dynein, dynactin and lis-1 (section 1.6.2; Table 1.1). There are 6 subunits that have been shown or predicted to be in the dynein (RO-1, NCU02610, NCU03882, NCU09095, NCU09142, and NCU09982), 7 subunits in dynactin (RO-2, RO-3, RO-4, RO-7, RO-12, NCU04043, NCU08375) and 3 subunits in LIS-1 (RO-11, NCU04312, NCU04534). The kinesin proteins that have been shown or predicted in *N. crassa* are NKIN, NKIN-2, NKIN-3, KIF-21A, KLP-2, KLP-3, KLP-4, KLP-5, KLP-6 and KLP-7

(Borkovich *et al.*, 2004; section 1.6.1; Table 1.1). Four myosin proteins, MYO-1, MYO-2, MYO-5, and an unnamed myosin fused to chitin synthase, have been predicted to be encoded in the *N. crassa* genome but their functions are unknown (section 1.6.3; Table 1.1).

The aims of the experimental research described in this chapter were to:

1. Show the influence that different motor proteins had on male and female nuclear behaviour during mating when male and female strains lacking different motor proteins were crossed.
2. Show how cytoskeletal inhibitors influence male nuclear behaviour during mating.

These aims were fulfilled by using confocal live-cell imaging of strains in which nuclei had been labelled with H1-GFP, deletion mutants lacking different motor proteins, and pharmacological treatments which disrupt microtubules and actin microfilaments, and inhibit myosin activity. All strains used in this study are either wild type 74 (*mat A* or *mat a*) or with 74 (*mat A* or *mat a*) wild type background (KO mutants [*mat A* or *mat a*] and GFP labelled strains [*mat A* or *mat a*]).

5.2 Results

5.2.1 Microtubule and actin inhibitors influence perithecial development and male nuclear movement

Microtubule and actin inhibitors (Table 5.1) were added to fertilized cultures and assessed 2 days later for perithecial formation (section 2.7.4). Both were found to prevent perithecial formation (Table 5.1).

Table 5.1 Analysis the influence of microtubule and actin microfilament inhibitors on perithecial development

Compound type of chemical	Working concentration	Target	Perithecial development
Benomyl	10 µg/ml	Microtubules	-
Latrunculin B	20 µM	actin	-

5.2.1.1 Microtubules are required for normal male nuclear behaviour

Benomyl treatment was found to cause the normally long microtubules in trichogynes (Fig. 5.1A) to fragment and the microtubule fragments seemed to clump or became bundled together (Fig. 5.1B). Within 1 h of treating trichogynes with benomyl, the movement of male nuclei passing through them slowed down and eventually stopped. This was typically associated with the nuclei that normally alternated between being elongated and condensed becoming permanently condensed (Fig. 5.2A). In addition, the male nuclei often developed protrusions (Fig. 5.2B). When trichogynes that had fused with macroconidia/CSTs were treated with benomyl, the female nuclei normally lost their rounded shape (Fig. 5.2C).

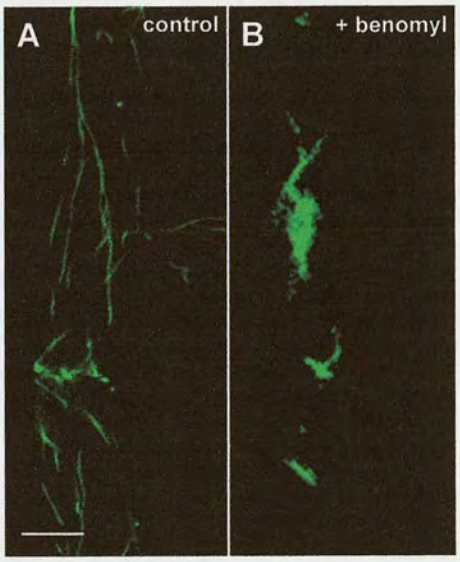

Figure 5.1 Effect of benomyl on microtubules in trichogynes (N2505 *mat a*). **A**. Normal microtubule organization. **B**. Depolymerized microtubules 15 h after treatment with 10 µg/ml benomyl. Note that the microtubule fragments seem to have clumped together. Bars = 5 µm.

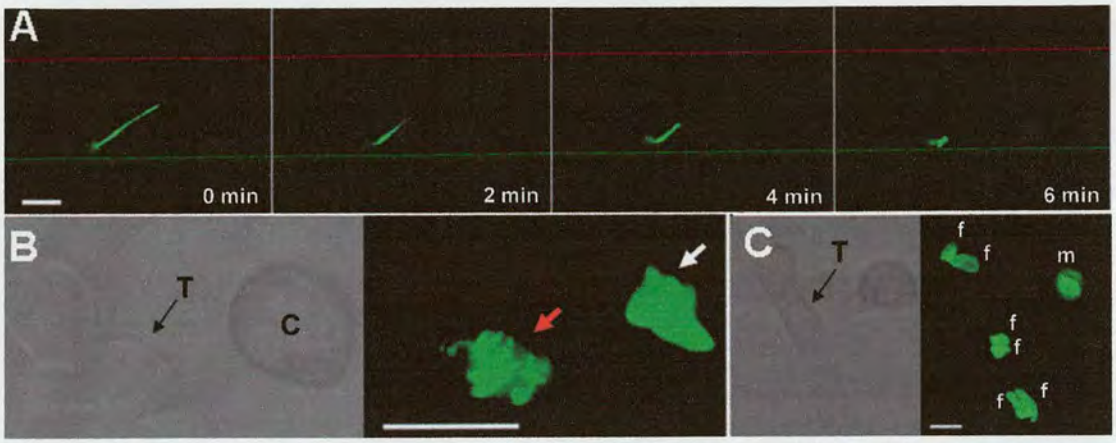

Figure 5.2 Effect of benomyl on male and female nuclei after conidium-trichogyne fusion. **A.** Time course showing a male nucleus (N2282 *mat A*) in a trichogyne (74A) not moving and becoming permanently condensed 1 h after treatment with benomyl. **B.** Male nucleus (N2282 *mat A*) with surface protrusions (red arrow) in a trichogyne (74a) (T) and a nucleus (N2282 *mat A*) without surface protrusions (white arrow) still in the conidium (C). **C.** Female nuclei in trichogyne (N2283 *mat a*) that have lost their rounded shape. The male (N2282 *mat A*) and female (N2283 *mat a*) nuclei have been labelled with H1-GFP. f, female nucleus. m, male nucleus. Bars = 5 µm.

5.2.1.2 Actin and myosin are required for normal male nuclear behaviour

The actin inhibitor, Latrunculin B, inhibited the movement of male nuclei. In contrast to benomyl-treated male nuclei, the male nuclei treated with Latrunculin B finally became more-or-less immobilized in an elongated rather than a condensed state (Fig. 5.3). Latrunculin B had no discernible effect on the female nuclei (data not shown).

Figure 5.3 A male nucleus immobilized in an elongated state after treatment with Latrunculin B. The male nuclei have been labelled with H1-GFP (N2282 *mat A*). Bars = 5 µm.

5.2.2 Dynein, kinesin and myosin mutants influence perithecial development and male and female nuclear behaviour

The motor protein mutants used in this chapter are listed in Table 5.2 (also see Tables 2.6 and 2.7). Protoperithecial, perithecial and ascospore formation were assayed by using a wide field compound microscope and a stereomicroscope. Experiments were performed on SC agar medium (section 2.3) at 24 °C under continuous light for 5 days and conidia of the opposite mating type were added and then left for another 14 days. The method of image analysis used to score the number of protoperithecia and perithecia formed is shown in Fig 5.4A and described in section 2.10. In addition, 10 mature perithecia were collected from cultures 10 days after fertilization and the numbers of ascospores formed (none, few or normal number) were assessed. Figures 5.4B and 5.4C show the experimental set up for investigating how each mutant partner influenced the wild type partners' nuclear behaviour.

Table 5.2 List of motor protein mutants and mutants expressing H1-GFP used in this chapter with orthologs that have been functionally analysed in *A. nidulans* (for more details about these strains, see Table 2.4; for more details about orthologs of these genes in *S. cerevisiae* and *S. pombe*, see Table 1.1)

Strain name*	Predicted protein	Orthologs in *A. nidulans*
	Dynein/Dynactin	
Δdica	Dynein intermediate chain	cytoplasmic dynein intermediate chain
ΔdicA	Dynein intermediate chain	cytoplasmic dynein intermediate chain
Δdlca	Dynein light chain	conserved hypothetical protein**
ΔdlcA	Dynein light chain	conserved hypothetical protein**
Δdyn-2a	Dynein light chain	None
Δdyn-2A	Dynein light chain	None
Δdyn-27a	Dynactin p27 subunit	None
Δdyn-27A	Dynactin p27 subunit	None

ro-1a	Dynein heavy chain	dynein heavy chain
ro-1a **(H1-GFP)**	Dynein heavy chain	dynein heavy chain
ro-2a **(H1-GFP)**	Dynactin p62 family	Dynactin p62 family
ro-3a **(H1-GFP)**	largest subunit of the dynactin (dynein activator) complex	p150 dynactin NUDM
Δ*ro-11a*	Nuclear distribution	NUDE
Δ*ro-11A*	Nuclear distribution	NUDE
	Kinesin	
Δ*kar-3a*	kinesin-related protein	KLPA
Δ*kip-2a*	kinesin-related protein	kinesin motor protein**
Δ*nkin-2a*	Neurospora kinesin 2	conserved hypothetical protein**
Δ*nkinA*	Neurospora kinesin	kinesin motor protein**
	Myosin	
Δ*myo-1a*	Class I myosin	myosin I myoA
Δ*myo-2a*	Class II myosin	AN4706: conserved hypothetical protein**
Δ*myo-5A*	Class V myosin	AN8862: conserved hypothetical protein**

*, Last letter of strain name refers to mating-type background. **, unknown function in *A. nidulans*.

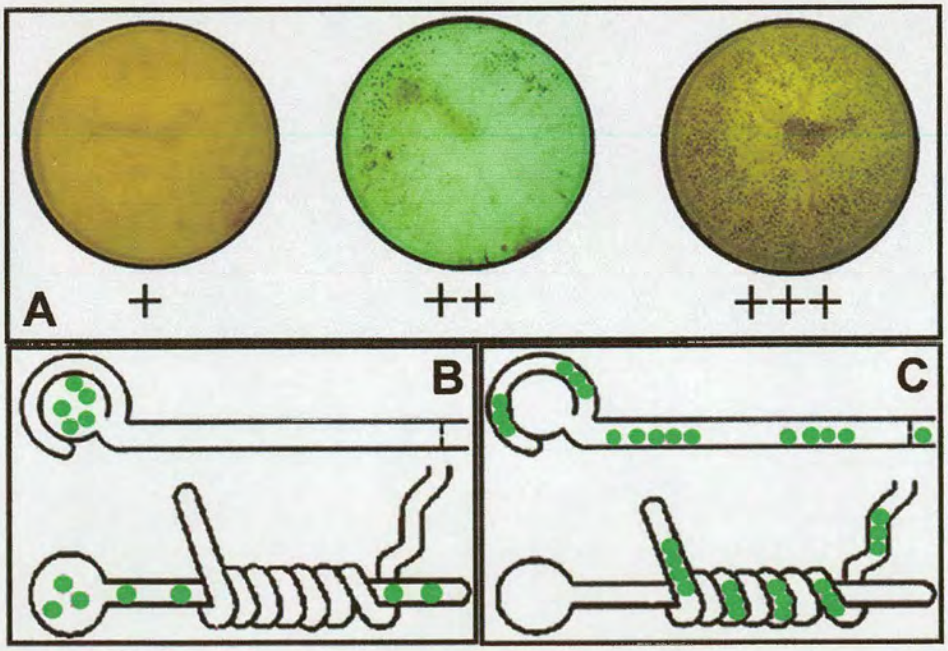

Figure 5.4 Methods used in this chapter. **A**. Unless otherwise stated, perithecial numbers per plate were scored as: - = < 10; + = 10^1-10^2; ++ = 10^2-10^3; +++ = > 10^3. **B**. The experimental set up for investigating how the female mutant influenced the behaviour of wild type male nuclei (nuclei in conidia or conidial sex tubes labelled with H1-GFP [74A/a wild type background]). **C**. The experimental set up for investigating how the male mutant influenced the behaviour of wild type female nuclei (nuclei in trichogynes labelled with H1-GFP[74A/a wild type background]).

5.2.2.1 Dynein, kinesins and myosins in the female partner influence sexual development

Wild types (74 *mat A* and 74 *mat a*) were used as male and crossed with motor protein mutants as the female. The results are shown in Table 5.3 and summarized as follows:

1. All the *ro* mutants (*ro-1*, *ro-2*, *ro-3* and Δ*ro-11*) used in this study were female sterile and none formed protoperithecia.
2. Almost all the motor protein mutants (Δ*dicA*, Δ*dlca*, Δ*dlcA*, Δ*dyn-2a*, Δ*dyn-2A*, Δ*dyn-27a*, Δ*dyn-27A*, Δ*kar-3a*, Δ*kip-2a*, Δ*nkin-2a*, Δ*nkinA*, Δ*myo-1a*, Δ*myo-2a*) produced numerous protoperithecia similar to the wild type, with the exception of Δ*dica*, which formed very few.
3. Only Δ*nkinA* formed normal numbers of perithecia.
4. Only Δ*nkinA*, Δ*myo-1a*, Δ*dyn-27A* and Δ*dica* formed normal numbers of ascospores.

Table 5.3 Mating assay when male is the wild type (74A/74a) and the female is the mutant (derived from wild type 74A/74a)

	Phenotype (mutant as female)		
Strain name (female)	**Protoperithecial formation**	**Perithecial formation**	**Ascospore formation**
	Dynein		
Δ*dica*	-	+	+*
Δ*dicA*	+++	-^{NP}	-
Δ*dlca*	+++	++^{PD}	+++
Δ*dlcA*	+++^{NT}	++^{PD}	-^{N}

Δdyn-2a	+++[NT]	+[PD]	-*
Δdyn-2A	+++	+[PD]	+++*
Δdyn-27a	+++	+	+
Δdyn-27A	+++[PPD]	++ [PD]	+++
ro-1a	-[NP]	-	-
ro-2a	-[NP]	-	-
ro-3a	-[NP]	-	-
Δro-11a	-[NP]	-	-
Δro-11A	-[NP]	-	-
	Kinesin		
Δkar-3a	+++	+[PD]	+*
Δkip-2a	+++[THD]	+[PD]	-[N]
Δnkin-2a	+++	+[PD]	+*
ΔnkinA	+++	+++	+++
	Myosin		
Δmyo-1a	+++	++	+++
Δmyo-2a	+++	+ [PD]	+*

*, very few ascospores and both asci and ascospore development were abnormal; N, no asci or ascospores were found; NT, no trichogynes were found; THD, trichogyne homing delayed; PD, perithecial development delayed; PPD, protoperithecial development delayed; NP, no protoperithecia.

5.2.2.2 Dynein, kinesins and myosins in the male partner influence sexual development

Mutants were used as the male and crossed with the wild type (74 *mat A* and 74 *mat a*) which was the female. The results are shown in Table 5.4 and summarised as follows:

1. Sexual reproduction was normal in Δ*dyn-2*, Δ*dyn-27,* Δ*nkin* or Δ*nkin-2*.
2. When Δ*dica* was the male, the numbers of perithecia and ascospores were reduced. Interestingly, female H1-GFP labelled nuclei were not observed in ascospores when Δ*dica* was crossed with the wild type female expressing H1-GFP.
3. When the Δ*dlc* male was used as either mating type, reduced numbers of perithecia were formed, but only in *mat A* were the number of ascospores reduced.

4. Δ*myo-1* and Δ*myo-2* formed few perithecia and none of these contained ascospores.
5. Δ*kar-3a* produced few perithecia and few ascospores.
6. The number of perithecia was reduced when Δ*ro-11* was used as male but only Δ*ro-11a* produced a reduced number of ascospores.

Table 5.4 Mating assay when female was the wild type (74A/74a) and the male was the mutant (derived from wild type 74A/74a)

	Phenotype (mutant as male)	
Strain name (male)	**Perithecial formation**	**Ascospore formation**
	Dynein/Dynactin	
Δ*dica*	+++	++
Δ*dlca*	+	+++
Δ*dlcA*	++	+
Δ*dyn-2a*	+++	+++
Δ*dyn-2A*	+++^{FT}	+++
Δ*dyn-27a*	+++	+++
Δ*dyn-27A*	+++	+++
Δ*ro-11a*	++	+
Δ*ro-11A*	++	+++
	Kinesin	
Δ*kar-3a*	+	+
Δ*nkin-2a*	++^{NT}	+++
Δ*nkinA*	+++	+++
	Myosin	
Δ*myo-1a*	+	-
Δ*myo-2a*	+	-

NT, no trichogynes were found; FT, few trichogynes were found.

5.2.2.3 How do motor proteins influence the behaviour of male and female nuclei during mating?

In the previous chapter (chapter 3), the behaviour of the wild type female and male

nuclei was characterized. After trichogyne-conidium fusion, the female nuclei became: (1) blocked in nuclear division, (2) immobilized, (3) rounded up, and (4) clumped together. In contrast, the male nuclei behaved in the following way: (1) they became blocked in nuclear division, (2) they moved unidirectionally towards the ascogonium, (3) they moved in succession through the trichogyne, (4) all of the male nuclei from a macroconidium passed through the trichogyne, (5) they usually transiently stopped and condensed as they passed through trichogyne septal pores, (6) they exhibited an 'inchworm-like' movement (i.e., repeated 'elongation and condensation').

The results of the mating assay showed that dynein, kinesins and myosins from both the male and female partners influence sexual development in *N. crassa* (sections 5.2.2.1 and 5.2.2.2; Tables 5.3 and 5.4). I next examined by time lapse imaging using confocal microscopy the influence of these motor proteins on male and female nuclear behaviour in which the mutant was used as one partner and the nuclear behaviour observed was that of the other partner in which the nuclei had been labelled with H1-GFP. In these experiments, therefore, I was analysing the influence of each motor protein encoded by one partner on the nuclear behaviour of the other partner. The results are summarized in Tables 5.5 and 5.6.

5.2.2.4 Motor proteins from the female influence male nuclear behaviour

In summary (Table 5.5), three dynein subunits (DYN-2, DLC and DIC), one dynactin subunit (DYN-27), two kinesins (NKIN-2 and KAR-3) and one myosin (MYO-2) from the female influenced the behaviour of male nuclei in trichogyne.

Table 5.5 Motor proteins encoded by the female influence nuclear behaviour in male

		male wild type nuclei labelled with H1-GFP		
		Nuclei moved through trichogyne	Nuclei exhibited unidirectional movement	Nuclei moved in succession
		Dynein		
	Δ*dic*	+	-	-
	Δ*dlc*	+	-	-
	Δ*dyn-2*	+	-	-
	Δ*dyn-27*	+	-	-
		Kinesin		
female	**Δ*kar-3***	+	-	-
mutants	**Δ*kip-2***	+	+	+
	Δ*nkin-2*	+	-	-
		Myosin		
	Δ*myo-1*	+	+	+
	Δ*myo-2*	+	-	+
	Δ*myo-5*	+	+	+

5.2.2.4.1 Four proteins in the dynein/dynactin complex from the female influence male nuclear behaviour

All *ropy* (*ro*) mutants examined in this study were female sterile (see Table 5.3), but the dynein/dynactin mutants, Δ*dic*, Δ*dlc*, Δ*dyn-2* and Δ*dyn-27*, formed protoperithecia. The influence on male nuclear behaviour of four proteins (DIC, DLC, DYN-2 and DYN-27) in the dynein/dynactin complex from the female partner was examined. Wild type male nuclei entered trichogynes of all four dynein/dynactin mutants but they were all unable to exhibit unidirectional movement or move in succession down the trichogynes (Figs. 5.5A-E). The male nuclei still moved in the overall direction of ascogonium but they look much longer to reach the ascogonium compared with wild type nuclei. However, each of the female deletion mutants had a different phenotype with regard to male nuclear behaviour.

DLC is a dynein light chain subunit protein with homologs in *S. pombe* and *A. nidulans* but not in *S. cerevisiae* (Tables 1.1 and 5.2). Figure 5.5A and movie 5.1 showed the male nuclei unable to exhibit unidirectional movement.

DYN-2 is a cytoplasmic light chain dynein subunit that has homologs in *S. cerevisiae* and *S. pombe* (Table 1.1) but not in *A. nidulans* (Table 5.2). In some cases, the male nuclei in Δ*dyn-2A* trichogynes became immobilized, ring-shaped (Fig. 5.5B) and seemed to stick to the plasma membrane (Fig. 5.5C). In movie 5.2, the ring-shaped male nucleus is spinning around with one point apparently stuck to the plasma membrane.

According to its protein sequence, DYN-27 is classified within the Dynactin p27 protein family but no homologs of this protein are present in *S. cerevisiae*, *S. pombe* or *A. nidulans*. In Δ*dyn-27A* trichogyne, the wild type male nuclei stopped at the septal pores and became very disorganized (Fig. 5.5D and movie 5.4) compared with the compact and condensed wild type male nuclei moving through septal pores in wild type trichogynes (Fig. 3.8) In addition, they tended to aggregate in the trichogynes and move to the ascogonium very slowly (Fig. 5.5E), and overall exhibited little dynamism in term of nuclear movement. The dynamics of the male nuclear movement in Δ*dyn-27a* trichogyne was completely abolished.

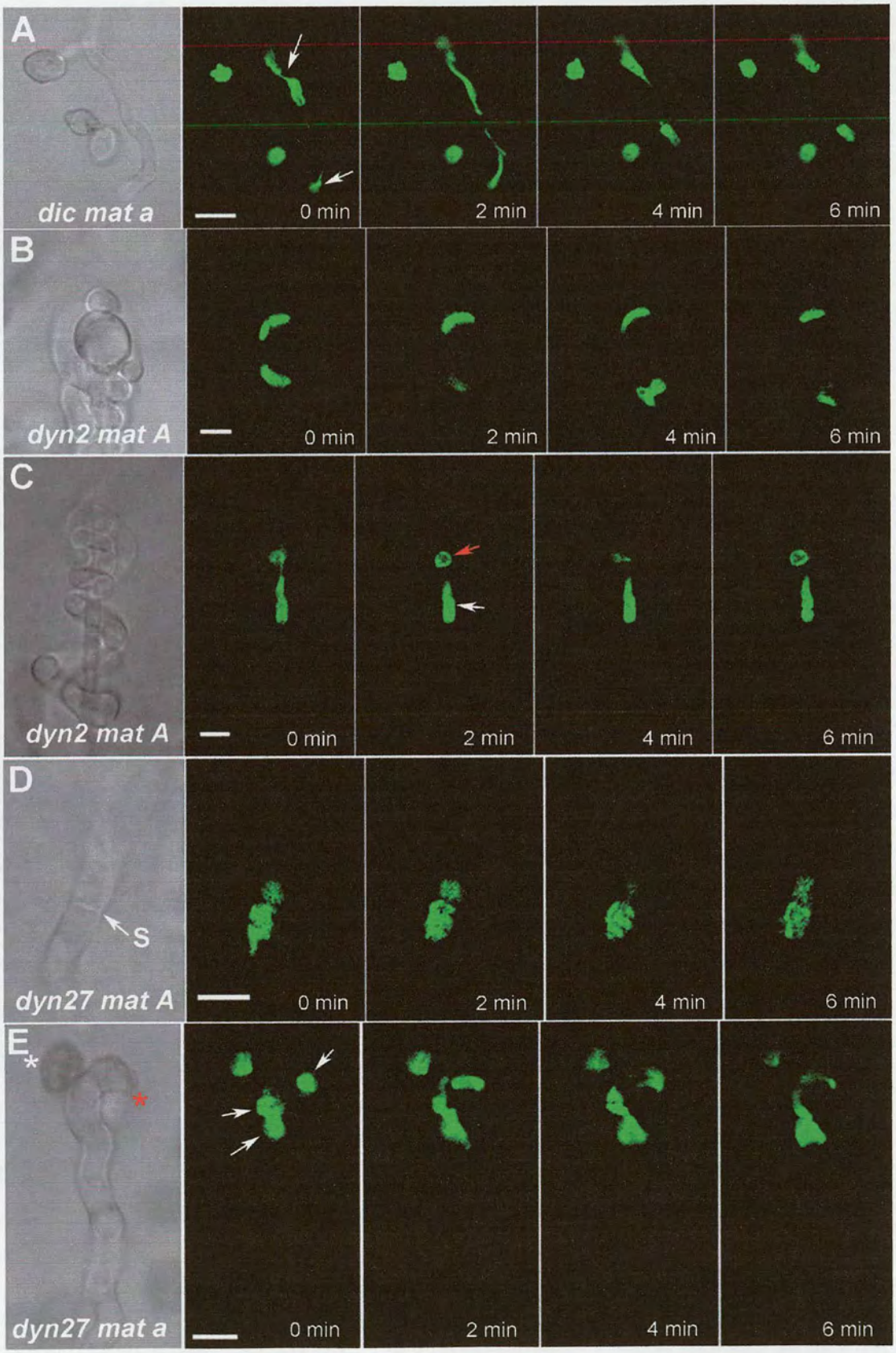
A
dic mat a
0 min
2 min
4 min
6 min
B
dyn2 mat A
0 min
2 min
4 min
6 min
C
dyn2 mat A
0 min
2 min
4 min
6 min
D
S
dyn27 mat A
0 min
2 min
4 min
6 min
E
*
*
dyn27 mat a
0 min
2 min
4 min
6 min

Figure 5.5 Time courses showing wild type male nuclear behaviour in the trichogyne or CST of dynein/dynactin female mutants. The male nuclei have been labelled with H1-GFP. Wild type male nuclei all moved slowly following conidium/CST fusion with a trichogyne through the trichogyne of the mutants but did not exhibit unidirectional movement or movement in succession. Adjacent nuclei tended to move back and forth. Arrows indicate male nuclei in trichogynes; nuclei without arrows are male nuclei in macroconidia or conidial sex tubes (see chapter 4). **A**. Δ*dlca*. Two male nuclei in trichogyne. White arrows indicate two male nuclei in the trichogyne. Also see movie 5.1. **B**. Δ*dyn-2A*. Two male nuclei in a trichogyne wrapped around a CST. Also see movie 5.2. **C**. Δ*dyn-2A*. One male nucleus (white arrow) in a CST and one male nucleus (red arrow) in a trichogyne after a CST has fused with the trichogyne. Also see movie 5.3. **D**. Δ*dyn-27A*. One male nucleus stuck in moving through a septal pore. S, Septum. Also see movie 5.4. **E.** Δ*dyn-27a*. Three male nuclei (white arrow) that have passed through into the trichogyne from a conidium (red asterisk). The other male nucleus is in a conidium (white asterisk) that has not fused with the trichogyne. Also see movie 5.5. Bars = 5 μm.

5.2.2.4.2 Two kinesins from the female influence male nuclear behaviour

The influence on male nuclear behaviour of three kinesins (KAR-3, KIP-2 and NKIN-2) encoded by the female was examined in the deletion mutants Δ*kar-3*, Δ*kip-2* and Δ*nkin-2* used as female.

KAR-3 is a kinesin-related protein and has homologs in *S. cerevisiae, S. pombe* and *A. nudulans* (Tables 1.1 and 5.2). Male nuclei were delayed in passing through Δ*kar-3a* trichogynes. In contrast to normal male nuclear behaviour (Fig. 3.8), the male nuclei started elongating before they passed into the trichogyne and all the male nuclei tended to crowd around the point where the female trichogyne and male cell fused (Fig. 5.6A). The male nuclei eventually passed through the Δ*kar-3a* female trichogynes but they did not become very elongated during movement and moved very slowly (e.g. < 15 μm in 6 min in Fig. 5.6B). The wild type male nuclear velocity in wild type trichogynes was 20-50 μm per min (section 3.2.9; Fig. 3.8). The male nuclei also did not exhibit unidirectional movement or move in succession through the Δ*kar-3a* trichogynes (see movie 5.6 and 5.7 in Appendix I).

KIP-2 is a kinesin-related motor protein and has homologs in *S. cerevisiae, S. pombe* and *A. nudulans* (Tables 1.1 and 5.2). Male nuclei became elongated whilst moving through Δ*kip-2a* trichogynes but were unable to maintain their unidirectional direction (Fig. 5.6C).

NKIN-2 is Δ*nkin-2,* a conventional kinesin motor protein that has been previously characterized in *N. crassa* (Steinberg & Schliwa, 1995) and has homologs in *A. nidulans* but none in *S. cerevisiae* and *S. pombe* (Tables 1.1 and 5.2). It is an unusually fast microtubule motor protein (Kallipolitou *et al.,* 2001). Male nuclei were impaired in unidirectional movement and did not move in succession down the trichogyne (Fig. 5.6D).

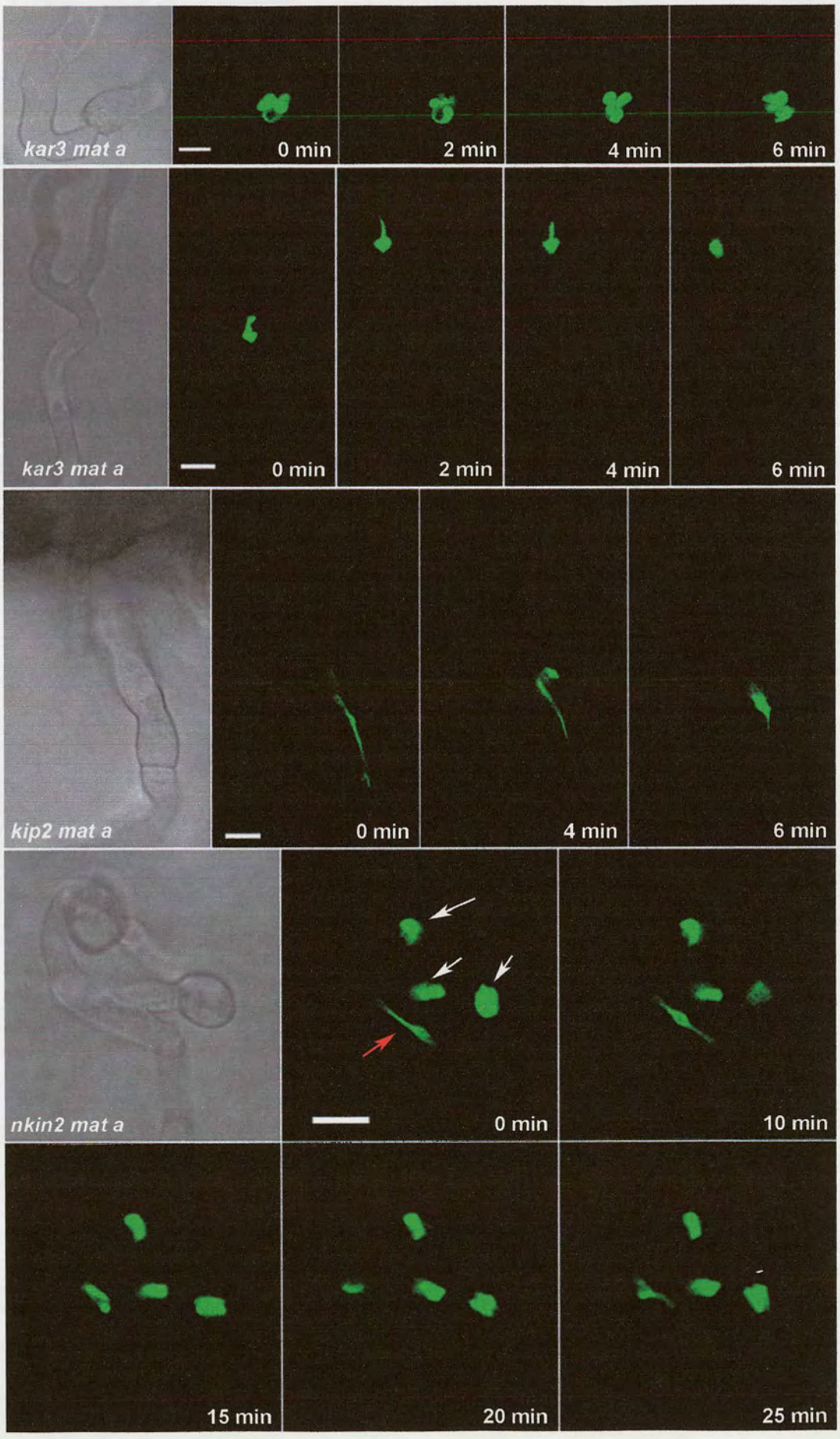
kar3 mat a
0 min
2 min
4 min
6 min
kar3 mat a
0 min
2 min
4 min
6 min
kip2 mat a
0 min
4 min
6 min
nkin2 mat a
0 min
10 min
15 min
20 min
25 min

Figure 5.6 Time courses showing wild type male nuclear behaviour in the trichogynes of kinesin female mutants. The male nuclei have been labelled with H1-GFP. Male fertilizing agents are macroconidia unless indicated. **A.** Δ*kar-3a*. The nuclei have aggregated around the tip of a CST that has fused with a trichogyne. Also see movie 5.6. **B.** Δ*kar-3a*. Male nucleus moving through a branched trichogyne. Also see movie 5.7. **C.** Δ*kip-2a*. Two adjacent male nuclei moving back and forth. Also see movie 5.8. **D.** Δ*nkin-2a*, the red arrow indicates the nucleus in a trichogyne and the white arrow indicates the nuclei that remained in the macroconidium. Also see movie 5.9. Bars = 5 μm.

5.2.2.4.3 MYO1 and MYO2 is the only myosin from the female that influences male nuclear behaviour

Myosins are a superfamily of motor proteins that move along actin filaments. The different classes of myosin also differ in the structure of their tail domains and ATP-hydrolyzing motor domains. There are three classes of myosins (class I myosin [MYO-1], class II myosin [MYO-2] and class V myosin [MYO-5]) in *N. crassa* and they all have homologs in *S. cerevisiae, S. pombe* and *A. nudulans* (Tables 1.1 and 5.2).

MYO-1 from female *mat a* trichogynes was found to be important for controlling *mat A* male nuclear movement (movie 5.10). The nuclei hardly moved at all but they found elongated extension (Fig. 5.7A). Interestingly, unlabelled female nuclei rapidly became labelled with H1-GFP encoded by the male wild type nuclei. This was not observed with any of the other mutant-wild type combinations (Fig. 5.7A).

Without MYO-2 encoded by the female, the wild type male nuclei did not exhibit unidirectional movement towards the ascogonium in the trichogynes. However, the male nuclei still moved in succession through the trichogyne but very slowly (Fig. 5.7B).

MYO-5 from the female did not influence male nuclear behaviour.

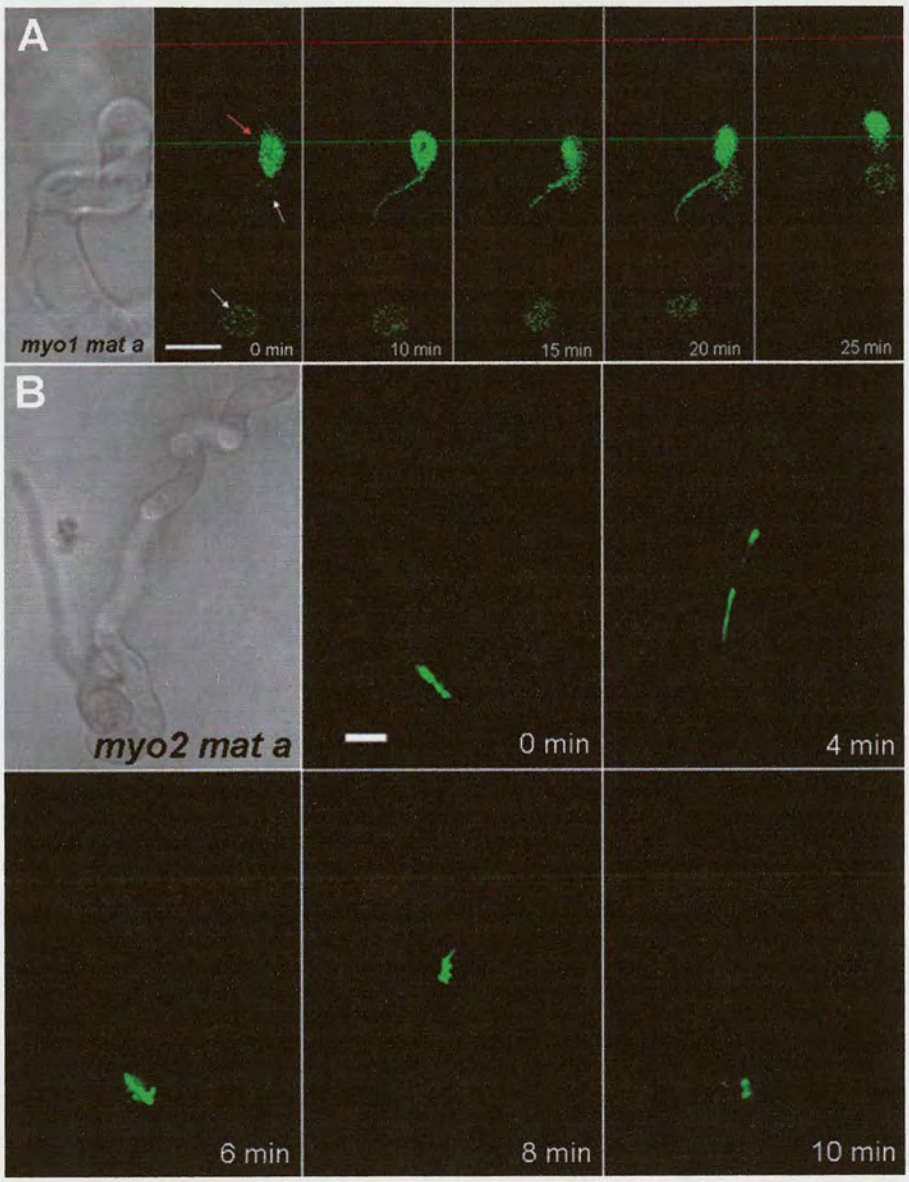

Figure 5.7 Time course showing wild type male nuclear behaviour in the trichogynes of myosin female mutants. The male nuclei have been labelled with H1-GFP. **A**. Δ*myo-1a*. The male nucleus hardly moved but has put out an elongated nuclear extension. Unlabelled Δ*myo-1a* female nuclei rapidly became labelled with H1-GFP encoded by the male wild type nuclei. Also see movie 5.10. Red arrow indicates the male nucleus and white arrows indicates the female nuclei. **B.** Δ*myo-2a.* When male as Δ*myo-2a*, the wild type male nuclei did not exhibit unidirectional movement towards the ascogonium in the trichogynes. Instead, they moved back and forth and appeared either elongated or condensed. Also see movie 5.11. Bars = 5 μm.

5.2.2.5 Motor proteins from the male influence female nuclear behaviour

In summary, one dynactin subunit (RO-3), one kinesin (KIP-2) and two myosins (MYO-1 and MYO-2) from the male were found to influence the behaviour of nuclei in the female (Table 5.6).

Table 5.6 Motor proteins encoded by the male cell influence nuclear behaviour in female

		female wild type nuclei labelled with H1-GFP		
		Nuclei become immobilized	Nuclei clumped together	Nuclei rounded up
		Dynein		
male mutant	**Δ*dic***	+	+	+
	Δ*dlc*	+	+	+
	Δ*dyn-2*	+	+	+
	Δ*dyn-27*	+	+	+
	ro-3	+	+	-
		Kinesin		
	Δ*kar-3*	+	+	+
	Δ*kip-2*	+	-	-
		Myosin		
	Δ*myo-1*	+	-	-
	Δ*myo-2*	-	-	-

5.2.2.5.1 RO-3 in the dynein/dynactin complex from the male influences female nuclear behaviour

DIC is a dynein intermediate chain and has homologs in *S. cerevisiae*, *S. pombe* and *A. nidulans* (Tables 1.1 and 5.2). DLC is a dynein light chain and has homologs in *S. pombe* and *A. nidulans* but none in *S. cerevisiae* (Tables 1.1 and 5.2). DYN-2 is another dynein light chain and has homologs in *S. cerevisiae* and *S. pombe* but none in *A. nidulans* (Tables 1.1 and

5.2). DYN-27 is a dynactin subunit and has no homologs in *S. cerevisiae*, *S. pombe* and *A. nidulans* (Tables 1.1 and 5.2). DIC, DLC, DYN-2 and DYN-27 from the male macroconidia had no influence on the female conidia. Δ*dyn-2* and Δ*dyn-27* of male showed no influence on female nuclei in trichogynes.

RO-3 is the largest subunit of the dynactin (dynein activator) complex and has homologs in *S. cerevisiae* and *A. nidulans* but none in *S. pombe* (Tables 1.1 and 5.2). Wild type female nuclei in the presence of *ro-3* male nuclei became immobilized and clumped together but were unable to maintain their rounded shape (Figs. 5.8). Sometimes the female nuclei became multilateral and they often produced extensions (Fig. 5.8). Sometimes the female nuclei formed ring-shapes (not shown). Female nuclei in the presence of *ro-3* male nuclei were found to be unable to maintain their shapes for at least 24 h following macroconidium-trichogyne fusion.

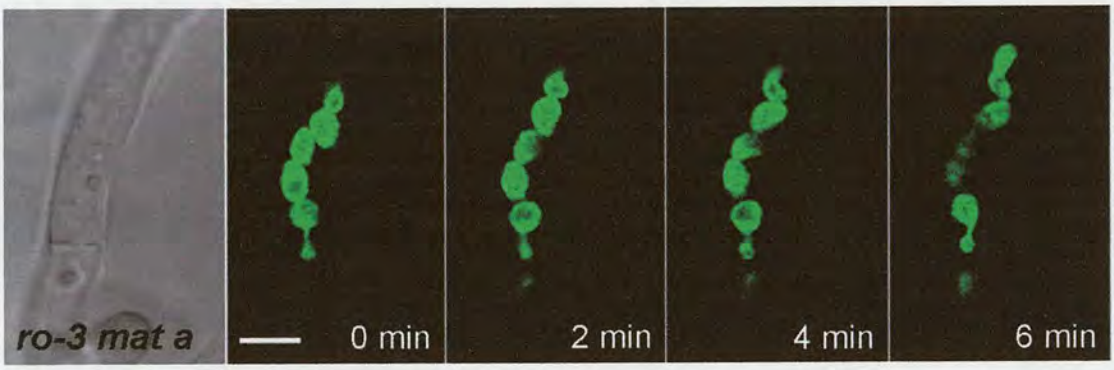

Figure 5.8 Time course showing wild type female nuclear behaviour in trichogynes after fusing with male *ro-3* mutants. The female nuclei have been labelled with H1-GFP. The female nuclei are unable to maintain their rounded shape. Also see movie 5.12. Bars = 5 μm.

5.2.2.5.2 KIP-2 from the male influences female nuclear behaviour

KIP-2 is a kinesin motor protein and has homologs in *S. cerevisiae, S. pombe* and *A. nidulans* (Tables 1.1 and 5.2). KIP-2 was the only kinesin protein in the male found to influence female nuclear behaviour. The female nuclei in the presence of KIP-2 male nuclei became immobilized and clumped together as normal but failed to maintain their rounded

shape and sometimes exhibited a ring shape (Figs. 5.9).

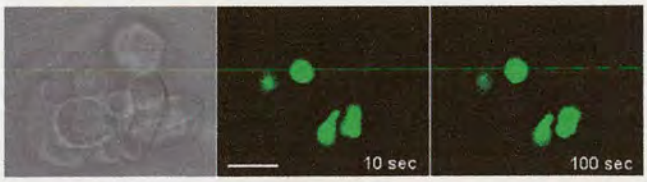

Figure 5.9 Three time courses showing wild type female nuclear behaviour after fusion with male kinesin mutant Δ*kip-2a*. The female nuclei are unable to maintain their rounded shape. The female nuclei have been labelled with H1-GFP. Bars = 5 μm.

5.2.2.5.3 Two myosins from the male influence female nuclear behaviour

Three myosins (MYO-1, MYO-2 and MYO-5) from *N. crassa* all have homologs in *S. cerevisiae, S. pombe* and *A. nidulans* (section 5.2.2.4.3; Tables 1.1 and 5.2).Without the MYO-1 protein provided by the male, female nuclei were unable to maintain their rounded shape or clump together (Fig. 5.10). Absence of MYO-2 from the male prevented the nuclei from becoming immobilized clumping together and rounding up (movie 5.14).

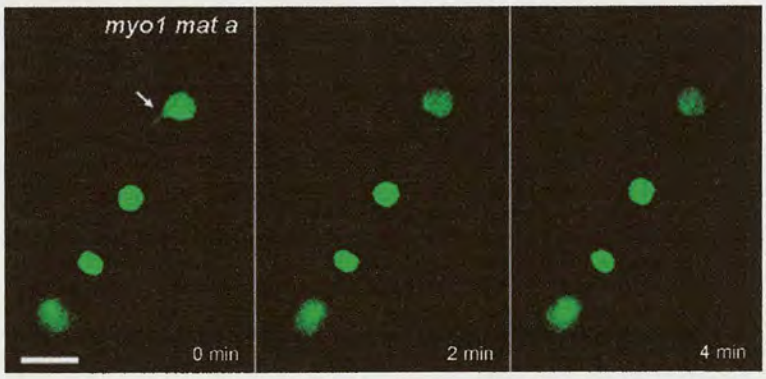

Figure 5.10 Time course showing wild type *mat A* female nuclear behaviour in a female trichogyne after fusion with a male Δ*myo-1a* mutant macroconidium. The female nuclei have been labelled with H1-GFP. The white arrow shows an extension that has been formed from one of the female nuclei. Also, the female nuclei have not clumped together. Also see movie 5.13. Bar = 5 μm.

5.3 Discussion

Once a trichogyne has fused with a macroconidium, the male nuclei from the macroconidium have to pass down the trichogyne to the ascogonium within the

protoperithecial body. Male nuclei eventually pair up with female nuclei in the ascogenous hyphae which grow out from the ascogonium, resulting in the formation of the dikaryon (Raju, 1980). I have provided evidence for the first time that male nuclear movement through the trichogyne involves transport along both microtubules and actin microfilaments, and that kinesins, dynein and myosins (encoded by both the male and female) mediate this process. Non-self recognition involves the co-operative functioning of motor proteins from the male and female. In addition, my results show for the first time that male-female (non-self) nuclear recognition during mating in *N. crassa* occurs immediately following macroconidium-trichogyne fusion rather than at the point the dikaryon gets established in the ascogenous hyphae (Thompson-Coffe & Zickler, 1994).

5.3.1 Both microtubules and microfilaments play roles in male nuclear movement

Depolymerization of microtubules and actin microfilaments inhibited male nuclear movement through trichogynes, and inhibited perithecial development. The latter is presumably because the male and female nuclei were unable to pair up and form a dikaryon. Interestingly, the microtubule and actin inhibitors used (benomyl and Latrunculin B, respectively) had different effects on male nuclear morphology. The male nuclei ended up condensed in the benomyl-treated trichogynes whist in Latrunculin B-treated trichogynes they became elongated. This suggests that the microtubules may play a role in elongating male nuclei, whilst actin microfilaments may play a role in condensing male nuclei, during their characteristic elongated-condensed, 'inchworm' pattern of movement down through the trichogyne.

5.3.2 Male nuclear movement and behaviour requires motor proteins encoded by the female

My results indicate that motor proteins encoded by the female are crucial for male nuclear behaviour following macroconidium-trichogyne fusion. Two kinesins (NKIN-2 and KAR-3), three dynein subunits (DYN-2, DLC and DIC), one dynactin subunit (DYN-27) and two myosins (MYO-1 and MYO-2) from the female were found to influence the behaviour of male nuclei moving through the female trichogyne because deletion of the genes encoding these proteins in the female resulted in abnormal male nuclear behaviour. Interestingly, when the female lacked MYO-1, I observed that male nuclear behaviour was strongly influenced (they hardly moved in the trichogyne) in the 5 examples I looked at. However, when the Δ*myo-1* female strain was crossed with a wild type male, some normal perithecial and ascospore development occurred but the number of normal perithecia formed was reduced 10-100 fold (Table 5.3). It may therefore be that 1-10% of wild type male nuclei when crossed with the Δ*myo-1* female actually reach the ascogonium and induce normal perithecial development. However, I did not observe this in the few (i.e. 5) times I analysed male nuclear behaviour in this cross.

Kar-3 has previously been described as having a microtubule destabilizing role in *S. cerevisiae* (reviewed by Steinberg, 2006). NKIN-2, which is an unusually fast conventional kinesin, has been shown to influence nuclear positioning in hyphae of *N. crassa* (Kallipolitou *et al.,* 2001). Dynein and dynactin have been previously shown to play roles in nuclear migration and positioning in *N. crassa* (Plamann et al., 1994; Vierula & Mais, 1997; Minke et al., 1999a,b; Riquelme et al., 2002). Nothing is known about class-II myosins in filamentous fungi. In *S. cerevisiae* and *S. pombe*, class-II myosin (Myo1p) is involved in cytokinesis. It is the only example of a myosin whose cellular function does not require a catalytic motor domain revealing a novel mechanism independent of actin binding and ATPase activity (Lord

et al., 2005).

5.3.3 Female nuclear behaviour requires motor proteins encoded by the male

My results show that motor proteins encoded by the male are essential for female nuclear behaviour following macroconidium-trichogyne fusion. One kinesin (KIP-2), one dynactin subunit (RO-3) and two myosins (MYO-1 and MYO-2) influenced female nuclear behaviour.

Kip2 has previously been shown to be involved in mitotic spindle positioning and nuclear migration during mitosis in *S. cerevisiae* (Cottingham & Hoyt, 1997). RO-3 has previously been shown to be involved in nuclear positioning in *N. crassa* (Plamann et al., 1994). Class-I myosin has been previously reported as being involved in endocytosis in *A. nidulans*, *Candida albicans* and *U. maydis* (Yamashita & May, 1998; Oberholzer *et al.*, 2002; Weber *et al.*, 2003).

5.3.4 Non-self nuclear recognition involves co-operative functioning of motor proteins from the male and female

My results have shown that non-self nuclear recognition of nuclei of opposite mating type occurs at immediately following macroconidium-trichogyne fusion and continues throughout nuclear transport. My data provides strong evidence for a novel mechanism underlying non-self (male-female) nuclear recognition in filamentous fungi. The recognition mechanism involves the co-operative functioning of motor proteins encoded by the male and female partners at different stages following macroconidium-trichogyne fusion. With one exception, the male and female partners each contributed unique motor proteins in this co-operation. Whether these different motor proteins are differentially pre-synthesized in the macroconidia and/or trichogynes or whether the genes encoding the motor proteins are

induced by pheromone signals from the opposite mating type remains to be determined.

MYO-2 was the only motor protein found to influence both male and female nuclear behaviour when encoded by the female or male, respectively. How deletion of the gene in one partner does not complement the deletion of the gene in the other partner is not clear.

5.3.5 Motor protein gene regulation is mating-type dependent

Results obtained with the Δ*dlc*, Δ*dyn-2* and Δ*dyn-27* dynein deletion mutants used as female gave very different results with regard to ascospore formation during perithecial development when in a *mat A* or *mat a* genetic background. These results indicate that some motor protein gene regulation is mating-type dependent and provides further support for differential expression of motor proteins occurring at different stages during perithecium development.

5.4 Summary

1. Pharmacological and genetic evidence was obtained for male nuclear movement through the trichogyne involving transport along microtubules and microfilaments
2. Two kinesins (NKIN-2 and KAR-3), three dynein subunits (DYN-2, DLC and DIC), one dynactin subunit (DYN-27) and two myosins (MYO-1 and MYO-2) from the female influenced male nuclear movement through the trichogyne.
3. One kinesin (KIP-2), one dynactin subunit (RO-3) and two myosins (MYO-1 and MYO-2) from the male influenced female nuclear behaviour in the trichogyne.
4. The class-II myosin, MYO-2, was the only motor protein found to influence the behaviour of both male and female nuclei when encoded by the female or male, respectively.
5. Non-self nuclear recognition of nuclei of opposite mating type occurs at immediately

following macroconidium-trichogyne fusion and continues throughout nuclear transport.

6. A novel mechanism underlying non-self (male-female) nuclear recognition in filamentous fungi is proposed, and involves the co-operative functioning of motor proteins encoded by the male and female partners at different stages following macroconidium-trichogyne fusion (summarized in Fig. 5.11)
7. Some motor protein gene regulation is mating-type dependent.
8. The differential regulation of motor protein genes is probably important during perithecium development.

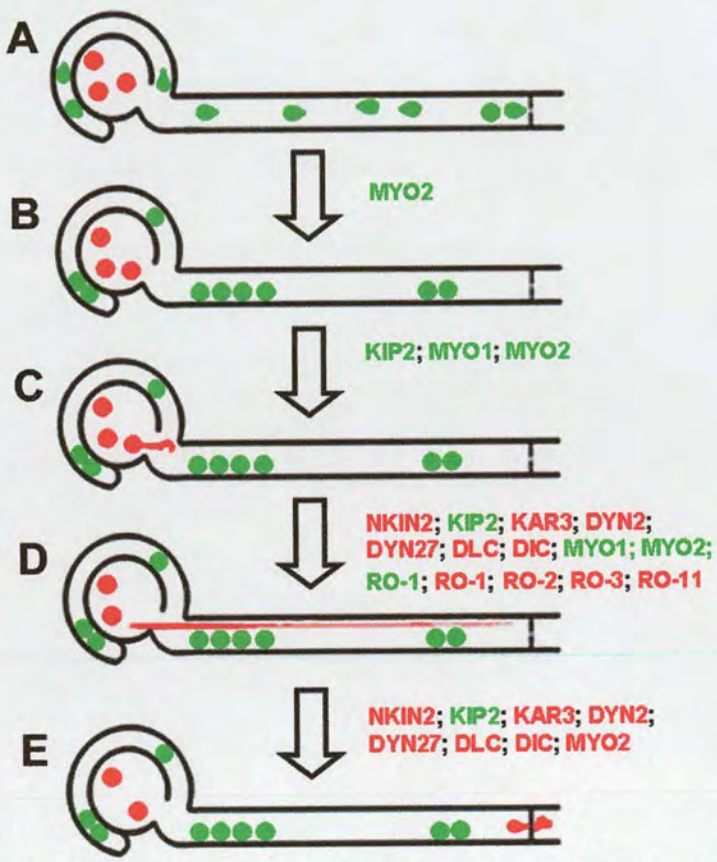

Figure 5.11 Summary of the proposed co-operative functioning of motor proteins encoded by the male and female partners at different stages following macroconidium-trichogyne fusion. **A**. Female trichogyne fused to male conidium. **B**. Female nuclei immobilized, clumped together and round up. **C**. Male nuclei passed through trichogyne. **D**. The first male nucleus elongated. **E**. The second male nucleus prepared to move into trichogyne. Nuclei in green are the female nuclei; nuclei in red are the male nuclei; proteins with green labelled by the female and

influence male nuclear behaviour; proteins with red labelling are encoded by the male and influence female nuclear behaviour.

References

Bistis, G.N. 1981. Chemotropic interactions between trichogynes and conidia of opposite mating type in *Neurospora crassa*. *Mycologia* 73, 959-975.

Bobrowicz, P., Pawlak, R., Correa, A., Bell-Pedersen, D., Ebbole, D.J. 2002. The *Neurospora crassa* pheromone precursor genes are regulated by the mating-type locus and the circadian clock. *Mol. Microbiol.* 45, 795-804.

Borkovich, K.A., Alex, L.A., Yarden, O., Freitag, M., Turner, G.E., Read, N.D., Seiler, S., Bell-Pedersen, D., Paietta, J., Plesofsky, N., Plamann, M., Goodrich-Tanrikulu, M., Schulte, U., Mannhaupt, G., Nargang, F.E., Radford, A., Selitrennikoff, C., Galagan, J.E., Dunlap, J.C., Loros, J.J., Catcheside, D., Inoue, H., Aramayo, R., Polymenis, M., Selker, E.U., Sachs, M.S., Marzluf, G.A., Paulsen, I., Davis, R., Ebbole, D.J., Zelter, A., Kalkman, E.R., O'Rourke, R., Bowring, F., Yeadon, J., Ishii, C., Suzuki, K., Sakai, W., Pratt, R. 2004. Lessons from the genome sequence of *Neurospora crassa*: tracing the path from genomic blueprint to multicellular organism. *Microbiol. Mol. Biol. Rev.* 68, 1–108.

Borlak, J., Zwadlo, C. 2004. The myosin ATPase inhibitor 2,3-butanedione monoxime dictates transcriptional activation of ion channels and Ca^{2+}-handling proteins. *Mol. Pharmacol.* 66, 708–717.

Bruno, K.S., Tinsley, J.H., Minke, P.F., Plamann, M. 1996. Genetic interactions among cytoplasmic dynein, dynactin, and nuclear distribution mutants of *Neurospora crassa*. *Proc. Natl. Acad. Sci. U.S.A.* 93, 4775-4780.

Cottingham, F.R., Hoyt, M.A. 1997. Mitotic spindle positioning in *Saccharomyces cerevisiae* is accomplished by antagonistically acting microtubule motor proteins. *J. Cell Biol.* 138, 1041-1053.

Fischer, R. 1999. Nuclear movement in filamentous fungi. *FEMS Microbiol. Rev.* 23, 39-68.

Kallipolitou, A., Deluca, D., Majdic, U., Lakamper, S., Moroder, L., Schliwa, M., Woehike, G. 2001. Unusual properties of the fungal conventional kinesin neck domain from *Neurospora crassa*. *EMBO J.* 20, 6226-6235.

Lee, I.H., Kumar, S., Plamann, M. 2001. Null mutants of the *Neurospora* actin-related protein 1 pointed-end complex show distinct phenotypes. *Mol. Biol. Cell* 12, 2195–2206.

Lord, M., Laves, E., Pollard, T.D. 2005. Cytokinesis depends on the motor domains of myosin-II in fission yeast but not in budding yeast. *Mol. Biol. Cell* 16, 5346–5355.

Minke, P.F., Lee, I.H., Plamann, M. 1999a. Microscopic analysis of *Neurospora ropy* mutants defective in nuclear distribution. *Fungal Genet. Biol.* 28, 55-67.

Minke, P.F., Lee, I.H., Tinsley, J.H., Bruno, K.S., Plamann, M. 1999b. *Neurospora crassa ro-10* and *ro-11* genes encode novel proteins required for nuclear distribution. *Mol. Microbiol.* 32, 1065-1076.

Minke, P. F., Lee, I. H., Tinsley, J. H., Plamann, M. 2000. A *Neurospora crassa Arp1* mutation

affecting cytoplasmic dynein and dynactin localization. *Mol. Gen. Genet.* 264, 433-440.

Morton, W.M., Ayscough, K.R., McLaughlin, P.J. 2000. Latrunculin alters the actin-monomer subunit interface to prevent polymerization. *Nat. Cell Biol.* 2, 376–378.

Oberholzer, U., Marcil, A., Leberer, E., Thomas, D.Y., Whiteway, M. 2002. Myosin I is required for hypha formation in *Candida albicans*. *Eukaryot. Cell* 1, 213–228.

Raju, N.B. 1980. Meiosis and ascospore genesis in *Neurospora*. *Eur. J. Cell. Biol.* 23, 208-223.

Riquelme, M., Roberson, R.W., McDaniel, D.P., Bartnicki-García, S. 2002. The effects of ropy-1 mutation on cytoplasmic organization and intracellular motility in mature hyphae of *Neurospora crassa*. *Fungal Genet. Biol.* 37, 171–179.

Plamann, M., Minke, P.F., Tinsley, J.H., Bruno, K.S. 1994. Cytoplasmic dynein and actin-related protein Arp1 are required for normal nuclear distribution in filamentous fungi. *J. Cell Biol.* 127, 139-149.

Pöggeler S., Kück, U. 2000. Comparative analysis of the mating-type loci from *Neurospora crassa* and *Sordaria macrospora*: identification of novel transcribed ORFs. *Mol. Gen. Genet.* 263, 292-301.

Seiler, S., Narang, F.E., Steinberg, G., Schliwa, M. 1997. Kinesin is essential for cell morphogenesis and polarized secretion in *Neurospora Crassa*. *EMBO J.* 16, 3025–3034.

Steinberg, G. Schliwa, M. 1995. The Neurospora organelle motor: a distant relative of conventional kinesin with unconventional properties. *Mol. Biol. Cell* 6, 1605-1618.

Steinberg, G. 2006. Preparing the way: Fungal motors in microtubule organization. *Trends Microbiol.* 15, 14-21.

Thompson-Coffe, C., Zickler, D. 1994. How the cytoskeleton recognizes and sorts nuclei of opposite mating type during the sexual cycle in filamentous ascomycetes. *Dev. Biol.* 165, 275-271.

Tinsley J.H., Minke, P.F., Bruno, K.S., Plamann, M. 1996. $p150^{Glued}$, the largest subunit of the dynactin complex, is nonessential in *Neurospora* but required for nuclear distribution. *Mol. Biol. Cell*, 7, 731–742.

Vierula, P.J., Mais, J.M. 1997. A gene required for nuclear migration in *Neurospora crassa* codes for a protein with cystein-rich, LIM/RING-like domains. *Mol. Microbiol.* 24, 331-340.

Weber, I., Gruber, C., Steinberg, G. 2003. A class-V myosin required for mating, hyphal growth, and pathogenicity in the dimorphic plant pathogen *Ustilago maydis*. *Plant Cell,* 15, 2826-2842.

Yamashita, R.A., May, G.S. 1998. Constitutive activation of endocytosis by mutation of myoA, the myosin I gene of *Aspergillus nidulans*. *J. Biol. Chem.* 273, 14644–14648.

CHAPTER 6

Light regulation of conidial sex tube production

6.1 Introduction

Neurospora crassa has more predicted photoreceptors (3 blue light [WC-1, CRY-1 and VIVID], 2 green light [NOP-1 and ORP-1] and 2 red light [PHY-1 and PHY-2)] photoreceptors) than any of the other fungi that have had their photobiology studied in detail (Purschwitz *et al,* 2006). A number of blue light activated photoresponses are already known in *N. crassa* including carotenoid biosynthesis, macroconidiation, and the regulation of circadian rhythms (Purchwitz *et al.,* 2006). No green light photoresponses have been previously reported in fungi and no red light/phytochrome-mediated responses have been previously reported in *N. crassa*.

The aims of the experimental research described in this chapter were to analyse:

1. The influence of different light and dark treatments, and different wavelengths on conidial sex tube (CST) formation.
2. The roles of the WC-1, CRY-1, ORP-1, PHY-1 and PHY-2 photoreceptors in CST

formation.

These aims were fulfilled by illuminating wild type and photoreceptor mutant strains with different wavelength of light.

6.2 Results

6.2.1 Light induced conidial sex tube formation is mating-type dependent

The initial photobiology experiments were done using Method 1 described in sections 2.9 and 2.9.1, and summarized in Fig. 2.2. In method 1, CST production was induced by sex pheromone of the opposite mating type supplied by female protoperithecia overlying male conidia (section 4.2.4).

Conidial sex tubes were only produced under white light in the mat *A* strain but in the mat *a* strain they were induced in both the light and dark (Fig. 6.1). In the *mat A* (but not the *mat a*) strain, CST induction was inhibited in the dark (Fig. 6.1). These results showed that CST production in *mat A* macroconidia appeared to be light-dependent, whilst in *mat a* macroconidia this did not appear to be the case. Red light was found to mimic the effect of white light on CST formation suggesting that red light is the main part of light spectrum responsible for CST production and that the response might be phytochrome-mediated. The results of Fig. 6.1 are from 74A and 74a wild type only. In the future, it will be important to examine whether these red light and mating type dependent effects also occur in other wild type strains.

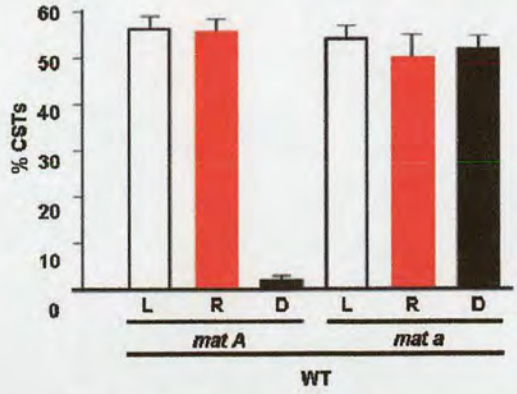

Figure 6.1 Conidial sex tube induction in wild type stains (74A and 74a) are stimulated by red light but this is mating-type dependent. L, white light. R, red light (600 ± 10 nm, photon fluence rate = 5.0 μM m^2 s^{-1}). D, dark. WT, wild type. % of CSTs indicates the percentage of macroconidia which produce CSTs from the total number of macroconidia. The error bars indicate standard errors of the mean.

6.2.2 PHY-1 and PHY-2 are more closely related to bacterial than plant phytochromes

Phytochromes in fungi are more closely related to bacterial phytochromes than plant phytochromes, but all phytochromes from plant, bacteria and fungi share the main features of phytochrome genes (i.e. they all have phytochrome-, histidine kinase- and cGMP-specific phosphodiesterases-domains, Blumenstein *et al.*, 2005; Fig. 1.12). The two phytochromes in *N. crassa* (PHY-1 and PHY-2) are most closely related phylogenetically to other fungal phytochromes, and are more closely related to bacterial than plant phytochromes (Idnurm & Heitman, 2005; Fig 6.2). Interestingly, only *N. crassa* and *Botryotinia fuckeliana* possess two predicted phytochrome genes; all other filamentous fungi only possess one, including *A. nidulans* in which the first phytochrome-mediated response in fungi was reported (Blumenstein *et al.*, 2005). The yeasts *S. cerevisiae* and *S. pombe* lack phytochrome encoding genes.

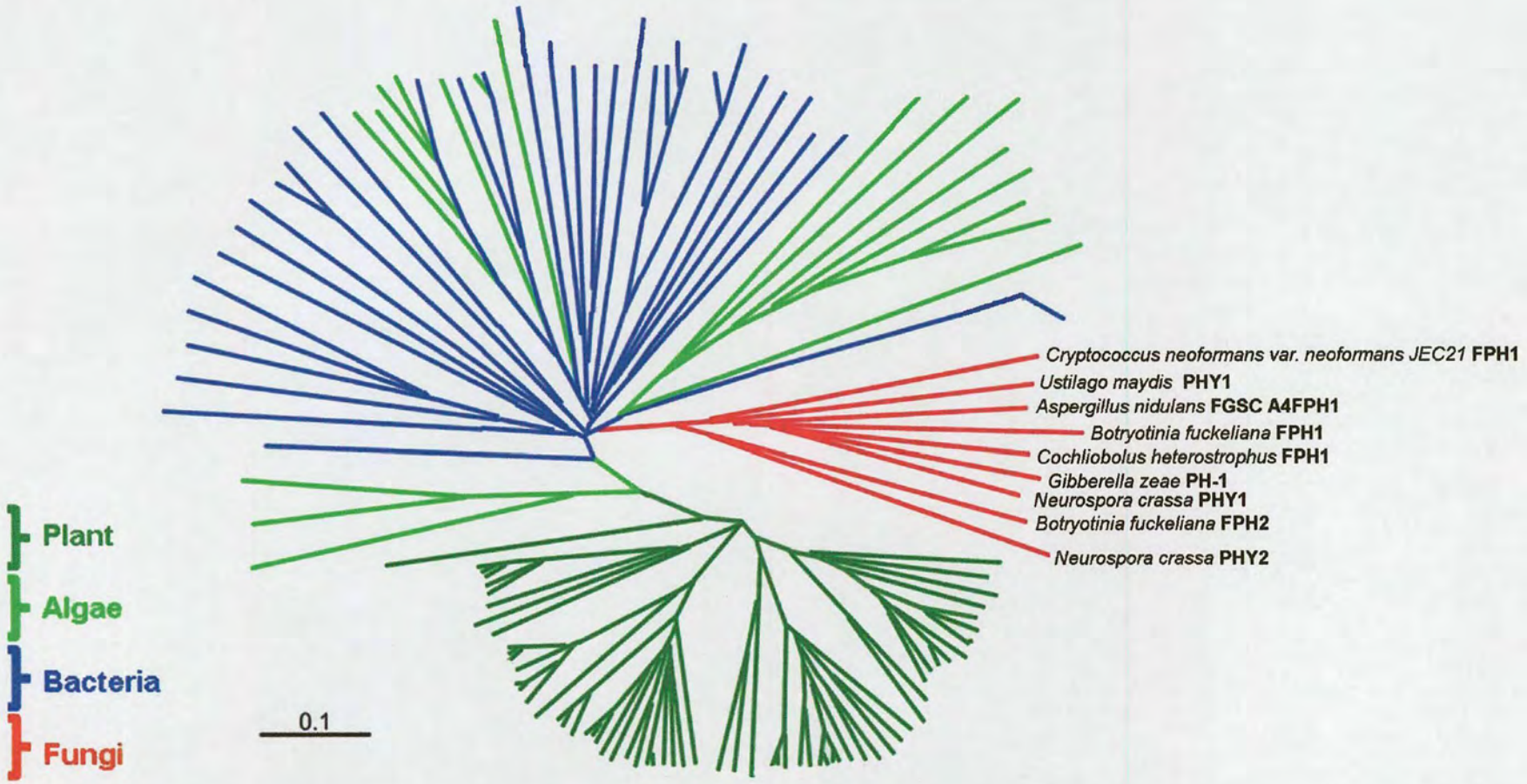

Figure 6.2 Phylogenetic tree of phytochrome proteins from plant (green), algae (light green), bacteria (blue) and fungi (red). The positions of the two *N. crassa* phytochromes PHY-1 and PHY-2 are shown in the red boxes.

6.2.2.1 PHY-2 influences the responses to red light of *mat A*

Similar to the last section, the experiments in this section were performed using Method 1 in which protoperithecia of opposite mating type provided the CST inductive pheromone (sections 2.9 and 2.9.1; Fig. 2.2). The conidia used as the male partner in these experiments were the deletion mutants, Δ*phy-1* and Δ*phy-2*.

Δ*phy-1* mutant macroconidia were found to produce CSTs in both red light and in the dark in both mating types. In contrast, CST production by Δ*phy-2* was inhibited in both mating types in both red light and the dark (Fig. 6.3). The percentage of CST formation by Δ*phy-1 mat a* under red light was ~ 50 % of that of Δ*phy-1 mat A* in the dark, Δ*phy-1 mat a* under red light or Δ*phy-1 mat a* in the dark (Fig. 6.3). Conidial sex tubes were only induced in the *mat A* wild type under light, whilst CST formation occurred in the light and dark in the *mat a* wild type.. This suggests that CST formation is not induced by light in *mat a*, and other regulatory factors may be involved. Comparing the results obtained with the wild type and phytochrome mutants, we can conclude the following:

1. PHY-1 plays a role in inhibiting CST formation in *mat A* in the dark but PHY-2 plays a role in the induction of CST in red light (Fig. 6.3).
2. PHY-1 activity is confined to *mat A*, where it has contrasting roles in the light and in the dark. Under red light PHY-1 promotes, whilst in the dark it strongly inhibits CST production (Fig. 6.3). In contrast, PHY-2 in *mat A* induces CST formation in a red light-dependent manner.
3. In the absence of PHY-2, PHY-1 is unable to stimulate *mat A* CST production in response to red light. This suggests that in this mating type the presence of PHY is required for PHY-1 activity.

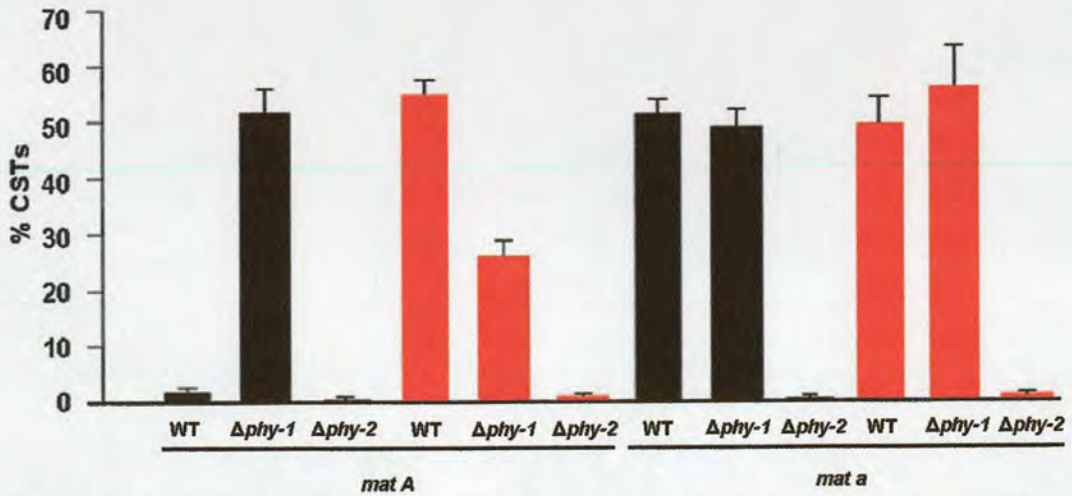

Figure 6.3 PHY-1 and PHY-2 phytochromes have different regulatory roles during CST induction. Red bars, red light (600 ± 10 nm, photon fluence rate 5.0 μM m^2 s^{-1}). Dark bars, dark. WT, wild type 74A/74a. % of CSTs indicates the % of conidia which produce CST from total number of conidia. The error bars indicate standard error of the mean.

6.2.2.2 Isolated macroconidia exhibit phytochrome-mediated red light responses in the presence of synthetic pheromone

The experiments in this section were performed by using Method 2 in which synthetic pheromone, rather than protoperithecia of opposite mating type, was used to induce CST formation (described in section 2.9 and 2.9.2, and summarized in Fig. 2.3). To avoid problems of light influencing the photobiology of the macroconidia prior to experimentation, macroconidia were produced in complete darkness in a darkroom and then manipulated during the experimental set up using 'night goggles' with a 800 nm infra red light source (section 2.9.3).

Previously it was shown that macroconidia of *mat A* genotype from cultures grown under continuous light can be induced to form CSTs with the synthetic sex pheromone MFa-1 in water at an optimum concentration of 25.6 µg/ml (section 4.2.4; Fig. 4.9). Applying MFa-1 to macroconidia from dark grown cultures resulted in CST formation similar to that produced by a female culture bearing protoperithecia as the source of pheromone (compare Figs. 6.4 and 6.1). Conidial sex tube formation was stimulated under both white and red light but few CSTs (~ 9%) were produced in the dark after 8 h. Without MFa-1, under white light the *mat A* strain produced virtually no CSTs (Fig. 6.4). In addition, the number of CST was very low (~ 6%) in the Δ*pre-1 mat A* strain lacking the pheromone receptor for MFa-1 (Fig. 6.4).

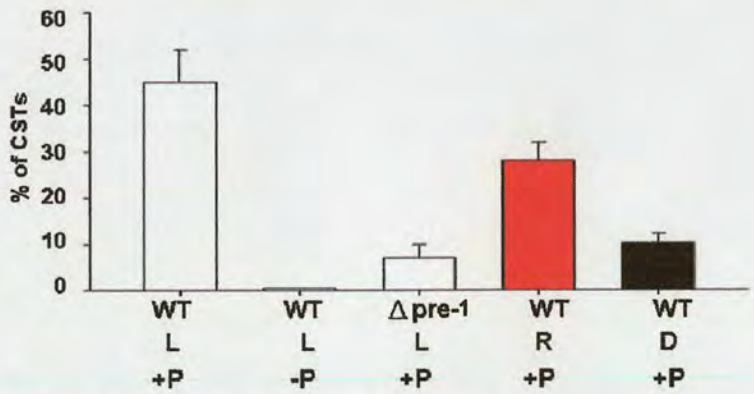

Figure 6.4 Synthetic sex pheromone MFa-1 induces CST formation in isolated dark grown *mat A* macroconidia. These responses were absent from the Δ*pre-1* mutant in *mat A* lacking the pheromone receptor to MFa-1. Isolated macroconidia also respond to red light in the presence of synthetic pheromone. L, white light. R, red light (600 ± 10 nm, photon fluence rate 5.0 µM m^2 s^{-1}) D, dark. WT, wild type. +P, with 25.6 µg/ml MFa-1 synthetic sex pheromone MFa-1. -P, no added synthetic MFa-1. % of CSTs indicates the % of conidia which produce CST from total number of conidia. The error bars indicate standard error of the mean.

6.2.2.3 Dark-grown macroconidia of both mating types respond differently to red and far red light

The experiments in this section were performed using Method 2 in which synthetic pheromone, rather than protoperithecia of opposite mating type, was used to induce CST formation (described in section 2.9 and 2.9.2, and summarized in Fig. 2.3). As in the last section, the macroconidia used for experimentation were produced in complete darkness and then manipulated in a dark room using night goggles (section 2.9.3).

In *mat A,* both red and far red light stimulated CST production (Fig. 6.5). In *mat a*, only red light, even with a short 5 min exposure, stimulated CST production very significant (Fig. 6.5 *mat a*, Dark *vs.* 5 min red light exposure, $p < 0.05$). Evidence was obtained for this being a classic phytochrome response in macroconidia of *mat a* (section 1.8.4; Fig. 1.13) because treatment with red light for 5 min followed by treatment with far red light for 1 min resulted in inhibition of CST formation (Fig. 6.5 mat a, 5 min red light exposure *vs.* 5 min red light and followed 1 min far red light exposure, $p < 0.05$). No evidence for red/far red photoreversibility was found in *mat A* (Fig. 6.5). Both *mat A* and *mat a* produced low levels (3 - 11%) of CSTs in the dark. The paired t-test is used to provide p values.

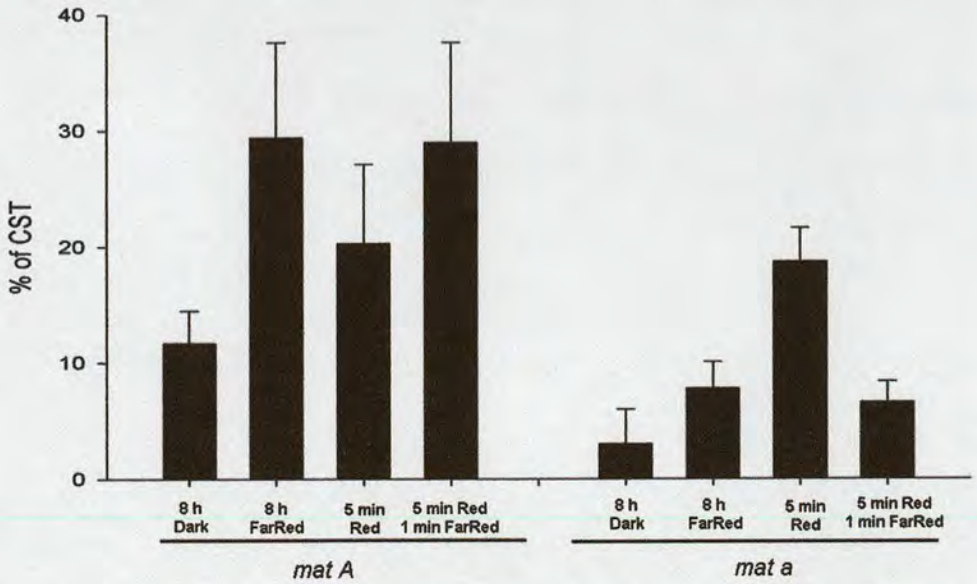

Figure 6.5 Conidial sex tube induction as red and far red light responses of dark-grown macroconidia. **A**. Percentage of CST formation in the *mat A* strain under different illumination conditions. **B**. Percentage of CST formation in the *mat a* strain under different illumination conditions. Macroconidia exposed for 5 min to red light only were followed by 7 h and 55 min in the dark. Macroconidia exposed to 5 min red light followed by 1 min of far red light were subsequently incubated for 7 h and 54 min in the dark. Red light (660 nm ± 10 nm, 5.0 μM m^2 s^{-1}). Far red (757 nm ± 20nm, 30.0 μM m^2 s^{-1}). % of CSTs indicates the % of conidia which produce CST from total number of conidia. The error bars indicate standard error of the mean.

6.2.3 Blue and green light influence CST induction

As in section 6.2.1, the experiments described in this section were performed using Method 1 (section 2.9 and 2.9.1; Fig. 2.2) in which CSTs were induced by sex pheromone supplied by protoperithecia of opposite mating type (section 4.2.3).

In other systems there is a strong interplay between different photoreceptors in the control of photoresponses (Jiao *et al.*, 2007). I therefore performed a series of experiments with *N. crassa* to analyse the influence of light of different wavelengths, and the effects of deleting different photoreceptors, on CST induction (Fig. 6.6).

In addition to red light, green and blue light also were found to stimulate CST production in both mating types. The percentage of CSTs produced under green light was significantly lower than for red light in *mat A* ($p < 0.05$), and significantly lower for both green ($p < 0.05$) and blue ($p < 0.01$) light than red light in *mat a* (Fig. 6.6). These results suggest roles for both blue and green light photoreceptors in CST induction. The paired t-test is used to provide p values.

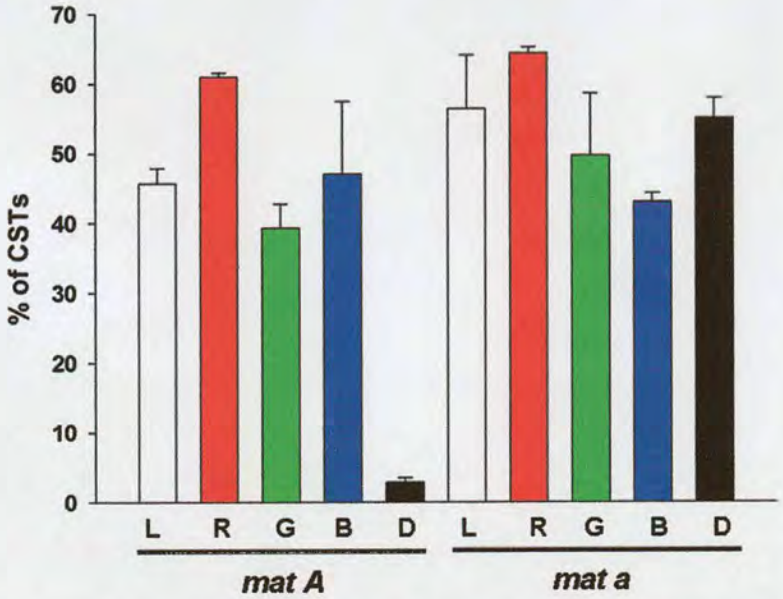

Figure 6.6 Influence of white, red, green and blue light on CST induction. L, white light exposure for 8 h. R, red light (660 ± 10 nm, photon fluence rate = 5.0 μM m^2 s^{-1}) exposure for 8 h. G, green light (530 ± 10 nm, photon fluence rate = 4.5 μM m^2 s^{-1}) exposure for 8 h. B, blue light (480 ± 10 nm, photon fluence rate = 6.0 μM m^2 s^{-1}) exposure for 8 h. % of CSTs indicates the % of conidia which produce CST from total number of conidia. The error bars indicate standard error of the mean.

6.2.4 Blue and green light photoreceptors are involved in regulating CST induction

As in section 6.2.1, the experiments described in this section were performed using Method 1 (section 2.9 and 2.9.1; Fig. 2.2) in which CSTs were induced by sex pheromone supplied by protoperithecia of opposite mating type (section 4.2.3). Analysis of CST

formation by deletion mutants of the genes encoding the blue light photoreceptors WC-1, CRY and one of the putative green light photoreceptors, ORP-1, and the clock regulatory protein, FRQ, indicated the involvement of all of these proteins in the control of CST induction (Figs. 6.7A - D).

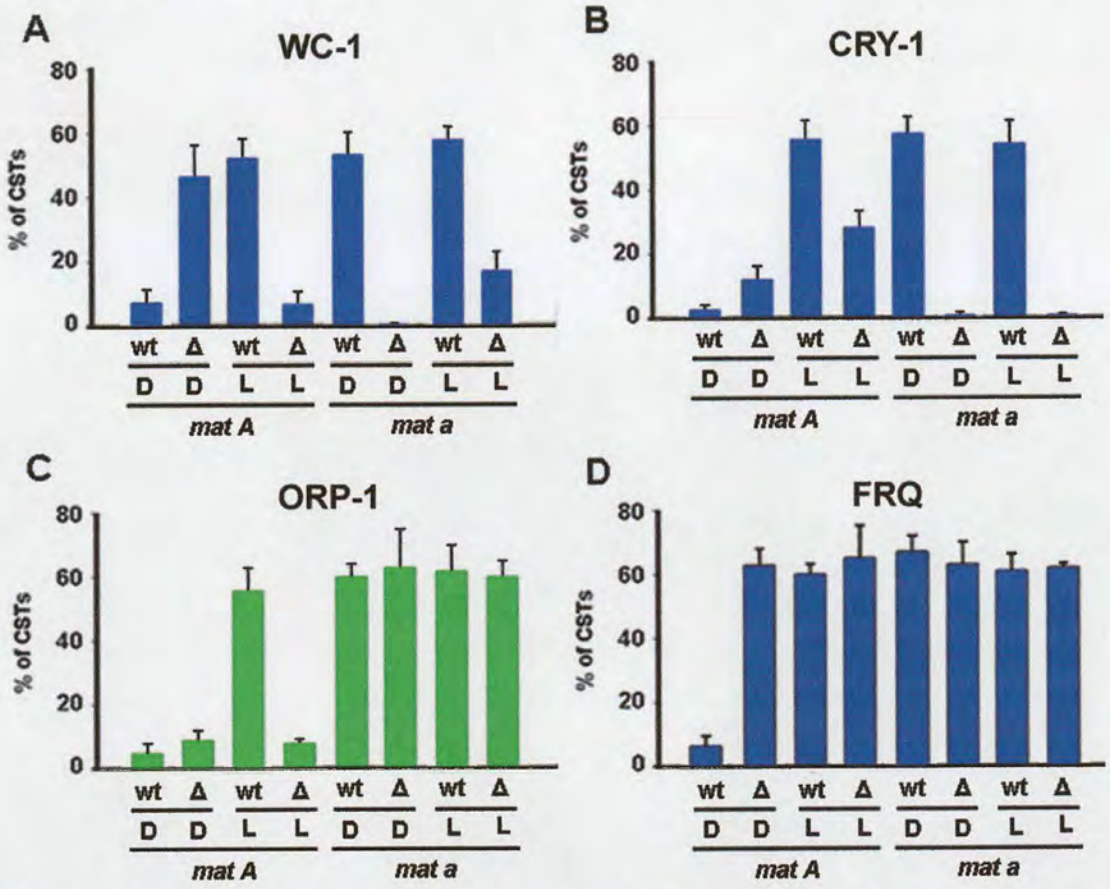

Figure 6.7 Green and blue photoreceptors influence CST formation. **A**. A role for the white collar-1 (WC-1) photoreceptor in CST induction. Δ = Δ*wc-1*. **B**. Possible role for putative blue light photoreceptor, cryptochrome (CRY-1), in CST induction. Δ = Δ*cry-1*. **C**. Possible role for putative green light photoreceptor ORP-1 in CST induction. Δ = Δ*orp-1*. **D**. A role for the frequency (FRQ) protein in CST induction. Δ = *frq*. % of CSTs indicates the % of conidia which produce CST from total number of conidia. The error bars indicate standard error of the mean.

WC-1 is a blue light photoreceptor and transcription factor (Purschwitz *et al.*, 2006). The Δ*wc-1* mutant was defective in its responses (i.e. CST formation) to both light and dark treatments in *mat A* (74A) (Fig. 6.7A). *mat a* (74a) even get the same response (the response of CST formation under light exposure) in the dark and it is complicated to make any conclusion about photoresponds in *mat a*.

CRY-1 is a predicted blue light photoreceptor for which a function has not yet been described in fungi. The Δ*cry-1* mutant was defective in its responses (i.e. CST formation) to both light and dark treatments in *mat A* (74A) (Fig. 6.7B). There were quantitative differences between CST formation in the Δ*cry-1* mutant compared with the Δ*wc-1* mutant (compare Figs. 6.7A and 6.7B).

ORP-1 is a predicted green light photoreceptor for which a function has not been described in fungi. The Δ*orp-1* mutant was only defective in CST formation in *mat A* in the light (Fig. 6.7C).

Based on an analysis of the *frq* mutant, FRQ only seemed to play a role in *mat A* in the dark.

6.2.4. The emergence of CSTs from conidia displays a positive phototropism

In these experiments, Method 1 was applied (section 2.9 and 2.9.1; Fig. 2.2) in which pheromone for CST induction was supplied by protoperithecia of the opposite mating type. When unilateral white light was applied, conidial sex tubes were found to predominately emerge on the side of macroconidia exposed to the light source (Fig. 6.8). However, only low fluence rates of light (< 1.0 μmol m^{-1} s^{-2}) were found to induce these positive phototropisms; with higher fluence rates, the phenomenon was not observed. I did not determine which of the photoreceptors participate in regulating this response.

Figure 6.8 Positive phototropism of CST formation in response to unilateral white light (from the right).

6.3. Discussion

For single-cell and multicellular systems to survive, they must accurately sense and respond to their intracellular and extracellular environments. Light is a nearly ubiquitous environmental factor, and most organisms have evolved the capability to respond in a range of ways to different forms of this external stimulus (Crosson *et al.*, 2003). Numerous photoreceptors underlie the activation of light-sensitive signal transduction cascades controlling these responses.

In *N. crassa*, blue light plays an important role in regulating circadian rhythms in conidiation, and this blue light-mediated signal transduction pathway has been well studied (Crosthwaite *et al.*, 1997; Liu & Bell-Pedersen, 2006; Tralau *et al.*, 2006; Yu *et al.*, 2007). When the genome of *N. crassa* was sequenced, a range of predicted photoreceptors were

identified. Three predicted blue light photoreceptors (White Collar-1 [WC-1], cryptochrome [CRY-1] and VIVID [VVD]), two predicted green light photoreceptors (*N. crassa* opsin photoreceptor [NOP-1] and Opsin related protein-1 [ORP-1]) and two predicted red light photoreceptors (Phytochrome 1 [PHY-1] and phytochrome 2 [PHY-2]) (Borkovich *et al.*, 2004; Fig. 1.10). So far, only WC-1 has been linked with functions, and it has been shown to be involved in regulating circadian rhythms (Crosthwaite *et al.*, 1997), carotenoid synthesis (Harding & Turner, 1981), conidiation induction (Harding & Turner, 1981), protoperithecial induction (Degli-Innocenti & Russo, 1984) and perithecial neck phototropism (Harding & Melles, 1983).

6.3.1 *Neurospora crassa* phytochromes are close to bacterial phytochromes in their protein sequences

In the last decade, accumulating genomic data has indicated that phytochromes are not restricted to plants. In fact, phytochromes are widely distributed amongst prokaryotes and eukaryotes (Karniol *et al.*, 2005). Plant, bacterial and fungal phytochromes are clearly separated from each other in the phylogenetic tree of these proteins (Fig. 6.2; Karniol *et al.*, 2005). The phytochromes of plant, algae and fungi evolved from bacterial phytochromes. Phytochromes then became adapted to the different lifestyles of these different organisms. The phytochromes of plants and bacteria now function in different ways: plant phytochromes absorb red light that photoconverts the inactive phytochrome (Pr form) into the active form (Pfr form) (Smith, 1995); in bacterial phytochromes, the opposite occurs - far red light is absorbed by the active Pfr form and photoconverts into the inactive Pr form (Yeh *et al.*, 1997). However, the bacterial Pfr form of phytochrome still plays a role in signal transduction (Yeh *et al.*, 1997).

Neurospora crassa phytochromes exhibit only ~ 20% similarity to plant and bacterial phytochrome protein sequences, and even the two phytochromes (PHY-1 and PHY-2) of *N. crassa,* only show ~ 40% similarity to each other. The latter contrasts with *Arabidopsis thaliana* phytochromes A-E show 60-83% similarity to each other and *Pseudomonas syringae* phytochromes that exhibit ~ 50% similarity to each other (Fig. 6.9). Nerveless, overall the phytochromes of *N. crassa* are more similar to bacterial phytochromes in their protein and domain structures (Fig. 1.12).

Phytochromes have so far only been investigated in two fungal species, *N. crassa* and *A. nidulans*. *Aspergillus nidulans* has only one phytochrome, which is involved in repressing sexual reproduction (Blumenstein *et al.*, 2005) whilst *N. crassa* possesses two phytochromes (PHY-1 and PHY-2) (Froehlich *et al.*, 2005). No functions for these phytochromes, nor phenotypes for phytochrome mutants, have been previously reported in *N. crassa*.

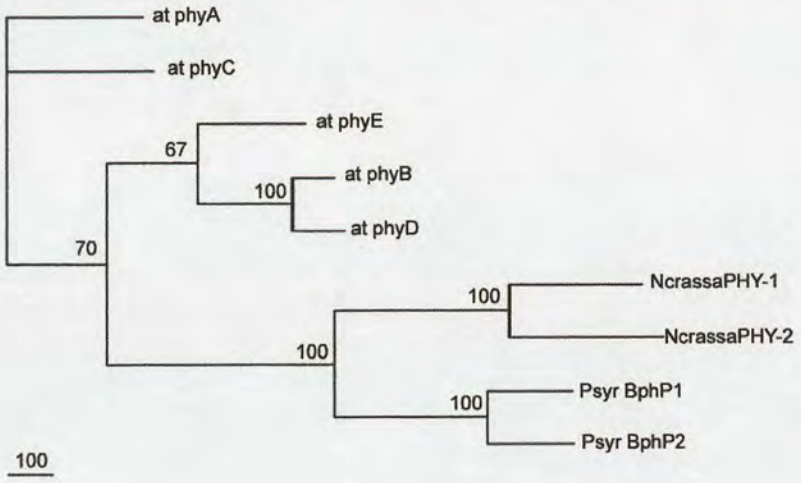

	1	2	3	4	5	6	7	8	9
1 At phyA	–	0.47873	0.47602	0.47230	0.50472	0.83008	0.82314	0.80197	0.78043
2 At phyB	529	–	0.48810	0.17693	0.42532	0.83289	0.83887	0.78303	0.77987
3 At phyC	526	533	–	0.49541	0.52277	0.82150	0.83733	0.76264	0.78533
4 At phyD	520	204	540	–	0.44128	0.83422	0.83801	0.78800	0.78009
5 At phyE	535	467	551	481	–	0.82532	0.82280	0.77031	0.77508
6 NcrassaPHY 1	894	942	879	936	893	–	0.61485	0.78838	0.81639
7 NcrassaPHY 2	619	656	628	657	626	621	–	0.78178	0.80741
8 Psyr BphP1	571	583	543	567	550	570	412	–	0.50838
9 Psyr BphP2	743	744	739	746	734	787	545	372	–

Figure 6.9 Phylogenetic relationship and pairwise distances between *Arabidopsis thaliana* phytochromes, *Pseudomonas syringae* phytochromes and *Neurospora crassa* phytochromes. **at phy A-E**, *Arabidopsis thaliana* phytochromes A-E; **NcrassaPHY1** and **NcrassaPHY2**, *Neurospora crassa* phytochromes 1 and 2; **Psyr BphP1-2**, *Pseudomonas syringae* bacterial phytochrome proteins 1 and 2. In the Table, the numbers shown below the diagonal indicate total amino acid differences and above the diagonal indicate the percentage of amino acid differences (adjusted for missing data). This is a neighbour-joining (NJ) tree and bootstrap values were obtained with 1,000 replications and shown at the notes. Numbers on tree branches indicate the percentage of bootstrap replications derived from 1,000 replications of NJ analysis and supporting the internal branches by ≧ 50 %.

6.3.2 Conidia formed in the dark or the light responded differently to red and far red light

Light is often important for fungal development, and in *N. crassa*, amongst other things it is important for the induction of conidiation (Linden *et al.*, 1997). I found that cultures of *N. crassa* produced very few conidia when grown in the dark. However, those produced were still able to act as male fertilizing agents during mating (data not shown) and thus seemed to function normally. Some of the experiments were performed with fully dark grown cultures to be sure that light had not influenced the photobiology of the macroconidia (e.g. by inducing

the formation of active phytochrome) prior to experimentation.

Collectively, data from my experiments with macroconidia from light grown and dark grown cultures suggest the following interpretation.

1. PHY-1 activity is *mat A* specific with opposing functions in the light and dark. In *mat A*, PHY-1 has no function in red light but plays a role in inducing CST formation in the dark.
2. Under red light conditions, PHY-2 is required for PHY-1 activity.
3. In *mat A*, PHY-2 seems to be the main protein that absorbs red light and functions in CST induction.
4. In *mat A*, PHY-2 activity is triggered by red light, but in *mat a* it operates independently of light.
5. In *mat a*, only PHY-2 seems to function and it plays roles in CST induction in both the light and dark.

Thus, PHY-1 and PHY-2 appear to have distinct characteristics that are mating-type dependent and are summarized in Fig. 6.10.

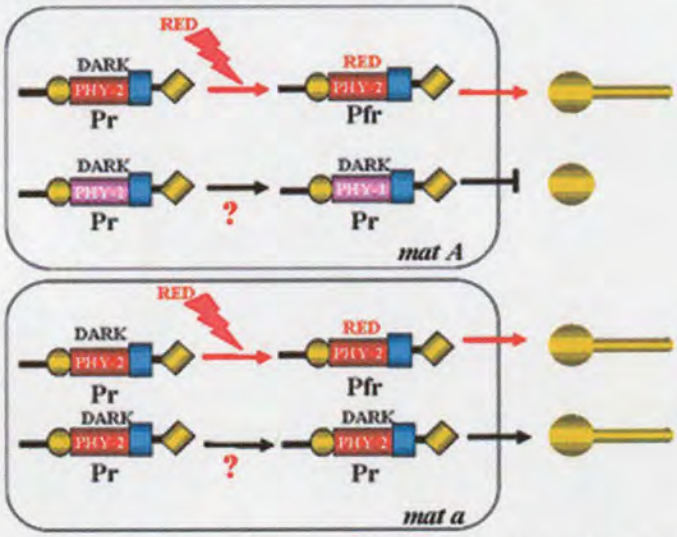

Figure 6.10 Summary of *Neurospora* phytochrome results. **1**. In *mat A*, PHY-2 seems to be the main protein that absorbs red light and functions in CST induction. **2**. In *mat A*, PHY-1 has no function in red light but plays a role in inhibiting CST formation in the dark. **3**. In *mat a*, only PHY-2 seems to function and it plays roles in CST induction in both the light and dark. Pr, inactive form; Pfr, active form.

6.3.3 The *mat a* strain exhibited a classic plant phytochrome type of behaviour

The central dogma of plant phytochrome photoconversion is that the inactive red-absorbing (λ_{max} ~ 660 nm) Pr form of phytochrome absorbs red light and is photoconverted to the active far red-absorbing (λ_{max} ~730 nm) Pfr form. The active Pfr form of phytochrome is then slowly converted to the inactive Pr form of phytochrome in the absence of light (under far red light illumination) (Rockwell *et al.*, 2006). This classic behaviour of plant phytochrome was only observed in the *mat a* strain in macroconidia that had been formed in the dark (i.e. the phytochrome was at 'zero status' in the inactive Pr form).

A short exposure to red light induced the *mat a* strain to produce CSTs whilst a short exposure of far red light followed by red light inhibited CST production (Fig. 6.5).

6.3.4 The phytochrome response to red/far red light in the *mat A* strain is not red/far red reversible

Far red light was found to induce CST formation in the *mat A* strain. However, CSTs were also induced in red light suggesting that phytochrome in *mat A* is also photoconverted to an active Pfr form. These results can be interpreted in different ways including: (1) this a phytochrome with Type I phytochrome or light labile properties similar to *phA* in plants (Franklin et al., 2005), or (2) the phytochrome is active its both the Pr and Pfr forms.

6.3.5 Conidial sex tube induction is controlled by a complex light signalling network

Not only were the two phytochromes found to play roles in CST induction, but also the putative green light opsin-like ORP-1 photoreceptor (Fig. 6.7C), the UV/blue light cryptochrome photoreceptor (Fig. 6.7B) and the blue light white collar-1 (WC-1) (Fig. 6.7A) were shown to be involved. Overall my results indicate that CST formation is controlled by a complex light signalling network.

As indicated earlier, WC-1 has been reported to regulate numerous processes (circadian rhythms, carotenoid synthesis, conidiation induction, protoperithecial formation and perithecial neck phototropisms, see section 1.8.1). My results indicate for the first time that it also involved in regulating CST induction. Since the clock regulatory protein FRQ is also involved in regulating CST induction, there may be a link here with WC-1 which also involved in regulating circadian rhythms in *N. crassa* (Liu & Bell-Pedersen, 2006). Perhaps CST formation itself exhibits a circadian rhythm.

Cryptochromes are present in bacteria, plants, animals and fungi. My results provide the first evidence for a cryptochrome-mediated response (i.e. CST induction) in fungi. In plants, cryptochrome can interact with phytochromes. For example, CRY2 can interact with PHYB (Martinez-Garcia *et al.,* 2000), CRY1 has been reported to interact with PHYA (Ahmad *et al.,* 1998), and CRY1 may also interact with PHYB indirectly (Yang *et al.,* 2001). This suggested that an important mechanism of cryptochrome signal transduction may be via altering phytochrome-mediated regulation of transcription (Mas *et al.*, 2000; Ni *et al.,* 1998). In

animals, cryptochrome can interact with opsins. (e.g. in the entrainment of the behavioral rhythms of flies, Stanewsky *et al.*, 1998). Thus in plants, cryptochrome seem to interact with phytochromes whilst in animals they interact with opsins (Cashmore *et al.*, 1999). It will be interesting to determine if cryptochromes interact with both in fungi.

Opsins are membrane proteins that are related to the protein moiety of the photoreceptive molecule rhodopsin; they typically act as light sensors in animals. Photoreceptive proteins similar to the animal opsins in three-dimensional structure but not in amino-acid sequence have been found in archaea, bacteria, fungi, and green alga. These non-animal opsins function as lightdriven ion pumps or light sensors but there is no evidence that they are structurally related to animal opsins (reviewed by Terakita, 2005) My results provide the first evidence for a green light response (i.e. CST induction), and for the involvement of a green light opsin-like photoreceptor in *N. crassa*.

6.3.6 Why do male macroconidia need to 'see' light during mating

Plants and animals use their photoreceptors to sense the environment where they in. The immature female fruitbodies (protoperithecia) of *N. crassa* need light to develop (Degli-Innocenti *et al.*, 1984), which may result in them forming predominately on the substratum surface. If light is so important for the development of female structures then it should also important for the male, which needs to meet and mate with the female - a process which involves female trichogynes sensing and growing towards sex pheromone emitted by the male cells (Bistis, 1981; Pöggeler & Kück, 2000; Bobrowicz *et al.*, 2002). This may be part of the reason why CSTs are regulated by light (and also by sex pheromone released from the female).

Neurospora crassa has recently been found beneath the bark of trees following forest fires (Jacobson *et al.*, 2004). Light that penetrates bark will tend to be of wavelengths towards the red end of the spectrum. This may be a reason for phytochrome signalling playing significant role in CST induction.

6.4 Summary

1. Conidial sex tube formation is light dependent in the *mat A* strain and the stimulatory effects of white light can be mimicked by red light; the *mat a* strain produces CST in the light and dark.
2. The protein sequences of PHY-1 and PHY-2 are more closely related to bacterial than plant phytochromes.
3. PHY-1 plays a role in inhibiting CST formation in *mat A* in the dark but PHY-2 plays a role in CST induction in both mating types in red light.

4. PHY-1 and PHY-2 have contrasting roles in CST induction: PHY-1 has a Pfr active form whilst PHY-2 seems to have both Pr and Pfr active forms.
5. Blue and green light play roles in CST induction.
6. The blue light photoreceptors, WC-1 and CRY-1, and putative green light photoreceptor, ORP-1, play roles in CST induction.
7. The clock regulatory protein FRQ plays a role in regulating CST induction in the *mat A* strain only.
8. The emergence of CST from macroconidia displays a positive phototropism to white light.

References

Ahmad, M., Jarillo, J.A., Smirnova, O., Cashmore, A.R., 1998. The CRY1 blue light photoreceptor of Arabidopsis interacts with phytochrome A *in vitro*. *Mol. Cell.* 1, 939–48.

Bistis, G.N. 1981. Chemotropic interactions between trichogynes and conidia of opposite mating type in *Neurospora crassa*. *Mycologia* 73, 959-975.

Blumenstein, A., Vienken, K., Tasler, R., Purschwitz, J., Veith, D., Frankenberg-Dinkel, N., Fischer, R. 2005. The *Aspergillus nidulans* phytochrome FphA represses sexual development in red light. *Curr. Biol.* 15, 1833-1838.

Bobrowicz, P., Pawlak, R., Correa, A., Bell-Pederson, D., Ebolle, D.J. 2002. The *Neurospora crassa* pheromone precursor genes are regulated by the mating-type locus and the circadian clock. *Mol. Microbiol.* 45, 795-804;

Borkovich, K.A., Alex, L.A., Yarden, O., Freitag, M., Turner, G.E., Read, N.D., Seiler, S., Bell-Pedersen, D., Paietta, J., Plesofsky, N., Plamann, M., Goodrich-Tanrikulu, M., Schulte, U., Mannhaupt, G., Nargang, F.E., Radford, A., Selitrennikoff, C., Galagan, J.E., Dunlap, J.C., Loros, J.J., Catcheside, D., Inoue, H., Aramayo, R., Polymenis, M., Selker, E.U., Sachs, M.S., Marzluf, G.A., Paulsen, I., Davis, R., Ebbole, D.J., Zelter, A., Kalkman, E.R., O'Rourke, R., Bowring, F., Yeadon, J., Ishii, C., Suzuki, K., Sakai, W., Pratt, R. 2004. Lessons from the genome sequence of *Neurospora crassa*: Tracing the path from genomic blueprint to multicellular organism. *Microbiol. Mol. Biol. Rev*, 68, 1–108.

Cashmore, A.R., Jarillo, J.A., Wu, Y.J., Liu, D. 1999. Cryptochromes: blue light receptors for plants and animals. *Science* 284, 760-765.

Crosthwaite, S.K., Dunlap, J.C., Loros, J.J. 1997. *Neurospora wc-1* and *wc-2*: transcription, photoresponses, and other origins of circadian rhythmicity. *Science* 276, 763-769.

Crosson, S., Rajagopal, S., Moffat, K. 2003. The LOV domain family: photoresponsive signaling modules coupled to diverse output domains. *Biochemistry* 42, 2-10.

Degli-Innocenti, F., Chambers, J.A.A., Russo, V.E. 1984. Conidia induce the formation of protoperithecia in *Neurospora crassa*: further characterization of white collar mutants. *J. Bacteriol.* 159, 808-810.

Degli-Innocenti, F., Russo, V.E. 1984. Isolation of new white collar mutants of *Neurospora crassa* and studies on their behaviour in the blue-light-induced formation of protoperithecia. *J. Bacteriol.* 159, 757–761.

Franklin, K.A., Larner, V.S., Whitelam, G.C. 2005. the signal transducing photoreceptors of plants. *Int. J. Dev. Biol.* 49, 653-664.

Froehlich, A.C., Noh, B., Vierstra, R.D., Loros, J., Dunlap J.C. 2005. Genetic and molecular analysis of phytochromes from the filamentous fungus *Neurospora crassa*. *Eukaryot. Cell* 4, 2140-2152.

Harding, R.W., Turner, R.V. 1981. Photoregulation of the carotenoid biosynthetic pathways in albino and white collar mutants of *Neurospora crassa*. *Plant Physiol.* 68, 745–749.

Harding, R.W., Melles, S. 1983. Genetic analysis of phototropism of *Neurospora crassa* perithecial beaks using white collar and albino mutants. *Plant Physiol.* 72, 996-1000.

Idnurm, A., Heitman, J. 2005. Photosensing fungi: phytochrome in the spotlight. *Curr. Biol.* 15, R829-R832.

Jacobson, D.J., Powell, A.J., Dettman, J.R., Saenz, G.S., Barton, M.M., Hiltz, M.D., Dvorachek, W.H., Glass, N.L., Taylor, J.W., Natvig, D.O. 2004. *Neurospora* in temperate forests of western North America, *Mycologia* 96, 66–74.

Jiao, Y., Lau, O.S., Deng, X.W. 2007. Light-regulated transcriptional networks in higher plants. *Nature Rev. Genet.* 8, 217-230.

Karniol, B., Wagner, J.R., Walker, J.M., Vierstra, R.D. 2005. Phylogenetic analysis of the phytochrome superfamily reveals distinct microbial subfamilies of photoreceptors. *Biochem. J.* 392, 103-116.

Liu, Y., Bell-Pedersen, D. 2006. Circadian rhythms in *Neurospora crassa* and other filamentous fungi. *Eukaryot. Cell* 5, 1184-1193.

Linden, H., Ballario, P., Macino, G. 1997. Blue light regulation in *Neurospora crassa*. *Fungal*

Genet. Biol. 22, 141-150.

Martinez-Garcia, J.F., Huq, E., Quail, P.H. 2000. Direct targeting of light signals to a promoter element-bound transcription factor. *Science* 288, 859–63.

Mas, P., Devlin, P.F., Panda, S., Kay, S.A. 2000. Functional interaction of phytochrome B and cryptochrome 2. *Nature* 408, 207–11.

Ni, M., Tepperman, J.M., Quail, P.H. 1998. PIF3, a phytochrome-interacting factor necessary for normal photoinduced signal transduction, is a novel basic helixloop- helix protein. *Cell* 95, 657–667.

Pöggeler S., Kück, U. 2000. Comparative analysis of the mating-type loci from *Neurospora crassa* and *Sordaria macrospora*: identification of novel transcribed ORFs. *Mol. Gen. Genet.* 263, 292-301.

Purschwitz, J., Muller, S., Kastner, C., Fischer, R. 2006. Seeing the rainbow: light sensing in fungi. *Curr. Opin. Microbiol.* 9, 566-571.

Rockwell, N.C., Su, Y.S., Lagarias, J.C. 2006. Phytochrome structure and signaling mechanisms. *Annu. Rev. Plant Biol.* 57, 837-858.

Smith, H. 1995. Physiological and ecological function within the phytochrome family. *Ann. Rev. Plant Physiol. Plant Mol. Biol.* 46, 289-315.

Stanewsky, R., Kaneko, M., Emery, P., Beretta, B., Wager-Smith, K., Kay, S.A., Rosbash, M., Hall, J.C. 1998. The cryb mutation identifies cryptochrome as a circadian photoreceptor in Drosophila. *Cell* 95, 681-692.

Terakita, A. 2005. The opsins. *Genome Biol.* 6, 213.1-213.9.

Thresher, R.J., Vitaterna, M.H., Miyamoto, Y., Kazantsev, A., Hsu, D.S., Petit, C., Selby, C.P., Dawut, L., Smithies, O., Takahashi, J.S., Sancar, A. 1998. Role of mouse cryptochrome blue-light photoreceptor in circadian photoresponses. *Science* 282, 1490-1494.

Tralau, T., Lanthaler, K., Robson, G.D., Crosthwaite, S.K. 2006. Circadian rhythmicity during prolonged chemostat cultivation of Neurospora crassa. *Fungal Genet. Biol.* 44, 754-763.

Whippo, C.W., Hangarter, R.P. 2004. Phytochrome modulation of blue-light phototropism. *Plant Cell Environ.* 27, 1223–1228.

Yang, H.Q., Tang, R.H., Cashmore, A.R. 2001. The signaling mechanism of Arabidopsis CRY1 involves direct interaction with COP1. *Plant Cell* 13, 2573–87.

Yeh, K.C., Wu, S.H., Murphy, J.T., Lagarias, J.C. 1997. A cyanobacterial phytochrome two-component light sensory system. *Science* 277, 1505-1508.

Yu, Y., Dong, W., Altimus, C., Tang, X., Griffith, J., Morello, M., Dudek, L., Arnold, J., Schüttler, H.-B. 2007. A genetic network for the clock of *Neurospora crassa*. *Proc. Natl. Acad. Sci. U.S.A.* 104, 2809-2814.

CHAPTER 7

Overall summary and future work

Chapter three provided a detailed description of the process of mating involving the macroconidium-trichogyne interaction in *Neurospora crassa*. Cognate pheromone and pheromone receptors (CCG-4 and PRE-2, MFa-1 and PRE-1) were shown to be involved and resulted in the chemotropic growth of specialized female hyphae called trichogynes towards male macroconidia. The most significant discovery reported in this chapter was that following macroconidium-trichogyne fusion the female nuclei became immobilized, rounded up and clumped together whilst all of the male nuclei from a single macroconidium moved unidirectionally and sequentially past the immobilized female nuclei towards the ascogonium with an inchworm-like, repeated elongation and condensation pattern of movement. In addition, both the male and female nuclei underwent cell cycle arrest following macroconidium-trichogyne fusion. Future work following on from the research described in chapter three could include:

- Differential labelling of the male and female nuclei during the mating process using GFP targeted specifically to one nuclear type and RFP specifically targeted to the other nuclear type. This will provide less ambiguous labelling of the two types of nuclei during the whole mating process.
- Labelling and localization of the PRE-1 and PRE-2 receptors with GFP. This should provide insights into whether pheromone-pheromone receptor interactions are localized to certain cellular regions of communicating trichogynes or macroconidia.

In chapter four I characterized a new cell type called the *conidial sex tube*. I showed that it is physiologically and morphologically different from other two types of hyphae (germ tubes and conidial anastomosis tubes) produced by macroconidia, and it is under separate

genetic control. Conidial sex tubes were clearly found to act as male fertilizing agents during mating in *N. crassa*. However, in the *mat A* strain they could also be induced by the synthetic sex pheromone, MFa-1, in the absence of the *mat a* female strain. My results showed for the first time that the male cell can exhibit a morphological response (i.e. CST formation) to the female in *N. crassa* (previously it was believed that it was only female trichogyne that responded to the male cell, Bistis, 1981). Future research following on from that described in chapter four could include:

- Determining whether the synthetic CCG-4 pheromone can induce CST formation in the *mat a* strain.
- Labelling the putative hydrophobin on the surface of CSTs with GFP. This would allow rapid identification of CSTs by fluorescence microscopy.
- Screening deletion mutants compromised in signalling to analyse the signal transduction pathways that are downstream of the pheromone-pheromone receptor interaction that stimulates CST formation.
- Determining whether the conidia of other fungal species produce CSTs.

In chapter five I provided evidence that male nuclear movement through the trichogyne involves both transport along microtubules and actin microfilaments, and that kinesin, dynein and myosins (encoded by both the male and female) mediates this process. Two kinesins (NKIN-2 and KAR-3), three dynein subunits (DYN-2, DLC and DIC), one dynactin subunit (DYN-27) and two myosins (MYO-1 and MYO-2) from the female were found to influence the behaviour of male nuclear movement through the trichogyne. One kinesin (KIP-2), one dynactin subunit (RO-3), and two myosin (MYO-1 and MYO-2) encoded by the male were found to influence the behaviour of the female nuclei. Non-self recognition of nuclei of opposite mating type occurs immediately following macroconidium-trichogyne fusion. A novel mechanism underlying non-self (male-female) nuclear recognition in filamentous fungi was proposed, and involves the co-operative functioning of motor proteins encoded by the male and female partners at different stages following macroconidium-trichogyne fusion. Future work following on from that described in chapter five could include:

- Analysing the influence of each of the motor proteins on male and female nuclear behaviour in the deletion mutant of each motor protein (in my study I only analysed the influence of each motor protein deletion mutant on the nuclear behaviour of the wild type of opposite mating type). Mutant strains expressing *h1-gfp* can be easily generated by crossing each deletion mutant with an *h1-gfp* expressing strain and selecting for recombinants containing both the gene deletion and *h1-gpf* from the ascospore progeny.
- Analysing whether the different motor proteins involved in non-self recognition are transcriptionally or post-transcriptionally regulated. This would be done using Northern,

Reverse Transcriptase Polymerase Chain Reaction (RT-PCR) and Western analyses.

- Complementing the motor protein deletion mutants by transforming them with the wild type motor protein genes to determine whether the wild type phenotype is recovered.
- Analysing the influence of other motor proteins on male and female nuclear behaviour during mating. Deletion mutants of the following motor proteins were not analysed in my study: dynein subunits (NCU02610, NCU03882, NCU09095, NCU09142 and NCU09982), dynactin subunits (RO-4, RO-7, RO-12, NCU04043, NCU08375), Lis-1 subunits (NCU04312 and NCU04534), kinesins (NKIN-3, KIF-21A, KLP-3, KLP-4, KLP-5, KLP-6 and KLP-7) and myosin (NCU04350).

In chapter six, CST induction was shown to be regulated by light but this was mating-type dependent. The effects of white light could be mimicked with red light and both the PHY-1 and PHY-2 phytochrome photoreceptors were shown to be involved. PHY-1 and PHY-2 have contrasting roles in this process: PHY-1 behaves like a plant phytochrome whilst PHY-2 behaves like a bacterial phytochrome even though both proteins are more closely related to bacterial than plant phytochromes. Blue and green light, and the blue light photoreceptors WC-1 and CRY, were also found to play a role in CST induction. The emergence of CSTs from macroconidia was shown to display a positive phototropism to white light. Future work following on from that described in chapter six could include:

- Screening and characterization of deletion mutants of genes encoding signalling and photoregulatory proteins in both mating types, and determine which are defective in CST induction and phototropism.
- Analysing the spectral and fluence responses, and thus action spectra, of the wild type and photoreceptor mutant strains. This could be analysed in a single experiment by placing a prism and continuous neutral density filter between the white light source and a slide on which macroconidia are incubated in the presence of synthetic pheromome of opposite mating type. The prism would provide a continuous spectrum of light wavelengths running in the xy plane, and a neutral density filter would provide light of different fluence running in the xz plane. Conidial sex tube formation could then be quantified in small defined quadrats across the whole slide. This quantitation could be easily automated by using a computer driven, motor driven stage with appropriate image analysis software to detectand quantify CST formation from macroconidia.
- Localizing the different photoreceptors with GFP labelling and monitoring their subcellular distribution in macroconidia after exposure to white, red, green or blue light. Phytochrome in its Pfr form in plants, translocates to the nucleus where it regulates transcription (Smith, 1999).

- Identifying proteins which interact with the phytochromes by two-hybrid analysis, and image their interactions (e.g. by using bifluorescence complementation, Hoff & Kück, 2005).

References

Hoff, B., Kück, U. 2005. Use of biomolecular fluorescence complementation to demonstrate transcription factor interaction in nuclei of living cells from the filamentous fungus *Acremonium chrysogenum*. *Curr. Genet.* 47, 132-138.

Smith, H. 1999. Tripping the light fantastic. *Nature* 400, 710-713.

Appendix 1 Supplementary movies on CD

Chapter 3 Male and female interactions during mating

Chapter 4 A new cell type produced by macroconidia that is involved in sexual reproduction

Chapter 5 Influence of motor proteins and cytoskeleton on nuclear behaviour during mating

Viewing instructions

The CD should autorun when inserted into the computer or with a double-click of the CD icon. If this does not happen, browse the CD and open the file *index.html* with a web browser (e.g. Internet Explorer or Mozilla Firefox, the later works best). Once open, click on the links to navigate through the chapters and files. For optimal performance copy the entire contents of the CD in to a folder on your hard drive, then open *index,html*.

.

Sexual mating in *Neurospora crassa*

Hsiao-Che Kuo
PhD Thesis

Appendix 1 - Supplementary movies

Chapter 3 -

Male and female interactions during mating

Chapter 4 -

A new cell type produced by macroconidia that is involved in sexual reproduction

Chapter 5 -

Influence of motor proteins and cytoskeleton on nuclear behaviour during mating

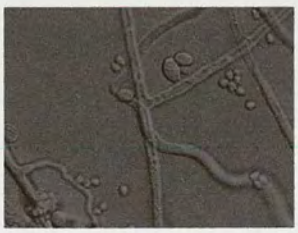

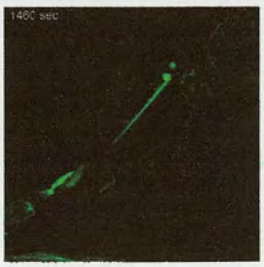

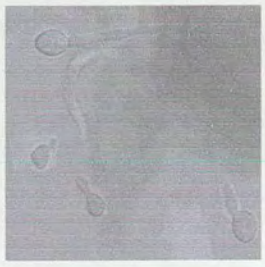

Home Chapter 3 Chapter 4 Chapter 5